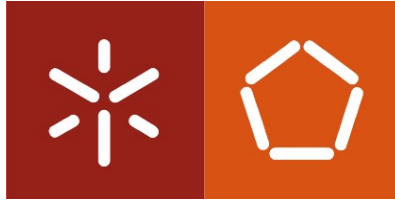


**Universidade do Minho**  
Escola de Engenharia

Luís Carlos Martins da Silva

**Analysis of Christchurch  
Catholic Basilica,  
New Zealand**





**Universidade do Minho**  
Escola de Engenharia

Luís Carlos Martins da Silva

**Analysis of Christchurch  
Catholic Basilica,  
New Zealand**

Dissertação de Mestrado  
Mestrado Integrado em Engenharia Civil

Trabalho efetuado sob a orientação do  
Professor Doutor Paulo José B. Barbosa Lourenço

e do  
Doutor Nuno Adriano Leite Mendes





To the memory of my Grandfather

*João António Viana,*

You will be always in my heart.



# ACKNOWLEDGMENTS

Firstly, I want to express my sincere gratitude to my thesis supervisor, Professor Paulo Lourenço. Thanks for believing in me, for your interest, patience, guidance, scientific advices and for your careful reading of the thesis.

I also would like to give a special acknowledgement to my thesis co-supervisor, Nuno Mendes. His guidance throughout this dissertation period was decisive. Thanks for the knowledge shared, advices, motivation, interest, discussions, careful reading and full availability.

A special thanks to my friend Gonçalo Leite for helping me in the development of the programming code, required to the model preparation.

I also would like to express my gratitude to the following PhD students: João Leite, which provided me important information about the Christchurch Catholic Basilica, Ana Araújo for giving a general description of the software DIANA and to Rui Silva for his interest.

Plus, thanks to all my friends and particularly to my course colleagues: Bruno, Hugo, Luís, Julien, João, Diogo and André for your friendship and help during this academic stage and to Filipe, Joana, Susana and Pedro for your help and support in this last year.

Lastly, I would like to express my gratitude to my parents, João Silva & Ana Luísa, and to my sister, Ana. Thanks for your sacrifices, friendship, patient, attention, advices and love. Thanks for being my family.



# ABSTRACT

Cultural heritage buildings are structures that enclose a set of particular values which symbolically allow to become part of a given culture identity and continuity. Nowadays, the conservation interventions on these particular structures aim to retain its historic integrity, identity and symbolism by taking into account centuries of ideological evolution, related to aesthetic and technical issues. The interventions in cultural heritage buildings should only be taken after a careful analysis, which includes a diagnosis, safety assessment and the design of possible solutions. Despite the need for some conservation interventions due to lack of maintenance and progressive deterioration, situations of sudden destruction of cultural heritage buildings deserves a special reflection. A numerical model is invariably a valuable tool to assess the structural behavior of these buildings and to influence the final act decision.

The present study case is the Christchurch Catholic Basilica, also known as Cathedral of the Blessed Sacrament. It is located in New Zealand and is listed as category I heritage in New Zealand – International or National significance. The four earthquakes events in an approximate period of nine months (September 2010 to June 2011) led to a progressive damage and local collapses. In order to study its structural behavior, a seismic analysis was carried out. The seismic assessment of the Cathedral involved the preparation and calibration of a tri-dimensional numerical model based on the Finite Element Method. Two models were prepared, an undamaged and a damaged one once the structure was already damaged at the time of the dynamic identification tests. The calibration process was not accomplished once the dynamic properties obtained from the dynamic identification tests do not fit well with the numerical results. The main cause is the interior damage that was not inserted (it is unknown). In order to evaluate the dynamic behavior of the Cathedral were carried out pushover analyses proportional to the mass in each direction. These analyses allowed collecting the damage patterns, the vulnerable elements and the ductile behavior using capacity curves. Having in account this information a comparison between the numerical and real behavior was affordable and a reasonable agreement was obtained.

*Keywords:* Cathedral, masonry, New Zealand earthquake, Pushover analysis, seismic performance.



# RESUMO

Edifícios pertencentes ao Patrimônio cultural são estruturas que integram um grupo particular de valores intangíveis que simbolicamente possibilitam que estas façam parte da identidade e continuidade de uma dada cultura. As intervenções de conservação têm em conta, atualmente, séculos de evolução ideológica relacionada com aspetos estéticos e técnicos que procuram reter a sua integridade histórica, identidade e simbolismo. A intervenção sobre este tipo de estruturas deve ser realizada após um estudo criterioso, que inclui um diagnóstico, avaliação da segurança estrutural e desenvolvimento de possíveis soluções. Apesar da necessidade de conservação de estruturas pertencentes ao patrimônio cultural devido à falta de manutenção e consequente progressiva deterioração, situações em que ocorre o seu colapso súbito merecem uma reflexão especial. Um modelo numérico é invariavelmente uma ferramenta valiosa para avaliar o seu comportamento estrutural e influenciar a tomada de decisão final.

O presente estudo trata do caso da Basílica Católica de Christchurch, também conhecida como Catedral do Sagrado Sacramento. Está localizada na Nova Zelândia e consta na categoria I da lista do patrimônio da Nova Zelândia – importância Nacional e Internacional. Os quatro eventos sísmicos num período aproximado de nove meses (Setembro de 2010 até Junho de 2011) levou a um dano progressivo e colapsos locais. Objetivando o estudo do comportamento estrutural foi realizada uma análise sísmica. A avaliação sísmica da Catedral envolveu a preparação de um modelo numérico tridimensional através do método de elementos finitos. Uma vez que a estrutura já se apresentava danificada, aquando os ensaios de identificação dinâmica, dois modelos foram preparados: um com dano e outro sem dano inserido. A calibração do modelo não foi conseguida uma vez que o dano interior, não inserido por não ser conhecido, impossibilitou um ajuste correto das propriedades dinâmicas obtidas nos testes de identificação dinâmica. Para avaliar o comportamento dinâmico da Catedral foram realizadas análises *pushover* proporcionais à sua massa em cada direção. Estas análises permitiram coletar o dano, os elementos vulneráveis e a ductilidade da estrutura através de curvas de capacidade. Tendo em conta esta informação, uma comparação entre o comportamento real e numérico foi possível, tendo sido obtido uma concordância razoável entre os mesmos.

*Palavras-Chave:* Catedral, alvenaria, Sismos na Nova Zelândia, análise Pushover, comportamento sísmico.





# TABLE OF CONTENTS

<b>ACKNOWLEDGMENTS</b> .....	I
<b>ABSTRACT</b> .....	III
<b>RESUMO</b> .....	V
<b>TABLE OF CONTENTS</b> .....	VII
<b>INDEX OF FIGURES</b> .....	X
<b>INDEX OF TABLES</b> .....	XV
<b>1 CHAPTER 1 - INTRODUCTION</b> .....	1
1.1 SCOPE AND MOTIVATION .....	1
1.2 RESEARCH OBJECTIVES AND OUTLINE .....	2
<b>2 CHAPTER 2 – OVERVIEW: SUDDEN LOSSES OF BUILT HERITAGE</b> .....	5
2.1 INTRODUCTION .....	5
2.2 LOSS INDUCED BY WAR .....	6
2.3 LOSS INDUCED BY WAR WITH RELIGIOUS CONTENTS .....	9
2.4 LOSS INDUCED BY TERRORISM .....	11
2.5 LOSS INDUCED BY EARTHQUAKES AND FIRE .....	12
2.6 LOSS INDUCED BY LONG-TERM GRAVITATIONAL LOADS .....	15
2.7 CONCLUSIONS .....	16
<b>3 CHAPTER 3 – CHRISTCHURCH CATHOLIC BASILICA</b> .....	21
3.1 BRIEF HISTORICAL OVERVIEW: NEW ZEALAND (NZ) .....	21
3.2 LOCATION .....	22
3.3 BUILDING DESCRIPTION .....	25
3.4 SEQUENCE OF EARTHQUAKES DAMAGE .....	30

3.4.1	<i>Earthquake of September 4, 2010</i> .....	30
3.4.2	<i>Earthquake of February 22, 2011</i> .....	31
3.4.3	<i>Aftershocks of June 13, 2011</i> .....	35
3.5	THE DICHOTOMY: DEMOLISH, PARTIAL OR TOTAL DECONSTRUCTION? .....	37
4	<b>CHAPTER 4 – NUMERICAL MODEL PREPARATION</b> .....	41
4.1	INTRODUCTION .....	41
4.2	FEM MODEL PRE-PROCESSING STAGE.....	42
4.2.1	<i>Methodology</i> .....	42
4.2.2	<i>Geometry definition</i> .....	43
4.2.3	<i>Material and physical properties</i> .....	46
4.2.4	<i>Mesh discretization</i> .....	48
4.2.5	<i>Boundary conditions</i> .....	52
4.3	UNDAMAGED FEM MODEL.....	53
4.3.1	<i>Linear static analysis</i> .....	53
4.3.2	<i>Modal parameters</i> .....	56
4.4	DAMAGED FEM MODEL .....	57
4.4.1	<i>Damage insertion</i> .....	58
4.4.2	<i>Calibration process</i> .....	60
5	<b>CHAPTER 5 – SEISMIC ASSESSMENT BY NONLINEAR STATIC ANALYSIS</b> .....	65
5.1	INTRODUCTION .....	65
5.2	MATERIAL CONSTITUTIVE MODEL AND NONLINEAR MATERIAL PROPERTIES .....	65
5.3	NUMERICAL INTEGRATION.....	67
5.4	ITERATIVE PROCEDURE.....	68
5.5	NONLINEAR STATIC ANALYSIS .....	72
5.5.1	<i>Direction +X</i> .....	72

---

5.5.2	<i>Direction -X</i> .....	75
5.5.3	<i>Direction +Y</i> .....	78
5.6	FINAL REMARKS .....	81
6	<b>CHAPTER 6 – CONCLUSIONS AND FUTURE WORKS</b> .....	83
6.1	CONCLUSIONS.....	83
6.2	FUTURE WORKS .....	84
	<b>REFERENCES</b> .....	87
	<b>ANNEX A</b> .....	93

# INDEX OF FIGURES

Figure 1 – The Mostar Bridge: (a) Destroyed after the war (Source: <a href="http://www.flickr.com">http://www.flickr.com</a> ); .....	7
Figure 2 – Church of Our Lady: (a) before destruction; (b) ruins in 1955, after the destruction by fire [14].....	8
Figure 3 – The Warsaw district of Muranów (a) After the World War I; (b) At present [22].....	9
Figure 4 – The smaller Buddha in 1977 (left) and in 2005 (right), after its destruction [10].....	10
Figure 5 – The taller Buddha in 1963 (left) and in 2007 (right), after its destruction [10]. .....	10
Figure 6 – Temples in Mali: (a) Restoration of Sankore mosque [25]; (b) Restoration of Djingareberre mosque [25]; (c) Destruction of a muslim saint tomb (Source: <a href="http://www.cnn.com">www.cnn.com</a> ).....	11
Figure 7 – (a) Terrorist attack upon the Twin towers (Source: <a href="http://cloudfront3.bostinno.com/wpcontent">http://cloudfront3.bostinno.com/wpcontent</a> ); (b) Freedom tower and the memorial - adjacent to tower (Source <a href="http://onewtc.com/">http://onewtc.com/</a> ). .....	12
Figure 8 – Wall system in Lisbon: (a) Before the earthquake; (b) After the earthquake, where an x-braced internal wooden frame is clear. ....	13
Figure 9 – Destruction of Chiado buildings by the fire in 1988 (Courtesy of <i>Lebreiro Henriques</i> : <a href="http://www.flickr.com/photos/lebreirohenriques/">http://www.flickr.com/photos/lebreirohenriques/</a> ).....	14
Figure 10 – The Cathedral of Pavia: (a) before the collapse of the civic tower in 1989 (Source: <a href="http://www.4thfirst.com/interesting_sites.html">http://www.4thfirst.com/interesting_sites.html</a> ); (b) After the collapse - ruins of the Civic Tower [43]; (c) At present (Source: Wikipedia). ....	15
Figure 11 – (a) Captain James Cook [46]; (b) Captains Cook’s ship – ‘Endeavour’[47].	21
Figure 12 – (a) New Zealand in the World Atlas; (b) location of Christchurch city – New Zealand South islands. (Source: <a href="http://wordatlas.com">wordatlas.com</a> ).....	22
Figure 13 – Number of Earthquakes (in $M_w$ – Moment magnitude scale) in the New Zealand Region (1960 to 2011) - (GeoNet data results).....	24

Figure 14 – (a) Identification of the existent plat boundary and the possible new fault of New Zealand South Island (Source: www.newscientist.com); (b) Maximum shear strain rate of New Zealand (Source: GNS Science). .....	24
Figure 15 – Number of earthquakes at Canterbury region from September 4 of 2010 to September 3 of 2012 (GeoNet data results). .....	25
Figure 16 – Map location of Barbadoes street– Cathedral of Blessed Sacramento top view. ....	26
Figure 17 – Cathedral of the Blessed Sacramento: (a) North and West façades; (b) South façade. ....	26
Figure 18 –Basilica of the Blessed Sacramento geometry (a) West elevation; (b) Top plan. ....	27
Figure 19 – West façade (left) and east façade (right) – the grey lines are elements in the background. ....	27
Figure 20 – South Elevation – the grey lines are elements in the background. ....	28
Figure 21 – North Elevation - the grey lines are elements in the background. ....	28
Figure 22 – Introduced elements in the 2004 strengthening of the Basilica of the Blessed Sacramento [3]. ....	29
Figure 23 – West façade of the Christchurch Catholic Basilica and the damage in the two bell towers, north (left) and south (right). ....	32
Figure 24 – Detail of the west wall collapse of the south bell tower. ....	32
Figure 25 – South transept facade. ....	33
Figure 26 – Detail of shear cracking around south transept window and local collapse of the architrave. ....	33
Figure 27 – Large diagonal crack in the entablature near to the north transept. ....	33
Figure 28 – Shear cracks in the transept-main nave connection. ....	33
Figure 29 – Lateral displacements of the main dome drum or rotunda. ....	33
Figure 30 – Collapse occurred in the north arch of the sanctuary. ....	34
Figure 31 – Severe damage to the south arch spandrel. ....	34
Figure 32 – Collapse of a part of the RC sanctuary flat. ....	34

Figure 33 – Damage to the south supporting wall of rotunda.....	34
Figure 34 – Shear cracks around the upper arcade of the North elevation. ....	34
Figure 35 – Diaphragm damage at the first floor (its exact position is unknown). ....	34
Figure 36 – Collapse of a fraction of North rotunda wall, part of the adjacent RC flat roof and north interior arch.....	35
Figure 37 – Damages to the key stone of the east arch.....	35
Figure 38 – Damage along the West arch. ....	36
Figure 39 – South arch severe damage. ....	36
Figure 40 – Visible damage to the main dome drum (after the removal of the internal dome in 25 August, 2011).....	36
Figure 41 – Developing of a diagonal block failure in the south transept façade. ....	36
Figure 42 – Crushing of the top south-west column.....	36
Figure 43 – Vertical crack in the east wall of the first floor. ....	36
Figure 44 – Schematic description of the FEM numerical model preparation. ....	42
Figure 45 – Main dome: (a) Interior dome of the rotunda during its removal; (b) Interior dome of the rotunda modeled in DIANA, using beam elements; (c) Wooden-frame of the main dome, after the copper cladding removal; (d) Wooden-frame of the main dome modeled in DIANA, using beam elements. ....	44
Figure 46 – Shell and solid elements: (a) General overview of the shell elements; (b) General perspective of solid elements; (c) West-East cut-away perspective with shell elements (colored as white) and solid elements (colored as grey).....	45
Figure 47 – The beam element L12BE, with a total of twelve degrees of freedom (DOFs). ....	48
Figure 48 – Curved shell elements: (a) Degrees of freedom per node (b) Quadrilateral curved shell element (Q20SH) [90]; (c) Triangular curved shell element (T15SH) [90].	49
Figure 49 – Solid elements: (a) The degrees of freedom of a solid element per node (three DOF); (b) Brick curved shell element (HX24L) [90]; (c) Wedge curved shell element (TP18L) [90]. ....	49
Figure 50 – Point mass: (a) Topology; (b) The three degrees of freedom (translations) of the PT3T element. [90] .....	49

Figure 51 – Tests of the mesh in a façade sample: (a) Obtained mesh using a Delaunay algorithm (automatic meshing); (b) Prescribed (manual) mesh using a structured rectangular approach (the crosses represent distorted elements). .....	50
Figure 52 – Mesh for the solid elements: (a) fine refinement; (b) coarse refinement. (c) Nodal vertical displacements due to the self-weight for both mesh discretizations.....	51
Figure 53 – Top view of the first type of boundaries constraints considered.....	53
Figure 54 – Deformation of the Basilica under its self-weight (magnification factor: 300). .....	54
Figure 55 – Stress of the analysis due to the self-weight: (a) Vertical stresses; (b) Principal tensile stresses for masonry elements; (c) Principal compressive stresses of RC slabs (top surface); (d) Principal tensile stresses of RC slabs (bottom surface).....	55
Figure 56 – First six global mode shapes of the non-damaged structure.....	57
Figure 57 – Damage in shell elements (shadowed elements): a) South elevation; (b) North elevation; (c) West elevation; (d) West façade of the transepts (d) East elevation; (f) Undamaged (left) and damaged (right) South bell tower; (g) Undamaged (left) and damaged (right) North bell tower. ....	59
Figure 58 – Damage in solid elements (shadowed elements): a) North-West perspective; b) South-East perspective; c) Deleted elements of the North arch. ....	60
Figure 59 – Experimental mode shapes and frequencies [58]. ....	61
Figure 60 – Comparison between the 1 <sup>st</sup> , 2 <sup>nd</sup> and 5 <sup>th</sup> experimental and numerical mode shapes.....	63
Figure 61 – Adopted hysteretic behavior for masonry and concrete [99]. ....	66
Figure 62 – Iterative methods [90]: a) Regular Newton-Raphson method; b) Modified Newton-Raphson method; c) BFGS method. ....	70
Figure 63 – Iterative methods: (a) Capacity curve in the main dome control node; (b) Capacity curve in the West tympanum wall control node; (c) Processing time. ....	71
Figure 64 – Pushover analysis: (a) Applied load directions (longitudinal – X; transversal – Y); (b) Control nodes defined. ....	72
Figure 65 – Capacity curve in +X direction: (a) Node 1; (b) Node 2.....	73
Figure 66 – Principal tensile strains of the south façade walls for a horizontal load of 0.3g in +X direction (the nave roof frame is not represented).....	74

Figure 67– Principal tensile strains for the West façade due to a horizontal load of 0.3g, in +X direction (External surface). ..... 75

Figure 68 – Bell tower stories’ displacements for a horizontal load of 0.3g (+X); (1st: storey; N3: node 3)..... 75

Figure 69 – Capacity curve in -X direction: (a) Node 1; (b) Node 2..... 76

Figure 70 – Principal tensile strains of the South façade walls for a horizontal load of 0.27g in -X direction (the nave roof frame is not represented). ..... 77

Figure 71 – Side interior view through a ..... 77

Figure 72 – Bell tower stories’ displacements for a horizontal load of 0.27g (-X); (st.: storey; N3: node 3)..... 77

Figure 73 – Capacity curve in +Y direction: (a) Node 4; (b) Node 5..... 78

Figure 74 – Principal tensile strains due to a horizontal load in +Y direction: (a) West façade; (b) East façade. .... 79

Figure 75 – Side interior view through a north-south cutaway: Principal tensile strains (external surfaces to façades, top surfaces of slabs and North surfaces to interior walls), direction +Y (interior damage, pointed out by the arrows). ..... 80

Figure 76 – Bell tower storeys’ displacements (+Y); (1st.: storey; N4: node 4). ..... 80

Figure 77 – (a) Damage at the interior transverse walls; (b) Global overview of the damage in the north elevation. .... 80



# INDEX OF TABLES

Table I – Case studies presented, cause for loss and intervention decision.....	16
Table II – Information about the Earthquake of September 4, 2010 (GeoNet, 29-10-2012). .....	30
Table III – Information about the Earthquake of February 22, 2011 (GeoNet, 29-10-2012). .....	31
Table IV – Damage and church typology [59]. .....	32
Table V – Information about the aftershock of June 13, 2011 (GeoNet, 30-10-2012).....	35
Table VI – Elastic material properties. ....	46
Table VII – Physical properties of the shell and beam elements. ....	47
Table VIII – Point mass groups, including their total weight and weight per node. ....	48
Table IX – Frequencies, period and cumulative effective mass in each direction. ....	56
Table X – Damaged numerical models used to evaluate the numerical modal response. .	62
Table XI – Comparison between experimental and numerical modal frequencies. ....	63
Table XII – Nonlinear material parameters. ....	67
Table XIII – In plane Gauss integration points and/or Simpson for linear and nonlinear analysis (in-plane x thickness). ....	68



# Chapter 1

## Introduction

### 1.1 SCOPE AND MOTIVATION

Cultural heritage buildings are structures that outline a set of particular values which symbolically allow to become part of a given culture identity and continuity [1].

Nowadays, the conservation interventions on these particular structures seek to “retain the historic integrity of heritage places by doing as much as necessary to preserve them”[2], by taking into account centuries of ideological evolution, related to aesthetic and technical issues [3, 4] aiming at maintaining the identity and symbolism. If, on one hand, the conservation aims to prevent building decay, by undertaking a methodology to increase its lifetime, on the other hand, the restoration intervention aims to re-integrate the decayed elements in its original features and building concept. When the introduction of new elements is necessary, they must be integrated harmoniously and, since a cultural heritage building is an historic document, the difference between the old and new should be visible [1]. The following famous sentence from Winston Churchill: “We shape our buildings, and afterwards our buildings shape us” describes the way which buildings are engaged to our emotional, cultural and social values. It is also implicit that continuous conservation and restoration interventions on these buildings are required to assure the preservation of those values.

The lack of intervention has been pointed out as the main cause of important cultural heritage buildings collapse, for example the Civic Tower of Pavia (Italy) in 1989, St. Marco’s Campanile at Venice (Italy) in 1902, St. Martinus Church at Kerksken (Belgium) in 1990, among others [5]. The sudden collapse of these cultural heritage buildings is associated to natural and human agents, and masonry long-term behavior. Natural disasters are an effect of natural hazards, as example floods, tornados, volcanic eruptions, landslides, tsunamis and earthquakes. Even human agents can also lead to cultural

heritage buildings destruction, as terrorism and war conflicts. The masonry long-term behavior can be associated to creep phenomena caused by high sustained loads, material aging and freeze-and-thaw phenomena.

The scope of the present study, i.e. analysis of seismic performance of the Cathedral of the Blessed Sacrament, also known as Christchurch Catholic Basilica, is related to the conservation and restoration of cultural heritage buildings, due to its symbolism and type of loss. The Christchurch Catholic Basilica is located in New Zealand (NZ) and is listed as category I heritage (International or National significance) [6]. The Basilica suffered a strengthening intervention in 2004 and its safety was assumed to be adequate. In this, the internal columns were post-tensioned, RC (reinforced concrete) slab and ring beams were added as well as a steel bracing system in the both tower bells. However, the four earthquakes occurred in a period of nine months, namely: (i) September 4 2010 earthquake; (ii) December 26 2010 earthquake; (iii) February 22 2011 earthquake; and (iv) June 13 2011 aftershocks, led to progressive damage and consequent local collapses. The constructive technique is unreinforced masonry (URM), which is associated to high seismic vulnerability, mainly due to: (i) low resistance to horizontal forces and lack of capacity to dissipate energy [7, 8]; (ii) the absence of seismic requirements in the construction [8].

The interventions in cultural heritage buildings should only be taken after a careful analysis [9], which includes a diagnosis, safety assessment and the design of intervention solutions [4], taking into account the guidelines presented by ICOMOS. The numerical modelling of these buildings is a valuable tool to assess their structural behavior. The intervention solution in cases where sudden collapse is expected should take into account economical, technical, social and cultural issues. Thus, the guidelines presented by ICOMOS will be fundamental to solve the dichotomy: demolish versus partial or total deconstruction of the Christchurch Catholic Basilica.

## **1.2 RESEARCH OBJECTIVES AND OUTLINE**

The present dissertation aims to accomplish the following main tasks:

- (i) The first task corresponds to the state of art and is presented at *Chapter 2*. A literature review is imperative to do this point. The aim is to develop a reflection point, whereas several case studies will be presented and exemplified with the special focus on

building restoration and reconstruction in cases of sudden collapse. It is also important to accomplish an understanding related to the pattern in which interventions relies on, identifying the reasons that allow undertaking or not a protection plan to preserve cultural heritage building integrity. The research on interventions after sudden collapse will be based on nine case studies: (1) Church of Our Lady in Dresden; (2) historic centre of Warsaw; (3) Mostar Bridge in Bosnia; (4) Bamian Buddha's in Afghanistan; (5) Mali Temples; (6) Twin Towers in New York; (7) earthquake of 1755 in Lisbon; (8) fire in Chiado, Lisbon; and (9) Civic Tower of Pavia. The described examples are addressed to five groups of loss causes: (i) loss induced by war (cases 1,2 and 3); (ii) loss induced by war with religious contents (cases 4 and 5); (iii) loss induced by terrorism (case 6); (iv) loss induced by earthquake (case 7); (v) loss induced by fire (cases 8); and (v) Loss induced by long-term effect of high sustained loads (case 9).

(ii) The second task is a brief description about the location, historic contents and main features of the Christchurch Catholic Basilica. Likewise, will be discussed the earthquake events and the respective induced damage. The last is presented at *Chapter 3*.

(iii) The third task corresponds to the preparation and calibration of the FEM (Finite Element Method) numerical model of the Christchurch Basilica and is presented at *Chapter 4*. The material properties, its constitutive law (nonlinear analysis) and material deterioration will be collected and inserted in DIANA software. Regarding to the calibration of the FEM model, it will be calibrated taking into account the experimental results obtained from the dynamic identification tests, namely the frequencies and modes shapes of the structure.

(iv) The fourth task is presented at *Chapter 5* and is associated with the seismic assessment of the numerical model. A nonlinear static analysis will be used to study the seismic response of the structure. The goal is to path the damage patterns, the vulnerable elements and the ductile behavior using capacity curves in order to enable a comparison between the numerical and real behavior.

(v) The last tasks contents the final remarks and conclusions of the present research. It also describes further steps that must be fulfilled in future works and are presented at *Chapter 6*.



# Chapter 2

## Overview: Sudden Losses of Built Heritage

### 2.1 INTRODUCTION

Cultural heritage is often expressed either as something tangible or intangible. In fact, the different parts that integrate such concept are similar and connected. The concept of cultural heritage is rather broad and could also be interpreted as a material or immaterial asset, defining the legacy and identity of a society.

As an example, it is possible to state that social standards, traditions and values (intangible cultural heritage) are a powerful tool of a society because they preserve its identity and, therefore, are so important as the physical heritage (tangible cultural heritage), such as a given building or monument. Together they forge the cultural value of a society and are inevitably connected. The tangible cultural heritage is particularly taken into account in this study, which addresses heritage buildings, including the importance of their continuous protection, conservation, maintenance and even reconstruction, as a way to accomplish also its intangible role, i.e. the symbolism.

Since antiquity several visions and theories point out distinct approaches to conservation and restoration works. Even if the purpose of this particular study is not to address the restoration theory and its history, some highlights of the most important theories are imperative, as they determine most interventions throughout history. The historical evolution includes: (i) Renaissance first theory of intervention by Leon Battista Alberti; (ii) Scientific revolution of the 18<sup>th</sup> century and its impacts on restoration; (iii) the first restoration theories during the 19<sup>th</sup> century – Archaeological and Stylistic; (iv) restoration theories by the end of 19<sup>th</sup> century – historical, modern and scientific; (v) the Athens Charter in 1931; (vi) ‘Restauro Critico’ proposed by Robert Pane and Cesare Brandi after World War II; (vii) the Venice Charter in 1964 and

the ICOMOS creation; (viii) the Italian Restoration Charter in 1989 and, finally, the (ix) Ravello's Charter in 1995 [10].

The modern principles and guidelines of interventions in historical structures, by ICOMOS/ISCARSAH (International Council on Monuments and Sites/ International Scientific Committee on the Analysis and Restoration of Structures of Architectural Heritage), take into account therefore centuries of ideological evolution, related to aesthetic and technical issues [3, 11]. Despite the need for some conservation interventions due to lack of maintenance and progressive deterioration, situations of sudden destruction of cultural heritage buildings deserves a special reflection. There are several sources of sudden deterioration due to natural disasters or human actions, e.g. armed conflicts, earthquakes, floods or fires. Selected case studies are addressed next, namely the (1) Mostar Bridge, (2) Church of Our Lady in Dresden (3) historic centre of Warsaw, (4) Bamian Buddha's, (5) Mali Temples, (6) Twin Towers in New York (7) earthquake of 1755 in Lisbon, (8) fire in Chiado in Lisbon, and (9) Civic Tower of Pavia.

Hence, the primary goal of the present discussion is to present a special field of building restoration and understand the pattern in which interventions relies on, identifying the reasons that allow undertaking a protection plan to defend cultural heritage building integrity [12].

## **2.2 LOSS INDUCED BY WAR**

### Case Example 1: *Mostar Bridge*

The first case example presented is the Mostar Bridge in Bosnia. Its construction (also called as *Stari Most*) in Bosnia and Herzegovina dates back to 1566 and was undertaken by the Turkish Empire. The bridge was designed by the renowned architect Sinan and became part of the UNESCO World Heritage List in 2005. The single span stone arch bridge had 29 and 20 meters of length and height, respectively, and was partially shattered in 1993 during the civil war in the former Yugoslavia - as other buildings of the historic town of Mostar, see Figure 1 (a). Figure 1 (b) shows the new bridge of Mostar. Its reconstruction, catalyzed by UNESCO in 1994 and finished in 2003 was financed by several nations. The reconstruction had an important role in the peace



treaty, in the recuperation of the economic and social aspects of the city and also in spreading the symbolism of peace and tolerance of culture heritage buildings [13].



a) b)  
Figure 1 – The Mostar Bridge: (a) Destroyed after the war (Source: <http://www.flickr.com>);  
(b) The new Mostar Bridge inaugurated in 2004 [UNESCO].

In the reconstruction, several principles were followed, in terms of: (i) aesthetics in order to preserve the ancient identity of the bridge; (ii) assurance of the original structural function by the usage of the same construction techniques and materials; (iii) usage of modern construction techniques of strengthening when their suitability is ensured in comparison to the ancient constructive methods [13]. To assemble the new portions of the bridge and to avoid aesthetical differences, the construction materials of the ancient *Stari Most* were used, i.e. similar stone for the arch (Tenelia stone) linked by mortar and by iron clamps sealed with lead [14]. Irreversible interventions as lime based injections were planned only in cases of strong structural stability demand [13] [15].

#### Case Example 2: *The Church of Our Lady in Dresden*

The ‘Frauenkirche’ or Church of Our Lady, see Figure 2(a), was designed by architect George Bähr and is located in Dresden (Germany). It was built in the first half of the 18<sup>th</sup> century (began in 1726 – completed in 1743) and was considered as a symbolic Protestant Baroque monument, with the great sandstone masonry dome as a main feature [16, 17]. Apart from the fact that the church suffered some interventions, firstly in 1790 and recently in 1938-1942, which guaranteed its safety, a tragic event occurred approximately two hundred years after its construction. An air raid in 1945, during the 2<sup>nd</sup> World War, caused severe damage to the city and to the Dresden masterpiece itself.

The collapse of the church was not directly caused by the bomb attack but to the resulting conflagration, which led to a thermal shock of the church and to the degradation of internal support structure strength, Figure 2(b) [17].



a) b)  
Figure 2 – Church of Our Lady: (a) before destruction; (b) ruins in 1955, after the destruction by fire [14].

A generalized interest of people from Dresden to accomplish the church reconstruction was only possible in 1993 due to a new political development (reunification of Germany) and private funds from 26 different countries. This integrated the Dresden people movement and provided the project financial support [16]. The reconstruction of Our Lady Church used the actual construction technology and stability assessment was done according to the actual structural engineering methods and safety standards. Still, it was attempted to reuse all possible materials of the old church, which were kept guarded. In order to fulfill the safety requirements, experimental and analytical studies were made to characterize the elements of the masonry, i.e. the used stones, mortar and the metal components, consisting of strength tests, creep tests, fire tests and durability investigation. Then, it was decided to use sandstone from local quarries, with high demands in terms of production (geometric tolerances), and a lime based mortar with hydraulic additives, tested to ensure adequate compatibility.

Due to construction rationalization requirements the mortar was ready-mixed [18]. In this context, the Church of Our Lady was one of the biggest reconstruction projects ever made and, also, a well-documented project, being a source of knowledge and experience that provides valuable information. The project allows discussing the importance of guidelines in the different project phases of a historical construction, i.e.

planning, execution and management, in a modern context. The intangible importance of historical buildings in the maintenance of peace, tolerance, forgiveness and, particularly, as a symbol of war effects is exalted by the distinctiveness feature of old and new facade elements [19].

### Case Example 3: *The Historic Centre of Warsaw*

The Historic center of Warsaw became part of the World Heritage List in 1980. This is a well-known example that again manifests the importance of cultural heritage to the society. About 85% of the historic center was destroyed in the World War II, mainly during the Warsaw Uprising in 1944, a 63-day resistance campaign against the German Nazi occupation [20], Figure 3(a). The action of the people from Warsaw was decisive to the after-war future of the old town.

The reconstruction project, from 1949 to 1963 [21], took in account the *historic urban and architectural form* (UNESCO), which was being carefully rebuilt. This near total reconstruction of the built heritage provided a strong social bond and identity to the country, making it unique due to its large scale, Figure 3(b).



a) b)  
Figure 3 – The Warsaw district of Muranów (a) After the World War I; (b) At present [22].

## 2.3 LOSS INDUCED BY WAR WITH RELIGIOUS CONTENTS

### Case Example 4: *Bamian Buddha's*

The Buddha's Temples from Afghanistan, corresponds to two 1.500 year old monumental statues, carved into a cliff and situated in the Bamian valley, central Afghanistan [23] (see Figure 4 and Figure 5).



Figure 4 – The smaller Buddha in 1977 (left) and in 2005 (right), after its destruction [10].



Figure 5 – The taller Buddha in 1963 (left) and in 2007 (right), after its destruction [10].

Both statues were destroyed in the Afghanistan war in 2001. Despite of the tense environment between the different sides of the conflict, there is consensus in condemning the act of the Taliban as proven by the public manifestations in several countries, which provides support and hope to achieve some solution. The present case is very sensitive, as it has been reported several times as ‘heritage at risk’ in ICOMOS reports (reports of 2000; 2002/03 and 2008/2010) [23]. After the destruction, since 2002, UNESCO and ICOMOS missions made several *in situ* interventions in order to recuperate and identify fragments, and to stabilize the walls of the Buddha’s statues.

Being the statues partial preserved before this event, it is difficult to perform a detailed description of some of their original elements and thereby, the most consensual decision is to reassemble and preserve their fragments. However, a final decision was not taken yet, and all depends on the will of the Afghan Government and stakeholders, as the possibility to reconstruct the smaller statue using an organic silicon compound is currently under analysis, involving extensive costs [24].

This case is an example of unexplained acts against a ‘culture heritage’ asset, and of the prevalence of radical ideals and extreme violence related not only with religion but especially to political divergences, which provides a loss to the Afghan culture but also to the World heritage.

#### Case Example 5: Mali Temples

Timbuktu is a regional capital located in the centre of Mali. It was established in the 12<sup>th</sup> century and had an important role in the dissemination of Islam in Africa and in the dissemination of science, literature and arts’ knowledge too, becoming a reference in

terms of intellectual and spiritual values. The historic centre of Timbuktu entered in 1988 on the *UNESCO World Heritage List*, evidencing the relevance of its monuments (specifically three Mosques, 16 cemeteries and several mausoleums) [25].

Similarly to the Buddha's monuments in Afghanistan, the cause of these temples' destruction is religious conflicts. Destruction was conducted by Islamist fighters and these tragic acts are quite recent, meaning that more developments are possible. Figure 6(a) and Figure 6 (b) show restoration interventions' prior to the incidents of two different Mosques: replacement of beams and gutters and repair of mud plaster to avoid erosion (interventions in accordance with the objectives of Timbuktu Cultural Mission – CMT established in 1993). Figure 6 (c) shows the destructive action against a muslim saint tomb.



Figure 6 – Temples in Mali: (a) Restoration of Sankore mosque [25]; (b) Restoration of Djingareberre mosque [25]; (c) Destruction of a muslim saint tomb (Source: [www.cnn.com](http://www.cnn.com)).

## 2.4 LOSS INDUCED BY TERRORISM

### Case Example 6: *The Twin Towers*

In September 11 of 2011, several attacks planned by the terrorist group Al-Qaeda marked the recent history of the United States. The massive consequences, in terms of loss of human lives and symbolic built heritage destroyed became a deep wound that had to be healed. The destruction of the Twin Towers, see Figure 7, had an enormous social impact and turned the World Trade Center site into a global heritage site [26].

The Freedom Tower as the successor of the Twin Towers has to recover the lost cultural and symbolic values of the site. Its construction represents a full example of integrated engineering. The new steel, glass and reinforcement concrete structure integrates sustainability issues such as renewable energy, daylight use, rainwater reuse, recycled construction materials from the debris [27] and also high life-safety demands. After its

completion, the Freedom Tower will be certainly one of the most important buildings of the 21st century [28].

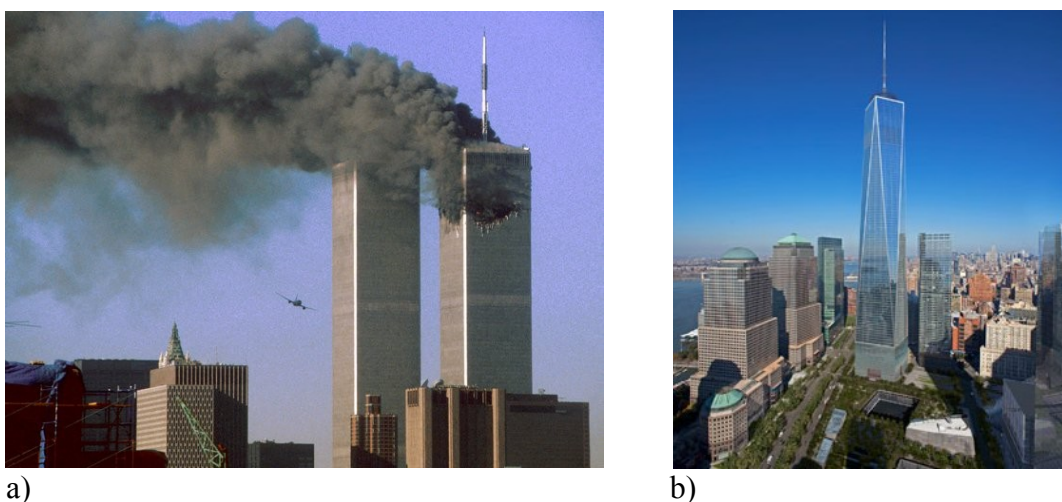


Figure 7 – (a) Terrorist attack upon the Twin towers (Source: <http://cloudfront3.bostinno.com/wpcontent/>); (b) Freedom tower and the memorial - adjacent to tower (Source <http://onewtc.com/>).

Additionally, a memorial centre was constructed in the site. The memorial ideally allows the fusion of the living with the dead as an act of remembrance [29], a retrospective tool which seeks to attenuate the negativity and impotence [30] aroused by the terrorist act.

## 2.5 LOSS INDUCED BY EARTHQUAKES AND FIRE

### Case Example 7: The Earthquake of 1755 in Lisbon

The earthquake of 1755, with an estimated intensity of  $X$  in Mercalli scale, shook Lisbon and had an enormous impact [31]. The earthquake was not itself the main source of devastation but the subsequent fires were. Many people died (estimation of 10.000 people) and the city center was severely damaged [32, 33].

The constructive techniques before the earthquake, in the so-called pre-Pombalino period (reference to Marquis of Pombal, the prime-minister that coordinated the reconstruction of the city) were very diverse, given the large temporal line of construction evolution. In general, constructions were based on stone masonry and with low quality of construction. Thus, it is reasonable to assume that the ruin of most buildings was due to their low capacity to dissipate energy, and to the high inertial forces of these construction types [32, 33].





a) b)  
 Figure 8 – Wall system in Lisbon: (a) Before the earthquake; (b) After the earthquake, where an x-braced internal wooden frame is clear.

The earthquake brought social concerns and a new conscious (also in Europe) of the real hazard of such a natural disaster. The severe social consequences increased the necessity to achieve a fast city reconstruction. The earthquake allowed the city to adapt its buildings to earthquakes, increasing also the health quality by adding new infrastructure systems. In addition, the disaster also triggered the need to reform the Portuguese economy and to reduce its economic dependency from Britain [34].

The reconstruction sought to construct buildings with seismic resistance. Its main feature is the so-called ‘gaiola Pombalina’ (‘Pombaline cage’), a wooden tridimensional frame that can resist to horizontal and vertical loads. The ‘gaiola’ structural behavior depends not only on a good connection between elements but also by the new timber truss framed with cross configuration adopted for the walls, see Figure 8 [35-37].

#### Case Example 8: The fire in Chiado – Lisbon

A discussion of disasters' repercussions in terms of what led to the subsequent works and what is the adequate level of intervention, should also provide a brief description of another dreadful event that occurred in the Portuguese capital: the Chiado fire. Chiado is one of the most famous neighborhoods in Lisbon, with a great number of important commercial establishments, but also theatres and cafés, which made the area a meeting point for the aristocracy, artists, and intellectuals at least until the 1960s. The fire consumed Chiado in August 1988 and brought serious physical consequences.

Seventeen large buildings were destroyed, being most of them from the Pombalino period [38, 39].

The reconstruction plan was headed by the renowned architect Siza Vieira, who wanted to ensure the preservation of the historical and social cultural values of Chiado and also to use the opportunity for an urban revitalization and rehabilitation of the area. The plan decided to maintain the volumetric dimensions of the ancient buildings and their façades, conserving the damaged ones, see Figure 9 [40]. The new buildings (as everything was lost) had to comply with the new standards and, whenever possible, to maintain the *Pombalino* period façades. The new structures were made in reinforced concrete. It is noted that being known that *any damage devalues a building* [3] in terms of cultural and symbolic value, also the rehabilitation of historic urban centers can be a source of economic, social and cultural development [41]. Chiado eventually became a beloved touristic site thanks to its picturesque streets and squares, cultural attractions, cafés and shops.



Figure 9 – Destruction of Chiado buildings by the fire in 1988 (Courtesy of *Lebreiro Henriques*: <http://www.flickr.com/photos/lebreirohenriques/>).

The tragic events that occurred in Lisbon: firstly the widely destructive earthquake of 1755 that led to the city reconstruction, currently called as Pombaline downtown, that allowed to define the beginning of earthquake engineering and that allowed to optimize construction materials, while adapting and integrating new structural systems; secondly, the recent localized fire disaster in Lisbon – Chiado, allowed again to rehabilitate an urban historic centre that had been deteriorating for decades.



## 2.6 LOSS INDUCED BY LONG-TERM GRAVITATIONAL LOADS

### Case Example 9: Civic Tower of Pavia

The Civic tower was located in Pavia, Italy, adjacently to Pavia Cathedral. The tower had been built during the 11<sup>th</sup> and 13<sup>th</sup> centuries and the belfry was added only in the 16<sup>th</sup> century [42]. The tower walls' were made by two thin external brick leaves and by an internal core made from random layers of broken bricks and stones in a matrix of mortar, i.e. a sort of concrete with coarse aggregates. The belfry was made by a regular masonry wall, see Figure 10(a).

The Civic Tower of Pavia suffered a sudden collapse on 17<sup>th</sup> March, 1989. The collapse was unexpected and beyond the physical consequences (severe damage to nearby buildings), four people died, see Figure 10(b) [42]. The study of its sudden collapse attracted many experts, which sought to explain the reasons for failure. The conclusion was that damage was mostly related to stress redistribution phenomena. The non-uniform stresses caused by masonry creep, shrinkage and carbonation associated to factors such as fatigue, due to wind and thermal actions, increased the compressive stress of the external walls due to redistribution. This failure mechanism is associated to tall structures or elements - as bell towers, columns, pillars and so on [42-44]. Thereby, the Civic Tower of Pavia sudden collapse was not an isolated accident, as corroborated by other similar examples: (i) St. Marco's bell tower at Venice (Italy) in 1902; (ii) the St. Martinus Church at Kerksken (Belgium) in 1990 (5) the St. Magdalena Church at Göch (Germany) in 1992 [5]. Despite the cultural importance of the Civic tower, as a symbol that integrated once the built heritage of Pavia city, it was not rebuilt, mostly due to the high cost involved and the impossibility to raise the necessary public and private funds, see Figure 10(c).

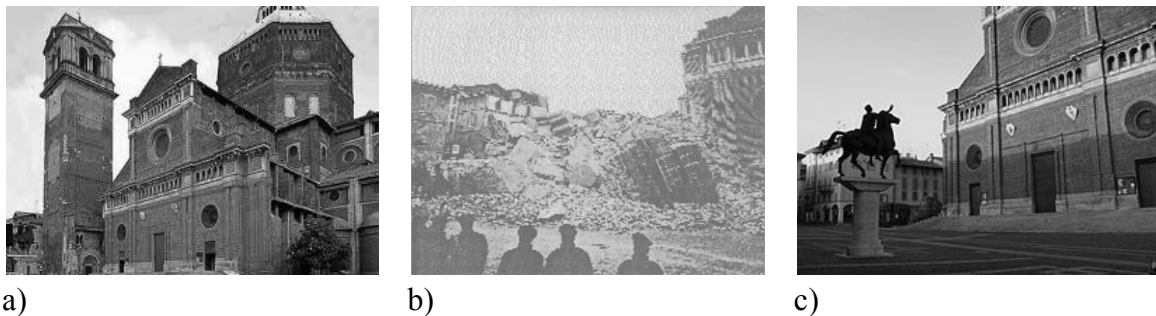


Figure 10 – The Cathedral of Pavia: (a) before the collapse of the civic tower in 1989 (Source: [http://www.4thfirst.com/interesting\\_sites.html](http://www.4thfirst.com/interesting_sites.html)); (b) After the collapse - ruins of the Civic Tower [43]; (c) At present (Source: Wikipedia).

This collapse allowed highlighting the importance of guaranteeing the structural stability of old buildings, particularly taking into consideration masonry long-term behavior.

## 2.7 CONCLUSIONS

As presented above, several sources of built heritage loss were considered. The described examples suffered a sudden collapse associated with war conflicts and terrorism – human origin, and earthquake, fire and long-term effects due to high permanent load (creep) – natural origin, see Table I.

Table I – Case studies presented, cause for loss and intervention decision.

Example Cases	Cause for loss	Intervention
Mostar bridge		
Our Lady Church in Dresden	War	Reconstruction <sup>(1)</sup>
Historic centre of Warsaw		
Bamian Buddha's Temples of Mali	War with religious contents	None, so far
Twin Towers	Terrorism	Rebuilt <sup>(2)</sup>
City of Lisbon in 1755	Earthquake	City rebuilt <sup>(2)</sup>
Chiado in 1989	Fire	Reconstruction <sup>(3)</sup>
Civic Tower of Pavia	Creep / Long-term effect of permanent loads	None

<sup>(1)</sup> Reconstruction of the ancient buildings

<sup>(2)</sup> The rebuilt of the city/building altered the built heritage aesthetics'

<sup>(3)</sup> Reconstruction maintained, when possible, the ancient buildings façades

Some conclusions about the case studies of cultural built heritage presented must be made. For this purpose, some questions have to be answered, such as the followings ones: (1) what to do in cases of cultural heritage buildings sudden destruction? The decision depends on which factors? (2) Is the decision influenced somehow by the cause that determined the built heritage loss? (3) If restoration/reconstruction is made, what criteria should be adopted in the process? (4) Which is the importance of the case studies in the *savoir fare* of restoration and reconstruction processes?

With respect to the first question, the difficulty is not associated to the possible choices, but what led to decide upon one of them. Citing Giorgio Croci, “a cultural intervention is required due to the historical building value” [9] so, it is possible to say that rebuilt

should be the decision, but it is also possible to say that the historical value does not lie only in the form and no post-disaster measure can reinstate the lost cultural heritage. The decision depends generally on some factors, as if it is possible to restore (i.e. if exist reliable information that guarantees the possibility of a restoration work), the economic aspects (i.e. if the necessary funds to execute the works are available and if the sustainability in the future of the building is guaranteed), the relative cultural importance of the building to the society.

The previous case studies allow corroborating the diversity of approaches. For instance, no intervention has made yet to the Bamian Buddha's and Timbuktu Temples, differently from Mostar Bridge, Lady of Our Church in Dresden and to the historic centre of Warsaw, which have been already reconstructed. Even if the cause of sudden destruction is the same in all cases, there are obviously differences between them which could have determined the final decision. The response is also conditioned by the spatial integration of the specific cultural heritage building or monument, by its relative importance to the community and to the different stakeholders. Even if international concerns and commitments seek for an intervention it is imperative to consolidate the meaning of culture significance in a local or regional scale. The importance of social pressure is well explicit in the example of Our Lady Church and historic centre of Warsaw. Additionally, in the Bamian Buddha's case, the lack of reliable information regarding parts of the small Buddha prior to its destruction, could preclude the restoration (as referred above, the reconstruction of the large Buddha is not an option). Thus, the technical criterion related to the possibility or not of reconstruction is also very important.

With respect to the second question, it seems that when the cause of loss is associated to war, the decision has been in some cases to proceed to a reconstruction. When the loss is associated to religious issues too, the option is often not to proceed to any intervention, even if technical, spatial, social and economic factors also play a role. When the cause of loss is a natural one (such as fire, earthquake and creep) with major losses, it seems that a real concern is to provide the new buildings with structural and technical features that guarantee their safety, comfort and modern use. In this context, is also possible to refer the case of the Twin Towers. The cause of loss is due to terrorism, a manmade disaster, but the decision made had a similar logic ad rebuilding from a

perspective of cultural heritage safeguard, while taking into account higher standards in buildings design.

With respect to the third question and specifically to the examples that suffered an intervention, a reconstruction work embraces the past, present and future [12] of a given cultural heritage building or monument and therefore, the intervention stages and decision should be taken *after a careful diagnosis and evaluation of the safety of the structure in its present state*, according to Giorgio Croci, also set on the ICOMOS principles [9]. Bearing in mind for instance the Mostar Bridge and the Our Lady Church examples, it is clear that an intervention would have to take into consideration its history and future, so the reconstruction measures and their social and cultural implications require a scientific methodology.

The intervention process was meticulously analyzed. In the Mostar Bridge, since the initial phase, an historical and structural analysis was made, followed by a diagnosis of the bridge and a structural study due to the new standards and lastly to the assurance that quality of the material and proper crafts work were used in the works, as detailed in [15], where aesthetic and structural behavior are permanent issues. The same occurred in the reconstruction of Our Lady Church in Dresden. It belongs to the vast set of cultural heritage buildings that were destroyed in Second World War and, curiously remained ruined for a considerable period of time, 40 years of indecision, due to social and political aspects. In this case, considered one of the major reconstruction projects ever made, all of the steps and decision implications were previously thought before any real intervention.

This attitude of careful intervention goes in favor with the real goal of restoration, i.e. alter as minimum as possible the original architectural heritage. In fact, an intervention based on scientific knowledge is less exposed to risk which according to Giorgio Croci could be associated to (i) a misconception of the building which leads to wrong interpretation of uncertainties in the information and consequently to lower safety levels than the required ones, and (ii) delays related to lack of information or need of additional detailed studies [12]. In this context, in order to minimize misunderstandings and avoid lack of information that is necessary to the intervention decision the scientific methodology should be flexible: it is an iterative process and includes several studies, as a historical one, inspections, monitoring actions and structural analysis [4]. An

analysis that integrates the modern technologies, materials and methods in the study of historic constructions is recommended. However, subjectivity and uncertainties are inevitable in the analysis due to economic and technical limitations in the information collected and to the impossibility to represent exactly the real structure [34]. The practicability of the scientific approach and its was proven in the cases studied where sudden destruction occurs – for example in the Mostar Bridge, Our Lady Church in Dresden and Freedom Tower (Twin Towers case).

Finally, brief commentaries will be made related to the potential impact of the studied cases in future restorations or reconstructions due to sudden collapse. As seen before, there is an impossibility to give a generic answer to what to do in cases of sudden collapse of built heritage, as each case has its own characteristics. However, that does not invalidate the fact that the studied cases could be good sources of knowledge to help a decision in similar situations in the future. Additionally, all case studied allow highlighting the importance of preserving the cultural heritage and provided useful lessons. The events in Lisbon – earthquake and Chiado’s fire, even if tragic led to improvements of buildings in order to assure their survival and to minimize repair in future similar events; the Civic tower of Pavia, even if no intervention has been done was critical to the stability works of strengthening of other ancient towers, and masonry structures subjected to large sustained loading. Furthermore, cases as the historic centre of Warsaw and Our Lady Church in Dresden had a great contribution to disseminate the importance of urbanization and cultural heritage buildings conservation.



# Chapter 3

## Christchurch Catholic Basilica

### 3.1 BRIEF HISTORICAL OVERVIEW: NEW ZEALAND (NZ)

New Zealand or *Aotearoa* (*Maori* term) was one of the last major landmasses settled by humans. The first settlers of the archipelago – separated from Gondwana’s continent 80 million years ago, were ancestors of the indigenous people, the Maori, denominated as Polynesians. The Maori people arrived from Polynesia in the thirteenth century [45]. The arrival of the first Europeans occurred in the seventeen century, by the Dutch explorer Abel Tasman in 1642 [45]. Despite this visit, the next Europeans’ visit was made by the well famous British explorer James Cook at 1769, Figure 11.



a)



b)

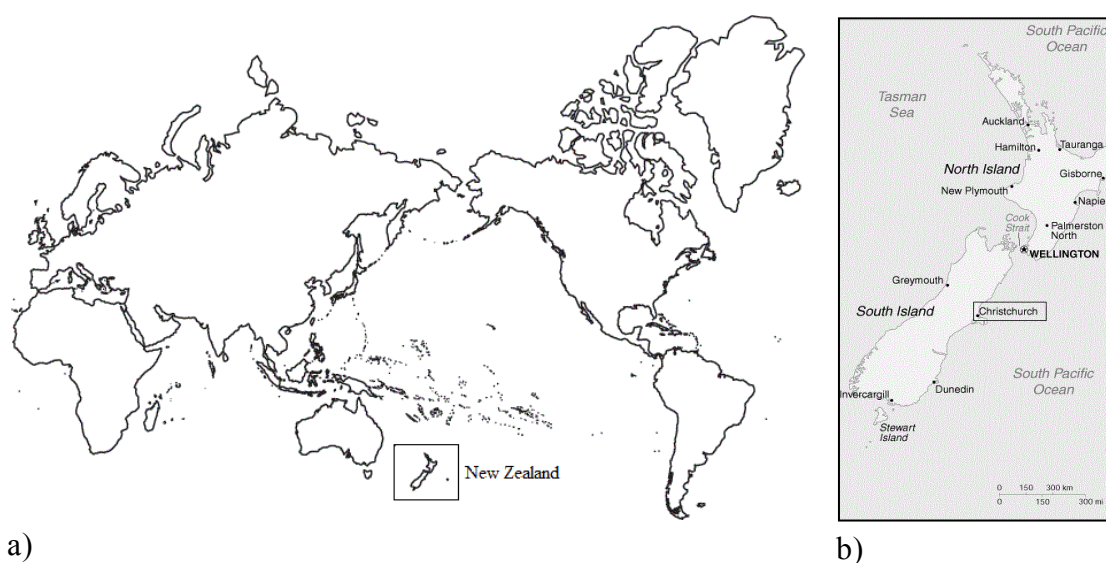
Figure 11 – (a) Captain James Cook [46]; (b) Captains Cook’s ship – ‘Endeavour’[47].

James Cook, considered as a worldwide skilful explorer, mapped almost the entire coast of New Zealand Islands. After James Cook voyages, a total of three, many others examples of arrivals are registered by numerous Europeans and North American sailors, whalers and trading ships – seeking for trading food, metal tools, weapons, artifacts and other resources. At the same time that more settlers arrived, the British Government sent Captain William Hobson to sovereignty New Zealand to Britain’s Queen Victoria and to sign a treaty with Maori people: The Treaty of Waitangi, on 6 February of 1840 [48]. Europeans with planned settlements arrived with a considerable scale in 1840,

after the Treaty. After 1890, NZ suffered social and cultural reforms. It is important to mention that it was the first country in the world that granted the right to vote to all women and that adopted compulsory arbitration between employers and unions [49]. In the 20<sup>th</sup> century New Zealand fought in the two of the World wars alongside the British Empire which causes a great depression in its economy. Although, the economy depress allowed NZ to adopt welfare measures: elected in 1935 the Labor government introduced policies to strength the economy, mitigate the economy vulnerabilities to external events and increased the social security of New Zealanders [50]. Nowadays, New Zealand is identified as one of the world’s most stable and less vulnerable nations, ranked as 7th according to Failed States index of 2012 [51]. In 2011 the country was ranked as the one with more transparency and less corruption at its public sector by the Transparency International Organization [52]. Additionally, New Zealand has in accordance with OECD (Organization for Economic Cooperation and Development) information, a high level of civic participation and political institutions confidence [53].

### 3.2 LOCATION

The Cathedral of the Blessed Sacrament, also known as Christchurch catholic Basilica [54], is located in New Zealand, Figure 12, specifically in Christchurch at Barbadoes Street. Christchurch is the second large city of New Zealand and has a population of 348,000 people (Source: Statistic New Zealand - according to the census date – held on March 5 2013).



a)

b)

Figure 12 – (a) New Zealand in the World Atlas; (b) location of Christchurch city – New Zealand South islands. (Source: wordatlas.com)



New Zealand is an island country in the southwest Pacific Ocean. It is located in an area called as the ‘Pacific Ring of Fire’. This area which encircles the Pacific Ocean is very unstable and the earthquakes are triggered by the set of 450 active volcanoes [WordAtlas], oceanic trenches and plate movements. These reasons are highlighted with statistical information, which indicates that the ‘Ring of fire’ contains 90% of the world’s earthquakes [USGS – U.S. Geological Survey].

NZ has an estimated number of 14,000 earthquakes each year, being its majority small enough not to be felt by the population. Information released by GeoNet allows compiling the occurred events since 1960 to 2011. Figure 13 demonstrates that most earthquakes have a magnitude of 4.0-4.9, as lower magnitudes were ignored. Additionally, is also important to observe the existence of a single event identified with a magnitude scale of 7.0-7.9, the one felt at Christchurch, on September 4 of 2010, which is the most damaging earthquake in NZ since Hawke’s Bay earthquake in 1931 [55].

These destructive natural phenomena could be explained mainly due to the relative movement between two lithosphere plates. New Zealand is simultaneously located between two distinct tectonic plates, the Pacific and the Indo-Australian ones, illustrated in Figure 14(a). It is possible to see two different types of subduction zones: one along all of the continental territory of South Island and another in the Oceanic crust, near to North Island.

The main difference between them is which plate dives into another, i.e. the Indo-Australian plate in the South Island and the Pacific plate in the North Island. Despite of the information in Figure 14(b), with the maximum shear stress located in a western region of Christchurch, the earthquake that took place on February 22th of 2011 allowed scientists to develop a new theory about the seismologic information of New Zealand and particularly to the Canterbury region.

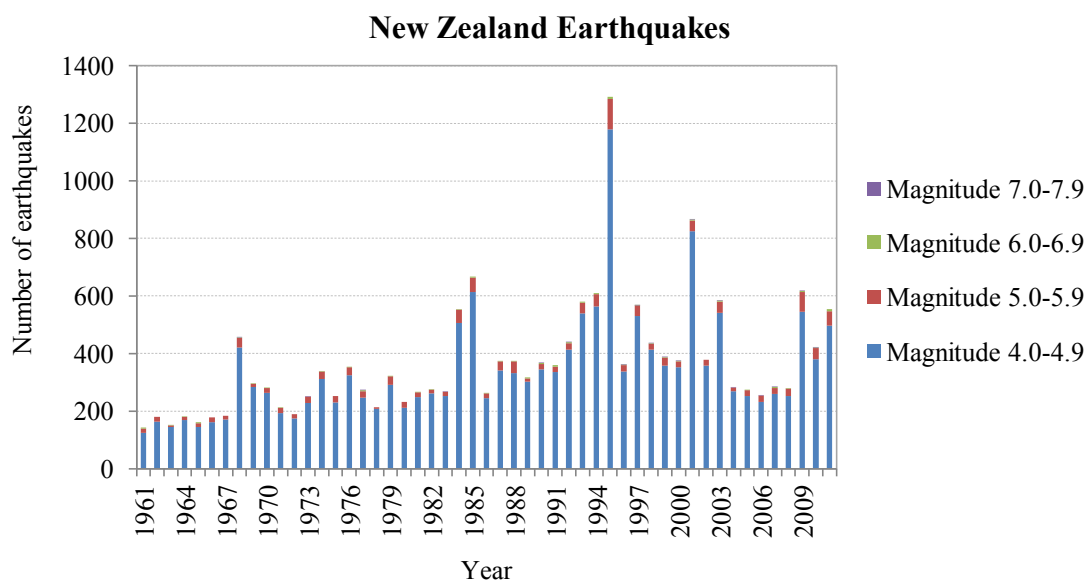


Figure 13 – Number of Earthquakes (in  $M_w$  – Moment magnitude scale) in the New Zealand Region (1960 to 2011) - (GeoNet data results).

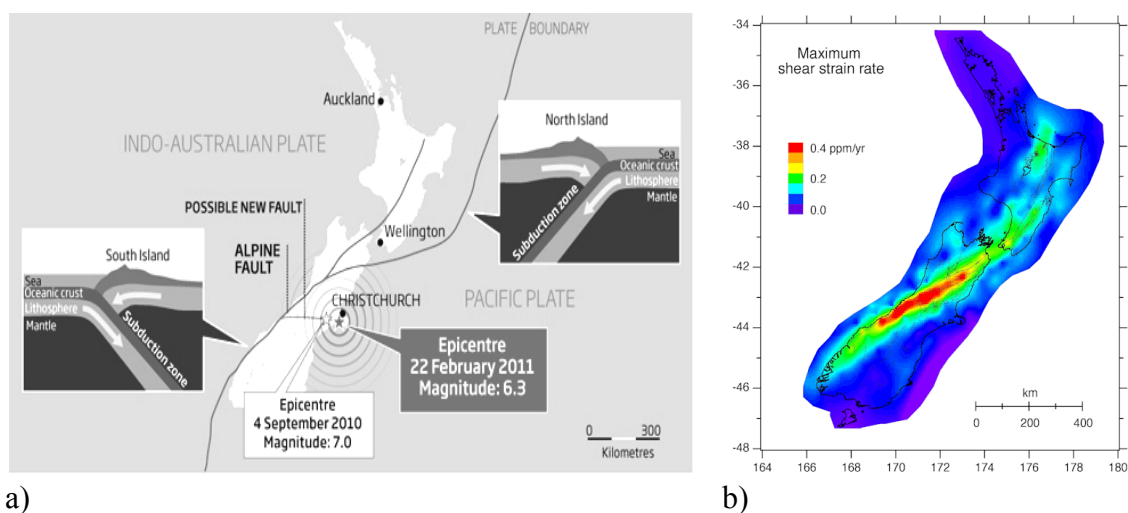


Figure 14 – (a) Identification of the existent plat boundary and the possible new fault of New Zealand South Island (Source: www.newscientist.com); (b) Maximum shear strain rate of New Zealand (Source: GNS Science).

The destructive event was caused by plates movement along a fault which does not appear to have broken the surface, in contrast to September 4<sup>th</sup> earthquake where was possible to measure the movement length of the longest fault segment. According to that and based on GPS data stations, satellite radar images, seismographs and strong-motion recorders, scientists conclude that a possible new and hidden fault was the origin [GNS Science].

On the other hand, the data record of earthquakes at Canterbury region between the time period of September 4 2010 and September 3 2012 indicates a very strong signal of a

strong seismic activity. According to Figure 15 and taking into account the seismic activity of Christchurch, it is possible to associate the earthquake of a magnitude higher than 7 as the one who occurred at September 4 of 2010 (real magnitude was 7.1) and the three earthquakes with magnitude of 6.0-6.9 as the ones who occurred at February 22 of 2011 (real magnitude was 6.3) and June 13 of 2011 (two large aftershocks at the same day with a real magnitude of 5.7 and 6.3, respectively).

**Number of Earthquakes at Canterbury region from September 4 2010 to September 3 2012**

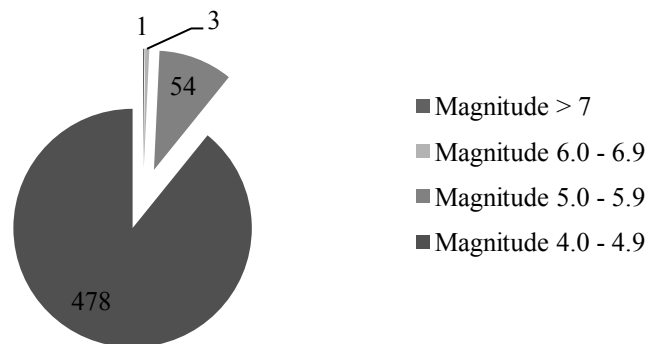


Figure 15 – Number of earthquakes at Canterbury region from September 4 of 2010 to September 3 of 2012 (GeoNet data results).

In fact, the seismic hazard in Canterbury Region is currently the highest one in the New Zealand Regions (total of 16). Moreover, the referred two earthquakes and two aftershocks are, as known, the main single events that damaged, in a huge scale, the Christchurch Catholic Basilica, bringing inevitable implications, not only to the particular case study and a two face problem (repair *versus* demolishing), but also implications related to the seismic design of all Christchurch buildings.

### 3.3 BUILDING DESCRIPTION

The Cathedral of the Blessed Sacrament, Figure 16, was designed by Architect Francis William Petre. The Cathedral is based on Roman style but features a neo-classical style. For its representative capacity to demonstrate heritage values and being an example of pleasant architecture appearance too, it is listed as category I heritage in New Zealand – ‘International or National significance’ [6].

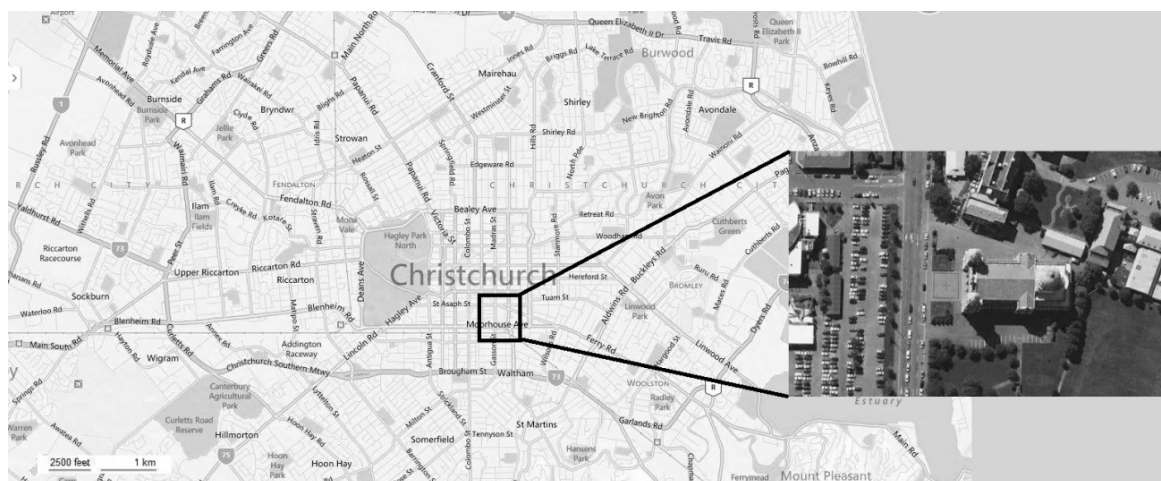


Figure 16 – Map location of Barbadoes street– Cathedral of Blessed Sacramento top view.

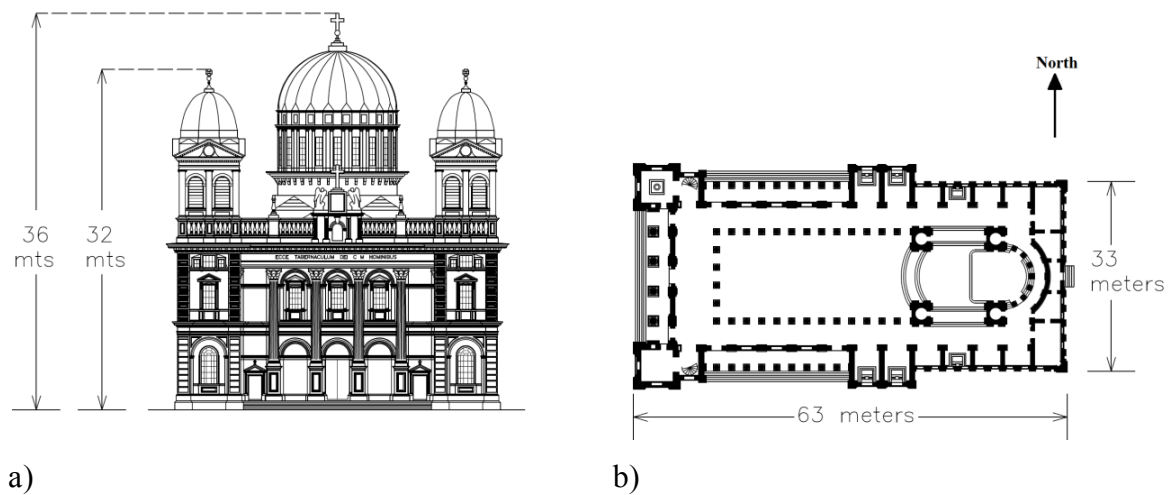
The Cathedral of the Blessed Sacramento, see Figure 17, was built in a time period of four years, between 1901 and 1905. The Cathedral was built in Oamaru limestone and has the typical arrangement of old Roman basilicas, i.e. a nave, a transept, chapels, apse, a dome and bell towers. As usual, the apse has an eastern orientation.



a) b)  
Figure 17 – Cathedral of the Blessed Sacramento: (a) North and West façades; (b) South façade.

According to a very common practice of the 19<sup>th</sup> and early 20<sup>th</sup> centuries, the construction technique adopted was unreinforced masonry (URM). The structural walls are made with two-leaf stone masonry, externally, and a concrete core in the middle. The stones are linked through grout-filled cavities and have generally 500 mm of thickness. The internal and external claddings have 125 mm thickness of limestone [7]. The domes are cooper lined and the main one is supported on four large arches, made from no-fines concrete, that spring from the first floor level. The arches are supported by large columns with an internal spiral [7]. With respect to the main dome, Architect

Francis Petre, considered it places above the sanctuary instead of the usual form, at the crossing of transepts and nave [54, 56].



a) b)  
Figure 18 –Basilica of the Blessed Sacramento geometry (a) West elevation; (b) Top plan.



a) b)  
Figure 19 – West façade (left) and East façade (right) – the grey lines are elements in the background.

The nave contains colonnades with diverse capitals and spacious arcades. Additionally, the Basilica has large stained glass windows, an uncommon feature on other Catholic churches in New Zealand [57]. The Basilica has, in plan, a length of 63 meters (North and South façades) and a width of 33 meters (West and East façades). The highest element of the church is the dome with 36 meters followed by the two bell towers with 32 meters, see Figures 18-21 [58].

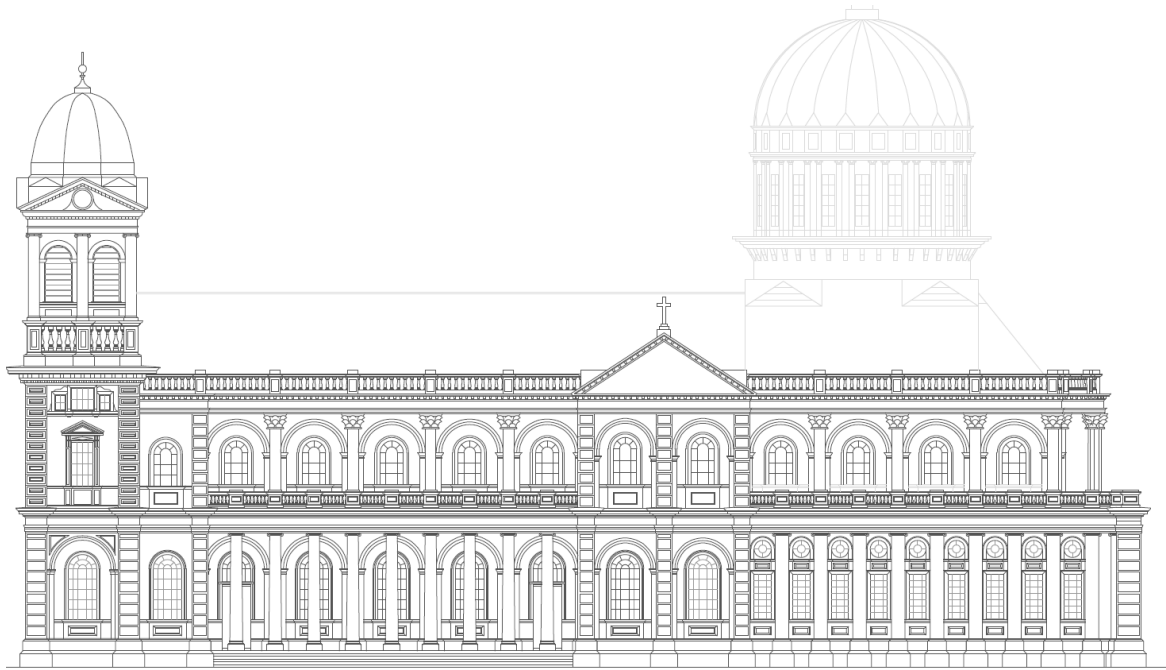


Figure 20 – South Elevation – the grey lines are elements in the background.

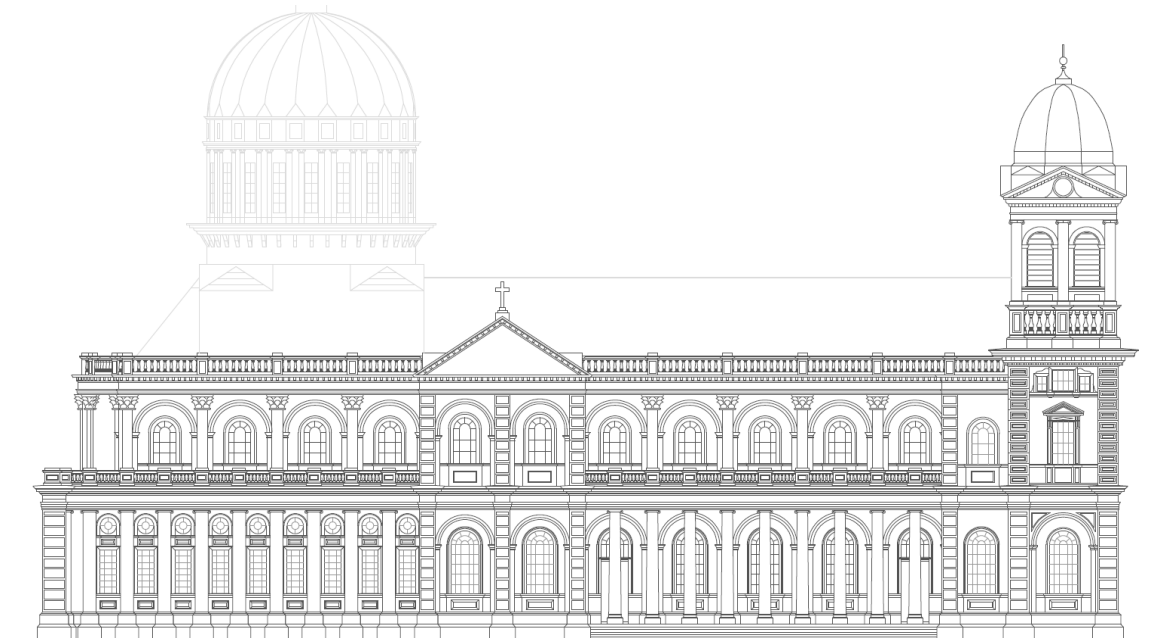


Figure 21 – North Elevation - the grey lines are elements in the background.

Traditional URM has proven to be a poor construction technique in terms of earthquakes resistance, mainly due to the low lateral forces' resistance and lack of capacity to dissipate energy [7]. In order to assure a satisfying behavior of the Basilica in seismic situations, a structural study was realized at 2002, adopting basic preliminary calculations and engineering practical knowledge for the conclusion [7]. In this report, the Basilica was considered unsafe in terms of earthquake behavior. Structural

strengthening was required and allowed to reach 45% of the design standard requirements (at the time the normative standard was NZS 4203<sup>1</sup>, 1992). After the strengthening the safety of the building was assumed to be adequate.

The strengthening process, see Figure 22, introduced: (i) a new reinforced concrete slab (RC) with 100 mm of thickness in the first floor and roof level, aiming a diaphragm action; (ii) a steel brace with 32 mm of thickness and RC ring-beams with a section 200 x 600 mm<sup>2</sup> in the front of the two bell towers, above and below the window openings; (iii) RC ring beams with a section of 200 x 600 mm<sup>2</sup> in the top section of the main dome, above and below the windows; (iv) post-tensioning in alternating columns of the nave colonnade and grouting of external parapets and ornaments; (v) fixing of the gable ends of the roof, the transepts and ornaments [7].

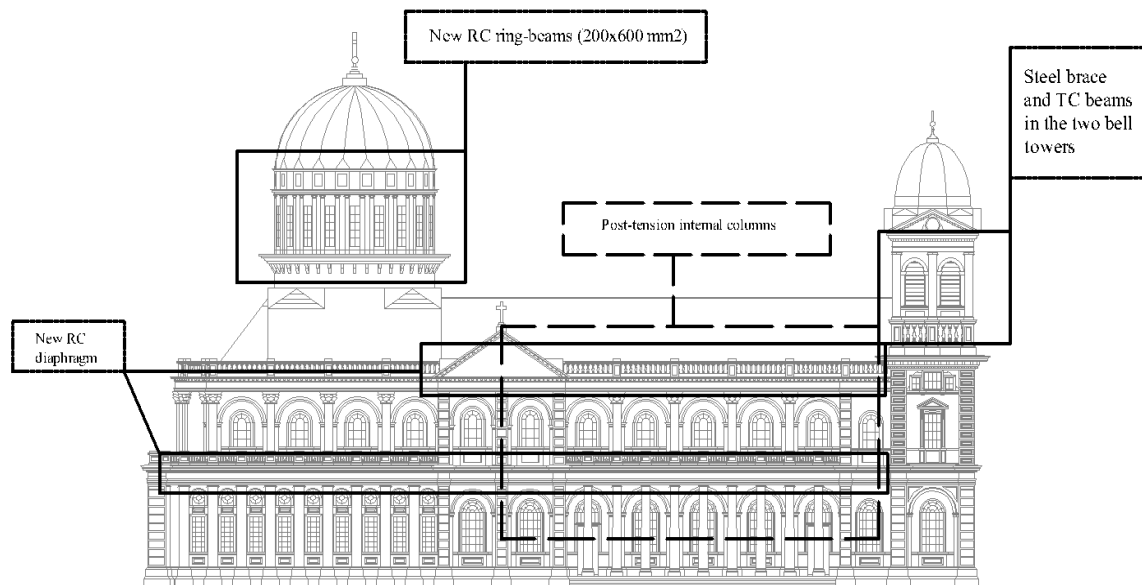


Figure 22 – Introduced elements in the 2004 strengthening of the Basilica of the Blessed Sacramento [3].

The strengthening operation aimed to increase the building capacity in a seismic situation. The solution adopted derived mainly from practical knowledge and tried to address the weakest elements of the buildings. This decision allowed to adjust the building response to the required standard values of lateral load capacity, resisting to the legal minimum of 0.05g ( $g$  is the gravitational acceleration) and 20% of the code value, i.e. 0.1g ( $g$  is the gravitational acceleration) (DBH, 1991) [7].

<sup>1</sup> NZS 4203:1992 was replaced in December 1<sup>st</sup>, 2008, by the AS/NZS and NZS 1170 series.

### 3.4 SEQUENCE OF EARTHQUAKES DAMAGE

In order to describe the damage which affected the Christchurch Catholic Basilica, the different events and corresponding dates will be presented below, so that damage to each particular event can be discriminated. Additionally, before each single condition overview, a short informative commentary is made about the behavior of unreinforced masonry buildings (URMB) in general, which will possibly bring a better understanding of the damage scale.

#### 3.4.1 EARTHQUAKE OF SEPTEMBER 4, 2010

The first earthquake occurred in the early morning of 4<sup>th</sup> September (4:35 am), with a magnitude of M7.1. The epicenter was located near Darfield town, a region of Canterbury located 40 km west of Christchurch [55, 59], see Table II.

Table II – Information about the Earthquake of September 4, 2010 (GeoNet, 29-10-2012).

Location	Focal depth (km)	Maximum Intensity (MM)	Magnitude (M <sub>L</sub> )	MSA* (m/s <sup>2</sup> )	Casualties
Darfield	11	9 (Severe)	7.1	0,85g	1 death

\*MSA – Maximum Spectral Acceleration.

The structural consequences due to the earthquake were, in general, minor in retrofitted URM buildings. The damage observed could be explained by insufficient lateral support [60]. Some damages were reported in the churches in the Christchurch area. In some cases, different damage scales to high proximity building were identified due to distinct architectural styles, structural systems and to the characteristics of local ground excitations – *site effects* [61]. Examples include [62]: (i) the Christchurch Chinese Methodist Church (URMB) was classified as unsafe to access, due to out of plane gable failure; (ii) the St Paul’s Catholic Church in Dallington (concrete portal frames and masonry infill walls) was determined as unsafe and ordered to be demolished, due to liquefaction and ground deformation in the church’s surrounding area; (iii) the Knox Presbyterian Church in central Christchurch (URMB) was to be restored.

The earthquake of September 4 of 2010 caused moderate damage to Christchurch Catholic Basilica [63]. The affected elements were the walls, with minor cracking and displacement of stones in West wall of the sacristy and evidence of an out-of-plane movement of the middle column of the North bell tower eastern elevation. Despite that,



cracks were also visible in retrofitted portions as the underside of the first floor diaphragm all around the nave and the main dome, with shear cracks at construction joints [58, 62]. After the visual assessment, the building was tagged with a red placard, which prohibits its usage [64].

### 3.4.2 EARTHQUAKE OF FEBRUARY 22, 2011

The earthquake of February 22 of 2011, felt at 12:51 p.m. was, quantitatively, less severe than the September 4 (2010) earthquake, with a magnitude of 6.3 instead of 7.1 ( $M_L$ ), see Table III. However, qualitatively, the 2011 earthquake caused more damage in Christchurch, possibly due to the vulnerability of many buildings, after the damage induced by the first earthquake. The higher damage can also be related, according to [65], to the proximity of the site, to the shallowness of the rupture and to the weak underlying soils. Another author [66] refers additionally: (i) the particular mode of rupture, associated to a near fault directive effect [67]; (ii) the amplification factor due to the transition of stiff rock to soil; (iii) the trampoline effect, defined by near surface material separation caused by high downward accelerations; and (iv) a hanging wall effect in the acceleration.

Table III – Information about the Earthquake of February 22, 2011 (GeoNet, 29-10-2012).

<b>Location</b>	<b>Focal depth (km)</b>	<b>Maximum Intensity (MM)</b>	<b>Magnitude (ML)</b>	<b>MSA* (m/s<sup>2</sup>)</b>	<b>Casualties</b>
Lyttelton	5	9 (Severe)	6.3	1,41g	185 deaths*

\*MSA – Maximum Spectral Acceleration.

\*\* A total of 185 people died and 4,400 were injured [68].

Taking into account the above mentioned points, even having a smaller magnitude, the earthquake of February 22<sup>th</sup> introduced to buildings substantially higher PGA's (peak ground acceleration) values [69]. In [59], different numbers corroborate the destructive nature of this event. The authors analyzed 112 churches, separated by different groups in accordance to its construction type and concluded about the relative fraction of churches, of each construction type, classified with green, yellow or red placards (Green placard – safe to re-enter; Yellow placard – restricted access; Red placard – unsafe), see Table IV. The damage was rather high and it is possible to highlight the value of 45% of tagged churches with a red placard and the value of 40% of tagged churches with a yellow placard. This acquires particular relevance if associated to the case study of the Christchurch Catholic Basilica.

Table IV – Damage and church typology [59].

Construction type	Clay brick masonry churches	Stone masonry churches	Timber framed churches
Green Placard	19 %	16 %	94 %
Yellow Placard	43 %	32 %	4 %
Red Placard	38 %	52 %	2 %

The main damage induced by the February 22, 2011 earthquake in the Basilica are described below [58, 64, 69], see also Figures 23-35.

- i. North and South tower belfries collapsed. Failure occurred in a north-west and south-west direction, respectively. Additionally to the top section complete collapse, the entire west wall of the south tower felt down.



Figure 23 – West façade of the Christchurch Catholic Basilica and the damage in the two bell towers, North (left) and South (right).



Figure 24 – Detail of the West wall collapse of the South bell tower.

- ii. Similarity to the North and South Elevation, a severe shear cracking behind the bell towers is visible. Spalling of the ground piers (due to in-plane rocking) and large displacements and cracking around the windows and doors also occurred. Additionally to the South elevation the collapse of the architrave on the both extremities is also reported.
- iii. Cracking of the outward wall of the North and South transepts. The North wall has a shear crack around one window on the ground level, which is non-significant comparatively to the South one. Shear cracks are identified in the South wall not only around the windows but also in the transept-main nave connection.



Figure 25 – South transept facade.



Figure 26 – Detail of shear cracking around South transept window and local collapse of the architrave.

- iv. Significant damage to the main dome drum occurs, with a permanent lateral displacement of approximately 75 mm and a vertical settlement of 100-200 mm, together with collapse of the supporting north arch and severe damage to the south arch.



Figure 27 – Large diagonal crack in the entablature near to the north transept.



Figure 28 – Shear cracks in the transept-main nave connection.



Figure 29 – Lateral displacements of the main dome drum or rotunda.





Figure 30 – Collapse occurred in the north arch of the sanctuary.

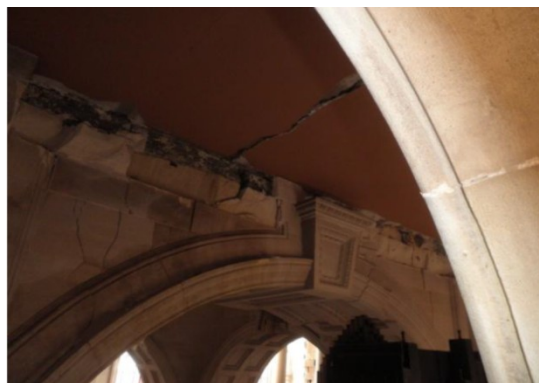


Figure 31 – Severe damage to the south arch spandrel.

- v. For the two levels that integrate the sanctuary, below the Dome and Rotunda, some concrete flat roof areas of the upper level (retrofitted in 2004), collapsed and present large shear cracks located around windows of the North, South, West and East arcade elevations. The ground level has minor damages.

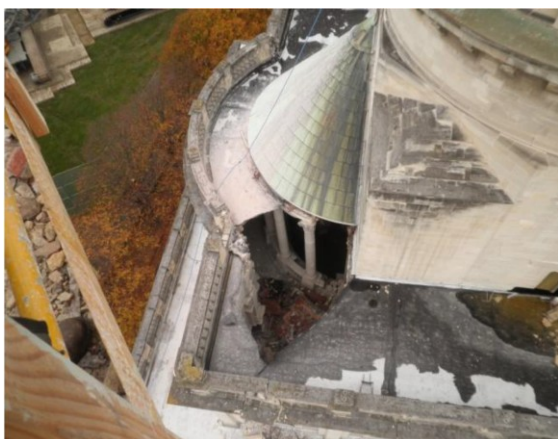


Figure 32 – Collapse of a part of the RC sanctuary flat.



Figure 33 – Damage to the South supporting wall of rotunda.

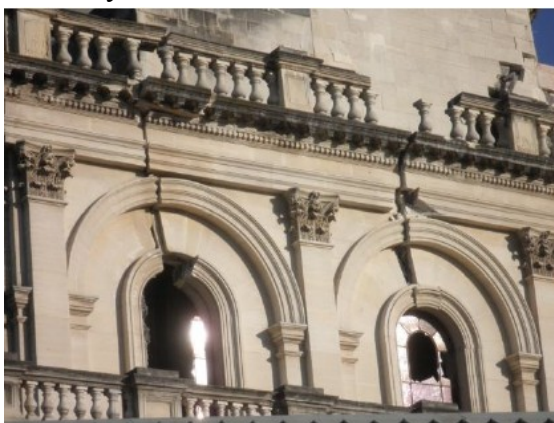


Figure 34 – Shear cracks around the upper arcade of the North elevation.

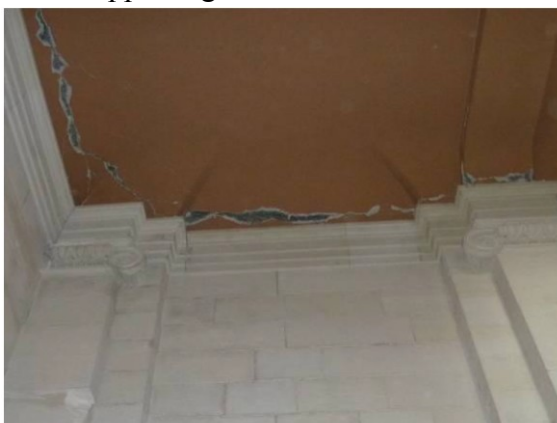


Figure 35 – Diaphragm damage at the first floor (its exact position is unknown).

### 3.4.3 AFTERSHOCKS OF JUNE 13, 2011

Aftershocks that occurred on June 13 of 2011, felt at 01:01 pm and 02:20 pm, see Table V, induced further damage to buildings, already vulnerable after the main earthquakes of September 2010 and February 2011 [59].

Table V – Information about the aftershock of June 13, 2011 (GeoNet, 30-10-2012).

Location	Focal depth (km)	Maximum Intensity (MM)	Magnitude (M <sub>L</sub> )	Casualties
10 km East of Christchurch (near Sumner)	9	>7 (Severe)	5.9	-
10 km East of Christchurch (near Sumner)	7	>7 (Severe)	6.3	-

In the case of the Christchurch Catholic Basilica, the two aftershocks had several repercussions. Besides of damage being aggravated, these events led to the necessity of changing the prior strategies to the main dome removal [69].

The main structural consequences of the aftershocks are described (see figures 36 to 43) now as:

- (i) A fraction of the North Rotunda Wall, parts of the adjacent reinforced concrete flat roof and the north interior arch, already with severe damaged, collapsed;
- (ii) The East and West arches suffered significant damage around the keystone;

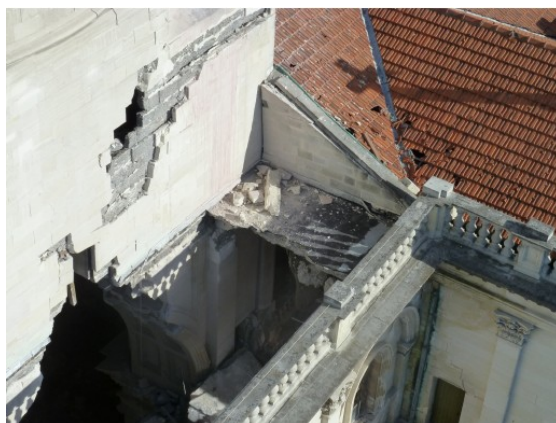


Figure 36 – Collapse of a fraction of North rotunda wall, part of the adjacent RC flat roof and North interior arch.



Figure 37 – Damages to the key stone of the East arch.



- (iii) The South transept façade suffered additional damage, exhibiting cracking and developing a diagonal block failure. A 25mm crack across the transept roof level is now present.



Figure 38 – Damage along the West arch.



Figure 39 – South arch severe damage.



Figure 40 – Visible damage to the main dome drum (after the removal of the internal dome in 25 August, 2011).



Figure 41 – Developing of a diagonal block failure in the South transept façade.



Figure 42 – Crushing of the top South-West column.

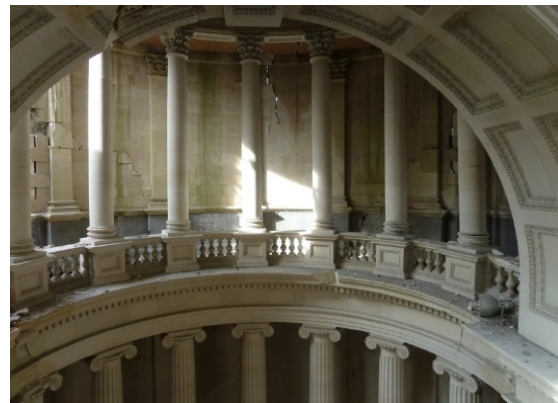


Figure 43 – Vertical crack in the East wall of the first floor.

- (iv) Failure of the first level floor around the main dome, due to rocking of the support structure. Thus, most of the first floor walls are top unrestrained.

### 3.5 THE DICHOTOMY: DEMOLISH OR DECONSTRUCTION?

The seismic activity felt in Christchurch in 2010 and 2011 brought considerable damage to several buildings. Despite the tragic consequences of the earthquakes sequence, it is important to stress the important role in developing and improving guidelines of rapid damage evaluation of the New Zealand Society of Earthquake Engineering [67] and the initial assessment provided by the Christchurch Emergency Response Task Force. But the high seismic exposure of New Zealand led to vulnerability studies, to seismic design reports and to the development of emergency plans and response actions. According to that, it is possible to name ‘The Resource Management Act – 1991’ [70], ‘The Building Act 1994’ [71], ‘The Civil Defense Emergency Management Act – 2002’ [72] and the models of *Smith and Berryman* (1986) [73] and *Stirling et al.* (2002) [74]. The latter was fundamental for the design spectra of New Zealand Standard NZS 1170.5:2004 (New Zealand Standards).

The cited legislation has inconsistencies, particularly with respect to the definition of natural hazards. As an example the ‘Building Act 1994’ does not take into account seismic and wind hazard and the implications of incorporating new information, such as the Canterbury seismic activity, that the National Seismic Hazard Model (NSHM) considered [75]. Despite the inconsistencies and bearing in mind that a ‘*new policy and regulatory framework*’ [76] is necessary to adequately reduce New Zealand’s exposure to natural hazards, the particular group of Heritage Buildings is specifically described.

Knowing that responsibilities to manage natural hazards requirements are attributed to the local governments, as referred in ‘The local Governmental Act 2002’ [72], and also the fact that local authorities have a ‘*primary role for historic and cultural heritage*’ [77], it is important to address the role of the Heritage Conservation Policy of Christchurch and the acts of the different stakeholders.

Apart from that, and citing the principles of New Zealand Committee of ICOMOS, there is a ‘*need to retain the historic integrity of heritage places by doing as much as necessary to preserve them*’ [2]. The last aim shows the inevitable concerning regarding buildings with cultural and historical values, and the difficulties of a final decision on the plan to be followed. In the case of the Christchurch Catholic Basilica, the difficulty to carry out a debate is related with two key points: total demolition or partial deconstruction. It is noted that reconstruction is guaranteed by the responsible entities.

The demolition-reconstruction versus partial deconstruction-reconstruction dichotomy must be solved and will define the Basilica's future. Before exploring the theme, the general meaning of these concepts are presented:

1. Demolition could refer to the act of 'pull' or 'throw down' an existing building [78]. Subsequently it is possible to construct, or not, a new building.
2. Deconstruction is seen commonly as a successive dismantlement that can be interpreted as the act of 'pull down' or 'take to pieces' [78] an existing building, in order to possibly, or not, reuse it.

The decision in NZ will be based, fundamentally, in the assurance of safety. In fact, the primary goal is to guarantee that, no matter the solution, the risk is acceptable. Nevertheless, as discussed in Chapter 2, a multi-objective decision must integrate also technical criteria, economic aspect, sustainability efforts, political constraints and, last but not least, the cultural and historical criteria, as such:

- (i) Technical criteria – the required solution must facilitate the coordination among the different participants of the process; guarantee the personal and collective safety and also use the possible non-damaged materials and building components. This process could be prepared on the basis of a deconstruction guide such as the 'Manual de Desconstrucció' (Institut de Tecnologia de la Construcció de Catalunya) [79] and 'A guide to deconstruction' [80];
- (ii) Economical overview – a critical point to the final decision. The cost of a total demolition work is the lower one and it is also known that a retrofitting solution is quite more expensive. The estimated cost to build a new cathedral is between 25 and 65 MEuro [81]. In this aspect, the reinsurance companies are a key factor in many instances. In New Zealand, the Earthquake Commission (EQC) administers the earthquake insurance (set of worldwide consortium of 30 reinsurance companies) and the decision of full reconstruction (demolish is implicit) brings a substantial financial shortfall [63];
- (iii) Sustainability efforts – for what the building represents in the Heritage Status of Christchurch, an important parameter in the final decision must be considered for a more generic building decision. It is accepted that sustainability is nowadays a universal concern, involving the environmental,



the economy and the society. New Zealand has a Waste Management Program with a set of aims, including the residuals from construction and demolition fields [2].

- (iv) Cultural, historical and political criteria – the cultural and historical values of the Basilica are undeniable and the reconstruction must conserve and respect its original aesthetic and avoid alienation. With respect to the political criteria, the local authorities' actions and interests are important to the final decision, so the recovery plans must integrate the communication of all stakeholders, in which the community has an effective participation in this process [82].

Analyzing the criteria above it is possible to conclude that the most important are the economical ones, once the other criteria are guaranteed. This criterion must take into account the different cost study plans. The plans must consider not only the initial necessary funds for the works but also future revenues, related to economical sustainability, as tourism can provide important funds to the Basilica's maintenance and conservation [83]. On the other hand, these plans depend on the solution adopted.



# Chapter 4

## Numerical Model Preparation

### 4.1 INTRODUCTION

The numerical model preparation of Christchurch Catholic Basilica could be done according to different approaches, as there are several strategies to idealize masonry structures. The differences are related to material and structural behavior assumptions, number of input parameters, modeling efforts, computational time required, post-processing results, among others. Simplified approaches, specially focused on collapse mechanisms, as the kinematic analysis (limit analysis) [84] and the analyses based on macro-elements [85], can hardly replace the more advanced tools in the analysis of complex study cases, as the present case.

George Box's (1987) stated [86] "*Essentially, all models are wrong, but some are useful*", even if particularly related to statistical analysis, this quote can be reinterpreted for structural modeling. Box [86] imposes an implicit quality evaluation of the available methodologies and their results, in this case the building safety assessment of the model. Nevertheless, finite element methods (FEM) [87] are nowadays a very common tool, mainly due to the computational evolution [88]. Masonry structures could be represented in FEM as continuous isotropic/orthotropic models (macro-modeling), which represent an homogeneous material, or micro-models, where the masonry units and mortar are considered separately [89]. In the present case of study, a FEM numerical model was prepared using the software DIANA [90], assuming masonry as an ensemble of continuous and homogeneous elements (macro-modeling).

This Chapter presents the aspects related to the FEM model pre-processing stage, which allow the preparation of the Basilica's numerical models. Thus, two main tasks are presented. The first task comprehends the geometrical preparation of the undamaged numerical model of the Christchurch Basilica, using shell, beam and solid elements. The adopted methodology is detailed, together with the steps related to the boundary conditions, material and physical properties, and the discretization process. The second task is related to the damaged numerical model that simulates the state of the Basilica in

June 2011, when the dynamic identification tests were performed. This model was prepared having as basis the undamaged model. The damage insertion was achieved using methodologies that locally affect the elements' stiffness and are in agreement with the collected damage observation.

## 4.2 FEM MODEL PRE-PROCESSING STAGE

### 4.2.1 METHODOLOGY

A description of the methodology adopted to achieve the construction of the numerical model is firstly presented. Afterwards, the modeling assumptions are detailed. A brief discussion about the used methodology allows better understanding the taken steps until reaching the final model.

As seen in Chapter 3, the Basilica has a width of 32 m and a length of 63 m, approximately. In addition to its substantial dimensions, the Basilica presents a set of architectonic features difficult to be modeled. Thus, and taking into account the possibilities that the software DIANA offers, it was decided to import the geometry from the AutoCAD software (AutoCAD 2009, student license). Figure 44 shows the methodology used to import the AutoCAD, after a study of the Basilica's structural arrangement.

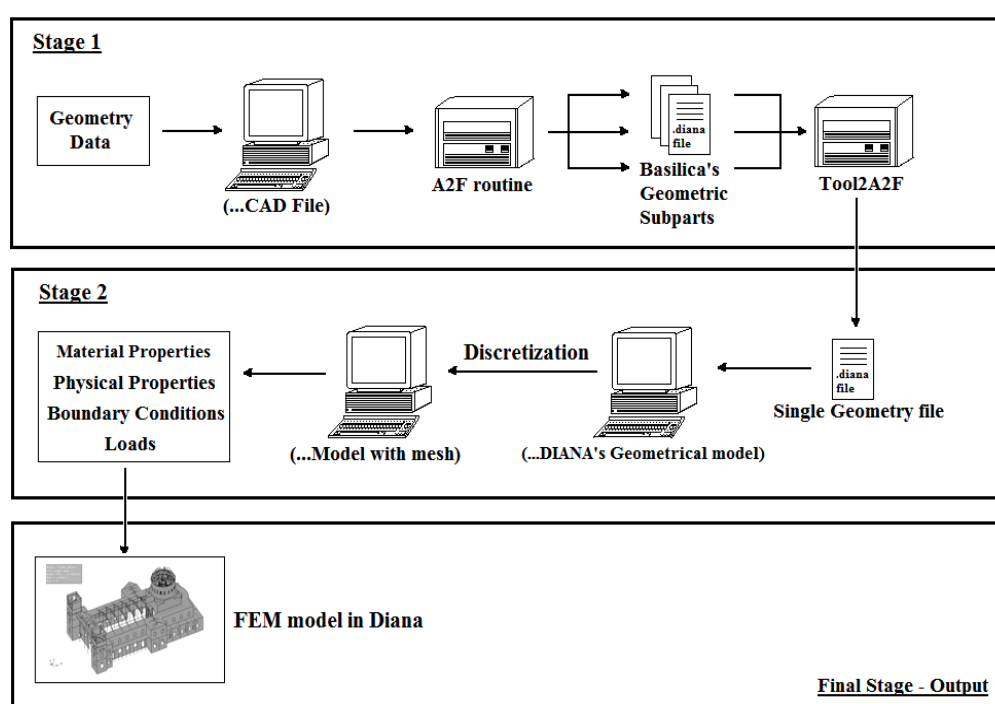


Figure 44 – Schematic description of the FEM numerical model preparation.

After the complete creation of the Basilica's geometry, the A2F [91] routine was used to read the AutoCAD file and write this data in a file format compatible with DIANA. The major inconvenience of A2F routine is its restriction, in terms of maximum number of elements. Thus, the geometry prepared in the AutoCAD was divided in multiple parts (i.e. files). These parts were put together into one unique input DIANA data file. Aiming at accomplishing the last purpose, a routine was developed in C# code language, named as Tool2A2F. After the first stage, the geometric input in DIANA is complete, allowing starting the discretization of the mesh. After the mesh, the preparation of the numerical model, the material and physical properties (linear or nonlinear), boundary conditions and loads must be added. According to the used methodology (Figure 44), the main steps of the FEM model preparation were: (i) the geometry; (ii) the elements discretization (mesh); (iii) material and physical properties; (iv) boundary conditions and (v) loads. These steps are described next in more detail being the loads description excluded. In fact, the loads allocation is taken into account during the performed analysis and by itself do not justify a single section point, once no-special features were considered (as overloads).

#### 4.2.2 GEOMETRY DEFINITION

The geometric definition has a key role in the modeling process. A thorough and detailed geometry construction is likely to yield better results than a simplified one. However, it leads to considerable time costs too. Insomuch it is desirable to adopt a simplified geometry that allows representing the main building features while the structural behavior is kept similar to the real system.

To represent the Basilica's geometry beam, shell and solid elements were used. The first geometry considerations are related to beam elements, in which it is assumed that the dimensions of the transversal sections are very small with respect to its axial length (one-dimensional elements). This element set includes all the interior beams, the West, North and South porch columns, the interior colonnades of the nave and altar, but also the steel crosses braces and Reinforced Concrete (RC) ring beams added to the bell towers in the 2004 strengthening. Aiming at reducing the structural global number of elements, the interior dome, the basilica's main dome and nave roofs were modeled as three-dimensional frames with shapes similar to the real elements (Figure 45), in order to capture the load path of the arch and truss system.

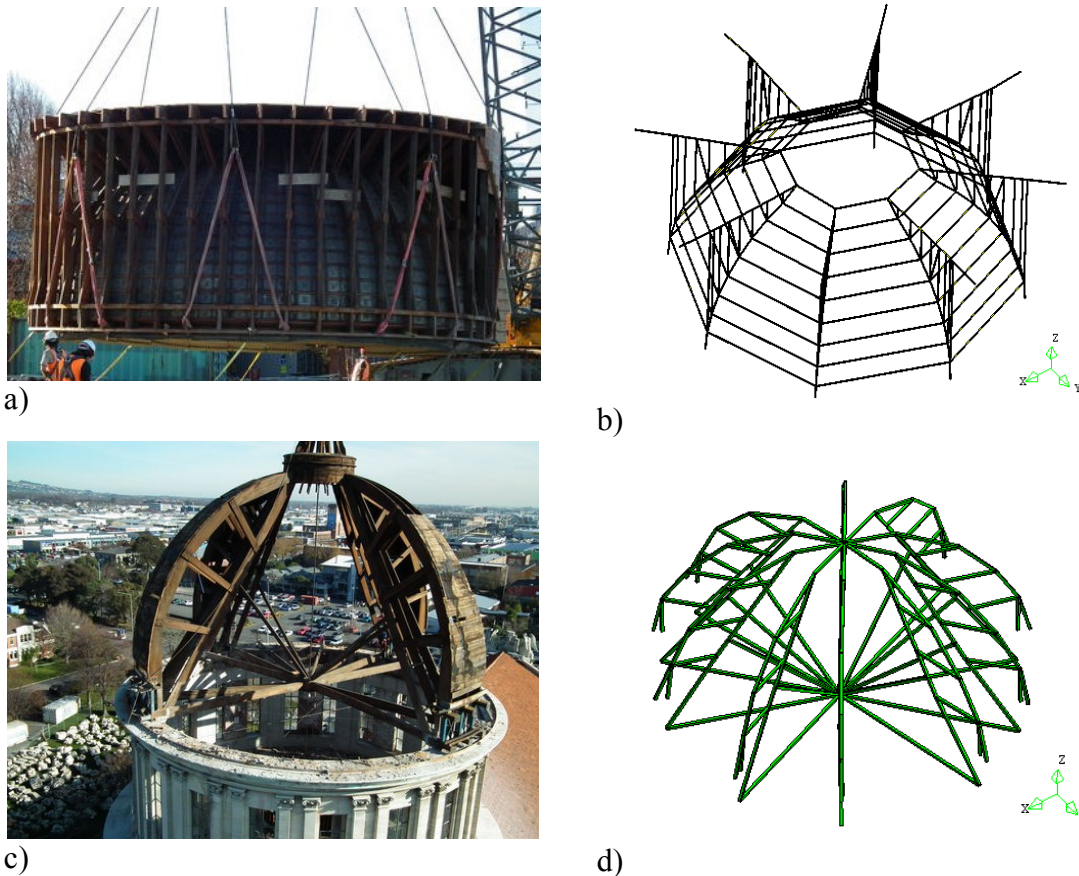


Figure 45 – Main dome: (a) Interior dome of the rotunda during its removal; (b) Interior dome of the rotunda modeled in DIANA, using beam elements; (c) Wooden-frame of the main dome, after the copper cladding removal; (d) Wooden-frame of the main dome modeled in DIANA, using beam elements.

In the shell elements (Figure 46a) it is assumed that the thickness is small in comparison to the other two geometric dimensions. They are used for all the façades considered to be load bearing walls, as well as the interior walls and arcades, the first floor RC slab that surrounds the Basilica's nave and the sacristy, the exterior RC slab above the sacristy and the RC slabs of the bell towers. The position of the shell elements refers to the middle plane of the elements and in all of them the thickness is constant.

As seen in Chapter 3, four arches arise from four large piers above the altar. These arches support the interior dome rotunda and the main dome structure. All the piers have interior openings with stairwells that allow the passage to the exterior balcony of the rotunda and to the main dome. Furthermore, the interior dome is supported by twenty four columns which are symmetrically positioned along the four arches, making possible another vertical path load – see Figure 40 (Chapter 3).

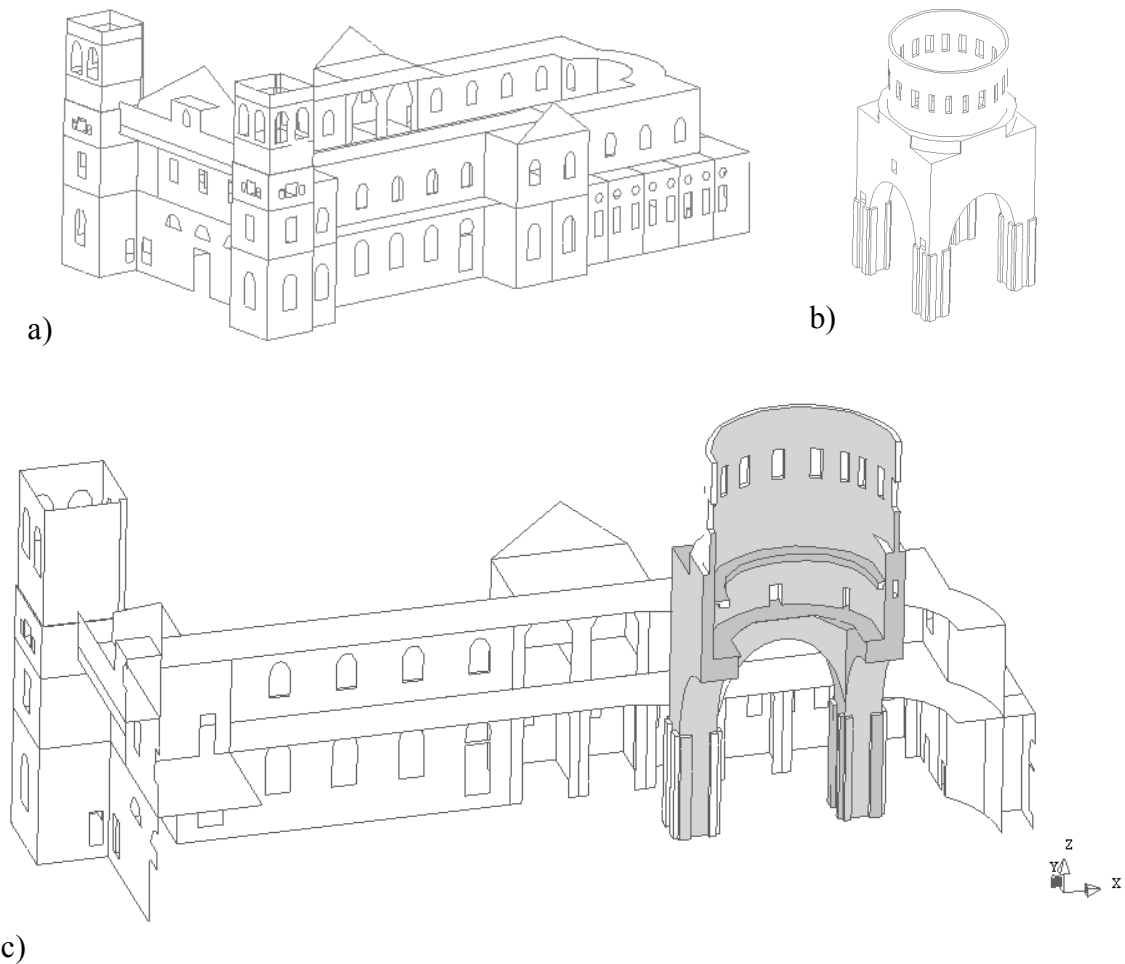


Figure 46 – Shell and solid elements: (a) General overview of the shell elements; (b) General perspective of solid elements; (c) West-East cut-away perspective with shell elements (colored as white) and solid elements (colored as grey).

The aforementioned structural elements could be represented by shell elements, instead of using solid ones. It would make easier the modeling process, not only in the geometric construction stage, but also in their connection to the shells and beam elements already considered. However, it was decided not to adopt this solution, mainly due to two reasons: (i) even if the geometric modeling process could have been faster, the structural arrangement through shell elements should be carefully studied, as the structural behavior of the numerical model could be diverse from the real one (different stiffness). Indeed, these elements form a three-dimensional and complex structure, with a lot of connections (arches-piers, arches-rotunda walls or rotunda walls-main dome walls). It would be hard to idealize an effective and reliable loading system between them; (ii) the calibration process by comparing the experimental and numerical vibration modes could be compromised. The dynamic identification was performed when the Basilica had a considerable level of damage. The insertion of this local damage in the numerical model

is a complex task. Thus, and aiming at accomplishing a consistent numerical model, these substructures were prepared by using solid elements (Figure 46(b)).

### 4.2.3 MATERIAL AND PHYSICAL PROPERTIES

As already stated, a macro-modeling approach was considered, in which homogeneous and isotropic materials are assumed. No experimental tests were performed in order to characterize the material properties of the Basilica. Therefore, information was required to the NZ institutions that are studying the Basilica too. The adopted values rely on this information even if it does not apply to all parameters, in particular those necessary for non-linear analysis. For selected parameters, literature recommendations were also followed to guarantee reasonable and coherent choices, in particular to masonry elements (the adopted values are within the range of the ones adopted in the literature [92-94]).

In this section only the elastic parameters needed to perform a linear static and modal analysis are presented, i.e. Young's modulus ( $E$ ), density ( $\gamma$ ) and Poisson ratio ( $\nu$ ) see Table VI. Material properties related to non-linear analysis, as compressive strength, compressive fracture energy, tensile strength and tensile fracture energy are presented in 5.2.

Table VI – Elastic material properties.

Material	Material Properties		
	$\gamma$ (kN/m <sup>3</sup> )	$E$ (GPa)	$\nu$ (Poisson)
Two leaf limestone masonry	20	2	0.15
Reinforced concrete	25	30	0.20
Steel	78	200	0.25
Timber	7	11	0.30

In what concerns physical properties, the solid elements have the geometric information needed for a given modeled element. On the other hand, beam or shell elements must have their cross section dimensions and thickness defined, respectively (see Table VII). This table also discriminates the adopted material for each beam and shell element. For all the solid elements a single material (masonry) was assigned.



Table VII – Physical properties of the shell and beam elements.

<b>Shell Elements</b>			
<b>Elements</b>	<b>Thickness (m)</b>	<b>Elements</b>	<b>Thickness (m)</b>
West Façade (M)	0.70	South elevation of the Sacristy	0.55
West tympanum wall (M)	0.35	South elevation of the nave	0.55
Slab of the West façade Porch (RC)	0.45	Inner transept walls	0.50
RC Slab of the West Porch (RC)	0.45	Bell towers – 1 <sup>st</sup> floor	0.70
West Entablature (M)	0.60	Bell towers – 2 <sup>nd</sup> and 3 <sup>rd</sup> floors	0.60
East Façade (M)	0.55	North/South Transepts	0.50
North elevation of the Sacristy (M)	0.55	Inner walls – 1 <sup>st</sup> floor	0.50
North elevation of the nave (M)	0.55	Inner walls – 2 <sup>nd</sup> floor	0.50
External slab – 1 <sup>st</sup> /2 <sup>nd</sup> floor (RC)	0.20	Inner slab – 1 <sup>st</sup> /2 <sup>nd</sup> floor <sup>(*)</sup>	0.30
Bell towers slabs (RC)	0.20		
<b>Beam Elements</b>			
<b>Elements</b>	<b>Section (m)</b>	<b>Elements</b>	<b>Section (m)</b>
North/South Entablature (M)	0.90 x 0.65	Roof frame above the nave (S)	$\phi = 0.10$
North/South Portico columns (M)	$\phi = 0.70$	Interior dome frame (T)	0.05 x 0.10
Inner Colonnade (RC+M)	$\phi = 0.70$	Bell tower steel braces	$\phi = 0.32$
West Porch columns (M)	$\phi = 1.00$	West tympanum reinforcement (S)	$\phi = 0.32$
Inner Beams (M)	0.6 x 0.70	Main dome roof frame (T)	0.10 x 0.30
Inner Columns of the Rotunda (M)	$\phi = 0.40$	Bell towers ring beams (RC)	0.2 x 0.6
M – Masonry    RC – Reinforced concrete    S – Steel    T – Timber			

Finally, it is important to refer that point mass elements were also considered. In a first elastic analysis, four groups of point masses were adopted to model the mass of the claddings of nave, main dome, belfry towers and rotunda's interior dome (see Table VIII). The values were estimated taking into account the materials densities and their volume. These masses were applied in the nodes distributed along these elements and the influence area of each node was computed to estimate the respective mass. The point masses in nave, main and inner dome, were applied in beam elements.

Table VIII – Point mass groups, including their total weight and weight per node.

Point Mass Group	Total weight (ton)	Weight per node (ton)
Nave claddings	24.00	1.00
Copper claddings of the main dome	32.80	0.80
Inner dome of the rotunda	2.00	0.04
Belfry towers roof	0.30	0.01

#### 4.2.4 MESH DISCRETIZATION

The mesh discretization is, alike to the geometry construction, a time-consuming procedure. In the present study, several reasons led to adjust single strategies of mesh discretization for shells and solid elements and each one is described below. The discretization of beams was not difficult, as their compatibility is assured by their nodes. Firstly, the selection of structural elements type from DIANA's library (beams, shells and solids) is presented. Next, the meshing strategy is described. For beam elements, a two nodes and three-dimensional beam was chosen, named as L12BE (Figure 47). This element has six degrees of freedom (DOF) per node (three translations and three rotations) and its formulation is based on Bernoulli theory, i.e. its cross-section remains plane and perpendicular relatively to the beam axis slope [90].

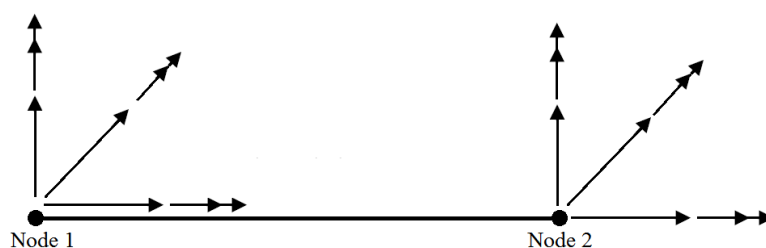


Figure 47 – The beam element L12BE, with a total of twelve degrees of freedom (DOFs).

For shell elements, three-dimensional degenerated curved shell elements according to Mindlin-Reissner theory were adopted. Thus, shear stress remains straight, but not normal to the reference plane of the element after deformation and the normal stress components are not considered. Furthermore, the adopted triangular and quadrilateral shell elements are isoparametric elements with linear interpolation [90], see Figure 48.

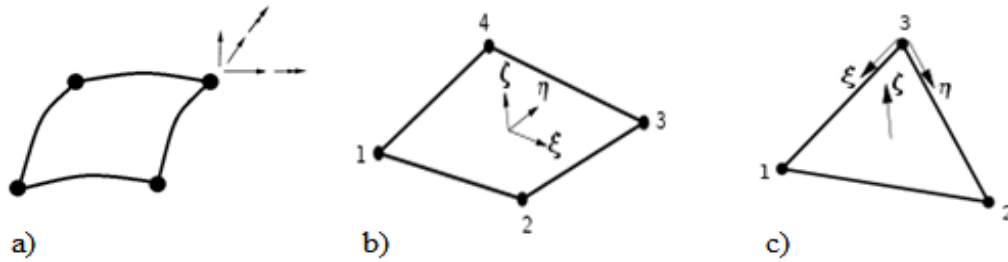


Figure 48 – Curved shell elements: (a) Degrees of freedom per node (b) Quadrilateral curved shell element (Q20SH) [90]; (c) Triangular curved shell element (T15SH) [90].

For solid elements, brick (hexahedral) and wedge (tetrahedral) elements were used. Solid elements have three degrees of freedom per node that corresponds to the three translations. In order to guarantee the connection compatibility between elements of different types (solid-solid, solid-shell and solid-beam) six-node and eight-node isoparametric elements with linear interpolation and Gauss integration for wedge and brick elements, respectively, were adopted, see Figure 49.

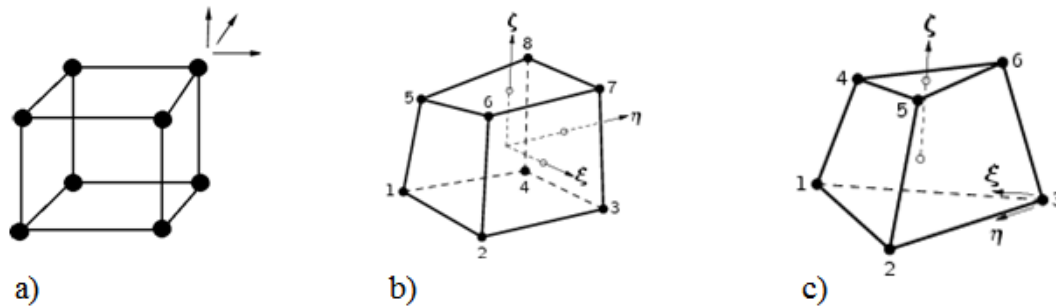


Figure 49 – Solid elements: (a) The degrees of freedom of a solid element per node (three DOF); (b) Brick curved shell element (HX24L) [90]; (c) Wedge curved shell element (TP18L) [90].

As seen in Section 4.2.3, four different nodal mass values were assumed. Point masses are concentrated masses adopted in the numerical model for all the nodes which have nodal masses applied. The chosen element was PT3T (Figure 50).



Figure 50 – Point mass: (a) Topology; (b) The three degrees of freedom (translations) of the PT3T element. [90]

The choice between linear and quadratic elements for beams, shells and solids is always an open discussion. Elements with more nodes, i.e. quadratic instead of linear, are more computational time demanding but offer a more accurate solution [95]. Nevertheless, owing the considerable dimensions of the Basilica, the use of these elements would greatly increase the number of nodes. Thus, linear elements are expected to allow achieving a solution with an acceptable number of degrees of freedom and avoid a huge numerical model.

In what concerns the mesh discretization, an automatic meshing strategy for surfaces using a Delaunay algorithm (a free-meshing option that uses triangular elements), which is a fast procedure, was tested. If applied to the case study it allows more flexibility to the mesh that will easily fulfill local geometric details. However, the drawbacks are related not only to the increase of the number of mesh elements but also with the decrease of the mesh quality, presenting a considerable amount of distorted elements in DIANA (see Figure 51a). The aim here is develop a mapped and rectangular mesh, avoiding bad shape elements in order to guarantee accurate results in the non-linear analysis (Figure 51b).

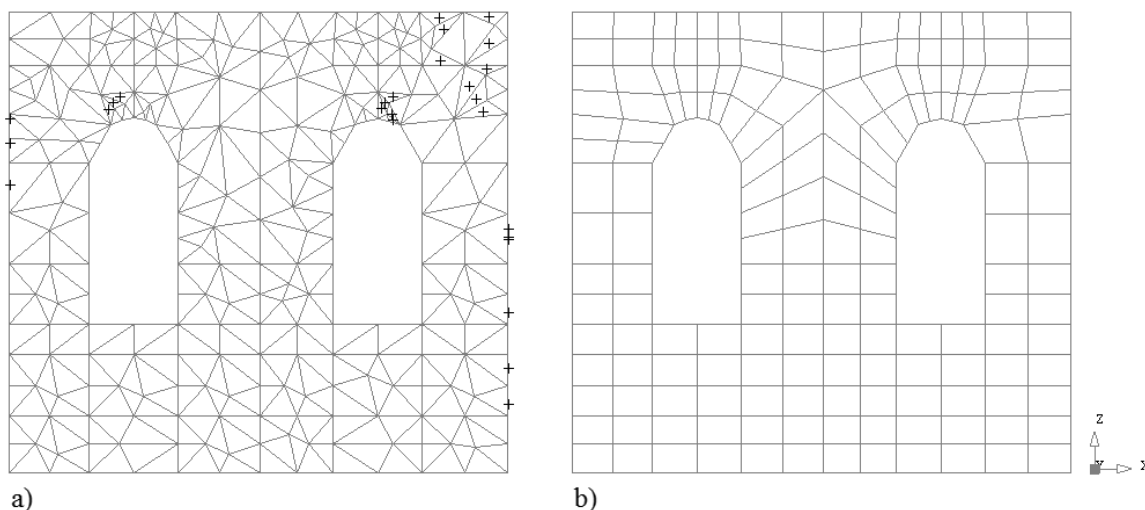


Figure 51 – Tests of the mesh in a façade sample: (a) Obtained mesh using a Delaunay algorithm (automatic meshing); (b) Prescribed (manual) mesh using a structured rectangular approach (the crosses represent distorted elements).

In the mesh discretization, two methodologies were taken into account: (i) for shell elements, the AutoCAD geometry was divided as a set of macro-elements whose layout was established to allow the construction of this mesh arrangement in DIANA; (ii) for

solid elements (applicable only to parts above the sacristy; see Section 4.2.2), a thorough geometric definition leads inevitably to increasing discretization complexity. As there are a significant number of geometrical boundaries, the process of creating regular macro-elements is not simple. Thus, in this case the mesh was already prepared in the CAD geometry, i.e. the solid elements mesh, represents the final geometry.

Two numerical models were created: (i) a numerical model with the finer mesh refinement for the solid elements (see Figure 52a); (ii) a numerical model with less refined mesh for the solid elements (Figure 52b). The goal is to obtain a proper and balanced mesh refinement for solids, presenting accurate results in the non-linear analysis. The created models reproduce the whole structure, i.e. beam and shell elements as well. However, to keep visualization clear, only solid elements are presented.

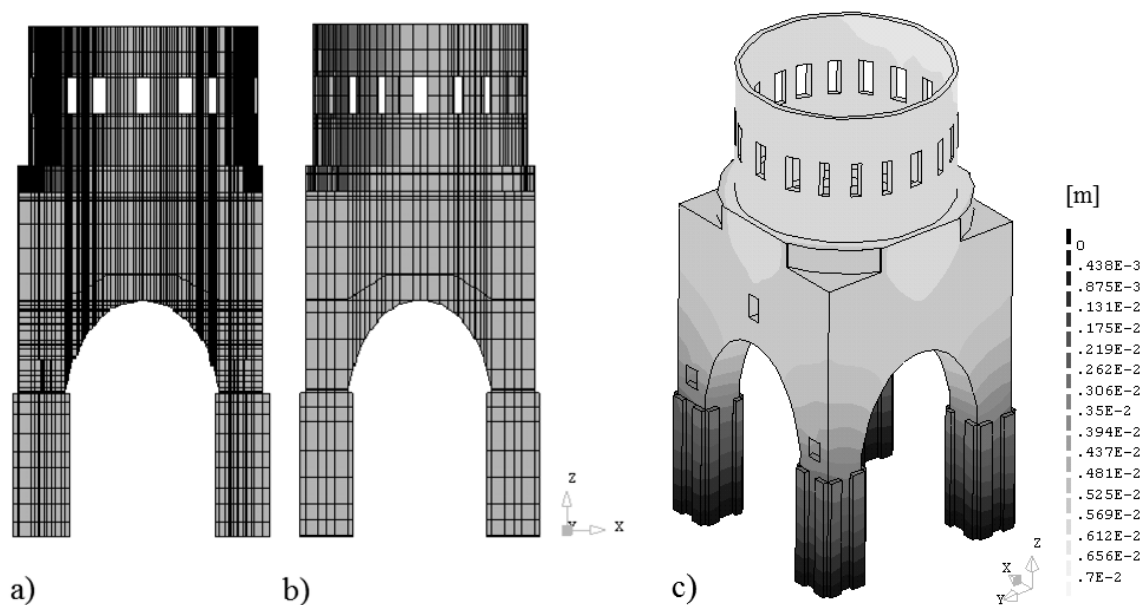


Figure 52 – Mesh for the solid elements: (a) fine refinement; (b) coarse refinement. (c) Nodal vertical displacements due to the self-weight for both mesh discretizations.

The fine model has a total of 109,366 nodes and 98,063 elements. The coarse model has 39,531 nodes and 36,758 elements. The relation between number of nodes and processing time is non-linear (depending on aspects such as solution procedures, material constitutive models, access to the database or available RAM memory). The tests made with both models in a computer with a processor Intel(R)-Core(TM) i7 3820 3.6GHz with 16GB of RAM, showed that the model with a finer mesh has approximately three more

times the number of nodes and a processing time for the self-weight (linear elastic analysis) of 12 hours, fifteen times higher than the coarser mesh.

A linear static analysis due to self-weight was carried out for both numerical models. The material and physical properties are presented in Section 4.2.3. Figure 52c shows that the maximum vertical displacement is 0.007 m. The results of both models did not present any difference up to three significant digits. Thus, the numerical model with a coarser mesh was adopted. The model has a total of 36,758 elements, in which 1,720 are beam elements, 27,919 are quadrilateral shell elements, 235 are triangular shell elements, 5,661 are brick elements and 1,223 are wedge elements. The total number of degrees of freedom is 178,719.

#### **4.2.5 BOUNDARY CONDITIONS**

The last step of the numerical model preparation is the definition of the boundary conditions. Scarce information related to the foundations of the Basilica is available. However, according to [68] the foundations probably have a concrete strip footing with 1.5-2.5 m of depth.

Two types of constraints were taken into account: (i) boundary conditions for the wall and columns foundations, and (ii) boundary conditions for the connection between different types of elements. The first group attaches all the mesh nodes at the bottom layer of the structure. At the base of the four piers, of the masonry walls (shells) and of the columns, supports that restrain all the degrees of freedom (fixed joints) were applied, see Figure 53. The second type of constraints was applied to all the interface nodes that connect different types of elements, i.e. elements with different number of DOFs, namely in all nodes that connect: shell elements to the solid elements; beam elements to the shell elements and/or beam elements to the solid elements. These constraints aim to guarantee their compatibility. For instance, a constraint condition is used to perform a connection between: (i) a curved shell element that has three translations and two rotations (5 DOFs) to a solid element which only has three translations (3 DOFs); (ii) between an extreme node of a beam, which has three translations and three rotations (6 DOFs), to a solid (3 DOFs) or a shell (5 DOFs) element.

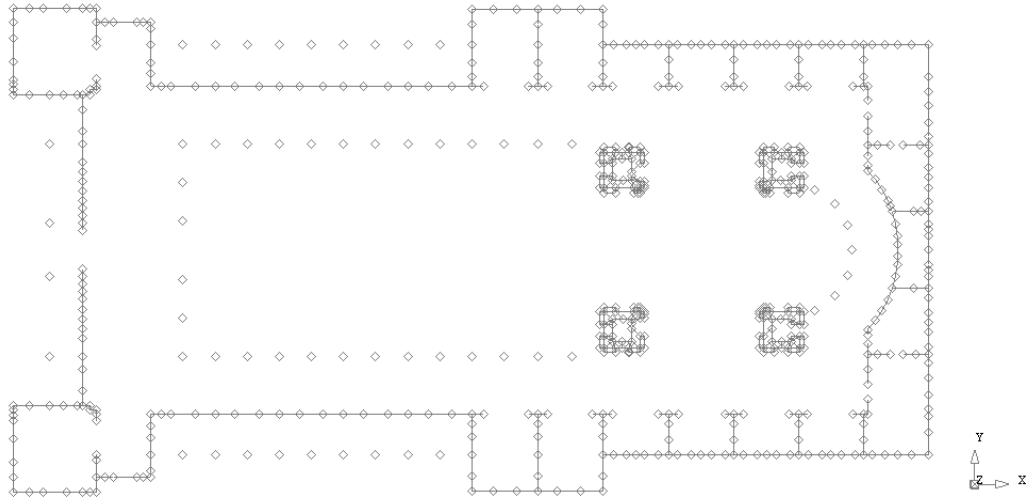


Figure 53 – Top view of the first type of boundaries constraints considered.

### 4.3 UNDAMAGED FEM MODEL

#### 4.3.1 LINEAR STATIC ANALYSIS

A linear static analysis due to its self-weight was performed to the Christchurch Catholic Basilica. The aim of this first analysis is to study the structural system stability, analyzing the displacements and stress concentrations. Furthermore, this analysis allows checking for mesh problems or inadequate modeling options. Figure 54 presents the structure deformation. The maximum vertical displacement is approximately 7 mm and occurs in the solid elements, i.e. elements above the sanctuary. It is also noted the large displacements occur in the second floor slabs which are connected to the rotunda and the deformed shape of the two bell towers is also clearly visible. Even if subjected only to a vertical load (self-weight), some out-of-plane movements are present in the masonry walls.

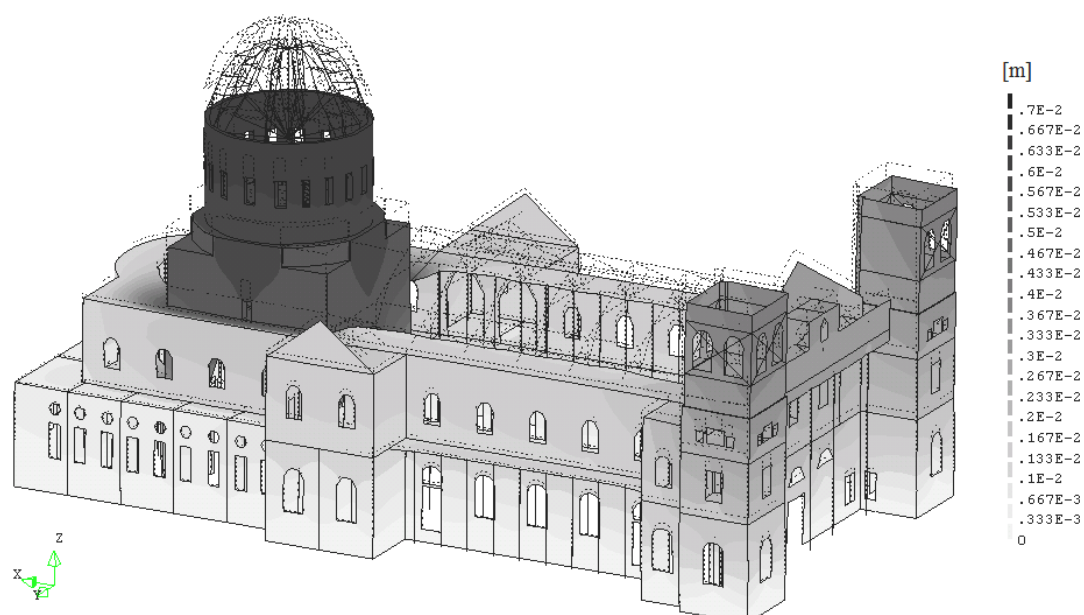


Figure 54 – Deformation of the Basilica under its self-weight (magnification factor: 300).

The vertical stresses (see Figure 55a) show, as expected, maximum compressive values of 1.8 MPa at the base of the altar piers. The maximum principal tensile stress of masonry elements is 0.2 MPa, located at the top of the North and South façades near the second RC floor of the rotunda (see Figure 55b). In these elements the maximum principal compressive stress is equal to 0.9 MPa. These stress values are justified due to curvature of the RC slab that is connected to the solid elements. In reality, it is likely that a small rotation of the slabs occurs in the connection and the stresses are much lower. This could be represented in the FEM model by releasing the bending degree of freedom but the option is not available in DIANA. It is also noted that the maximum stress values are indicative and they depend to some extent from the mesh discretization.

The maximum value of principal compressive stresses is located in the connection of West façade columns. The columns were simulated by beam elements, which lead to a point loading system causing high stresses in these areas. The values of compressive and tensile principal stresses for masonry elements mainly range the 0.3 MPa and 0.02 MPa, respectively, which seems to be adequate.



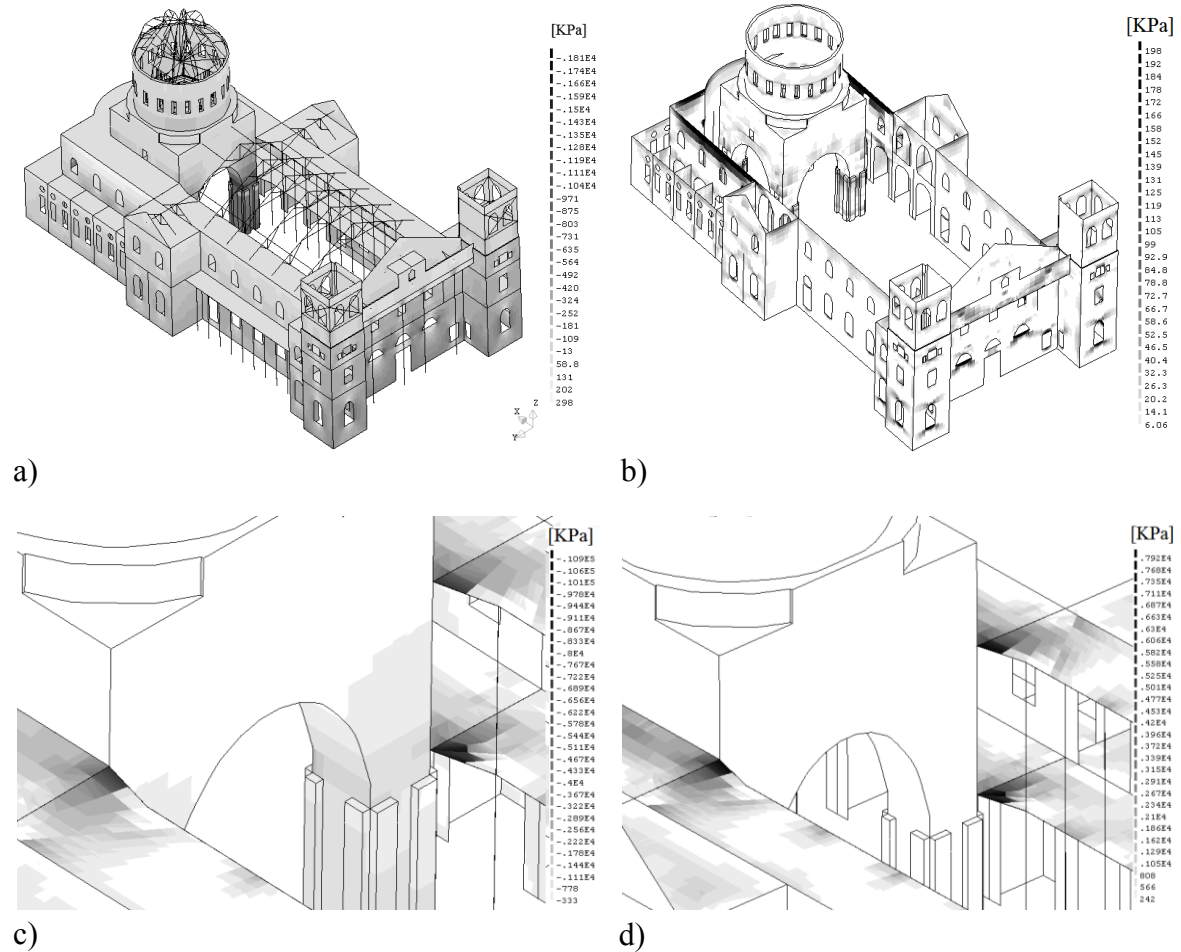


Figure 55 – Stress of the analysis due to the self-weight: (a) Vertical stresses; (b) Principal tensile stresses for masonry elements; (c) Principal compressive stresses of RC slabs (top surface); (d) Principal tensile stresses of RC slabs (bottom surface).

In general, the compressive and tensile stresses values for the RC slabs are 2 MPa and 0.2 MPa, respectively. The maximum stresses are located around the base and the top of sacristy arches, namely between the connections of beam elements from nave, RC slabs and solid elements (see maximum stress areas of Figure 55c and Figure 55d). As already mentioned, the solid elements have higher vertical displacements than the surrounding façades. The modeling process assumed a perfect connection between the slabs and respective solid and shell elements. Thus, the rotational stiffness terms that imposes a restriction to the generated deformed curvature (negative flexural moment near the façades, see Figure 55b and positive flexural moment, near to solid elements, see Figure 55c and Figure 55d) led to considerable stresses. Bearing in mind the last, the maximum principal compressive stresses of RC slabs (top surface) is approximately 11 MPa, about one third of the strength value. The maximum principal tensile stress (bottom surface) is

0.8 MPa, which is a high value that cannot be more reduced as it derives from the modeling strategy and not from mesh misrepresentation. In any case, reinforcement is present to provide capacity to the tensile stresses found.

#### 4.3.2 MODAL PARAMETERS

An eigenvalue analysis was performed to obtain the frequencies and mode shapes of the structure. The first six global frequencies range from 2.92 Hz to 5.84 Hz (Table IX). For one hundred modes, it was possible to obtain a cumulative mass participation of 86.4% in the x direction, 85.4% in the y direction and 48.8% in the z direction. Considering two hundreds modes it is possible to obtain a cumulative mass participation of 73.3% in the z direction. This unexpected (and very large) number of modes considered is due to the high number of local modes.

Table IX – Frequencies, period and cumulative effective mass in each direction.

Mode	Frequency (Hz)	Period (s)	Cumulative effective mass in direction X (%)	Cumulative effective mass in direction Y (%)	Cumulative effective mass in direction Z (%)
1	2.92	0.34	≈ 0	62.2	≈ 0
2	3.02	0.33	68.6	62.2	≈ 0
3	3.30	0.30	68.6	62.6	≈ 0
4	3.66	0.27	68.6	67.8	≈ 0
5	4.36	0.23	74.5	67.8	≈ 0
6	5.84	0.17	76.4	69.3	≈ 0
100	12.44	0.08	86.4	85.4	48.8
200	17.78	0.05	87.8	88.2	73.3

Selected mode shapes are presented in Figure 56. The first mode is global and translational (y direction, see Table IX) mode. The maximum modal displacements occur in the main dome, in the bell towers, and West and nave façades. Due to the considerable stiffness of the sacristy piers, the surrounding façades present minor modal displacements. The second, third, fourth and fifth modes are characterized mainly by bell towers' movements. The second mode is also a translational one (x direction, see Table IX), in which the two bell towers have an outward movement. The third mode, also a translational one (y direction, see Table IX), shows an out-of-plane movement in the lower inertial direction. The fourth mode shape is similar to the second one, but mobilizes

more mass in the y direction, due to the opposite movements of each bell tower. The fifth mode is also similar to the second one, but presents a slight torsion effect due to the out-of-plane movement of the West façade. Finally, the sixth mode is a local mode of the West tympanum wall. In general, the first six modes shows that the bell towers, main dome and nave façades are the more flexible elements and are the more relevant elements for the Basilica's dynamic behavior.

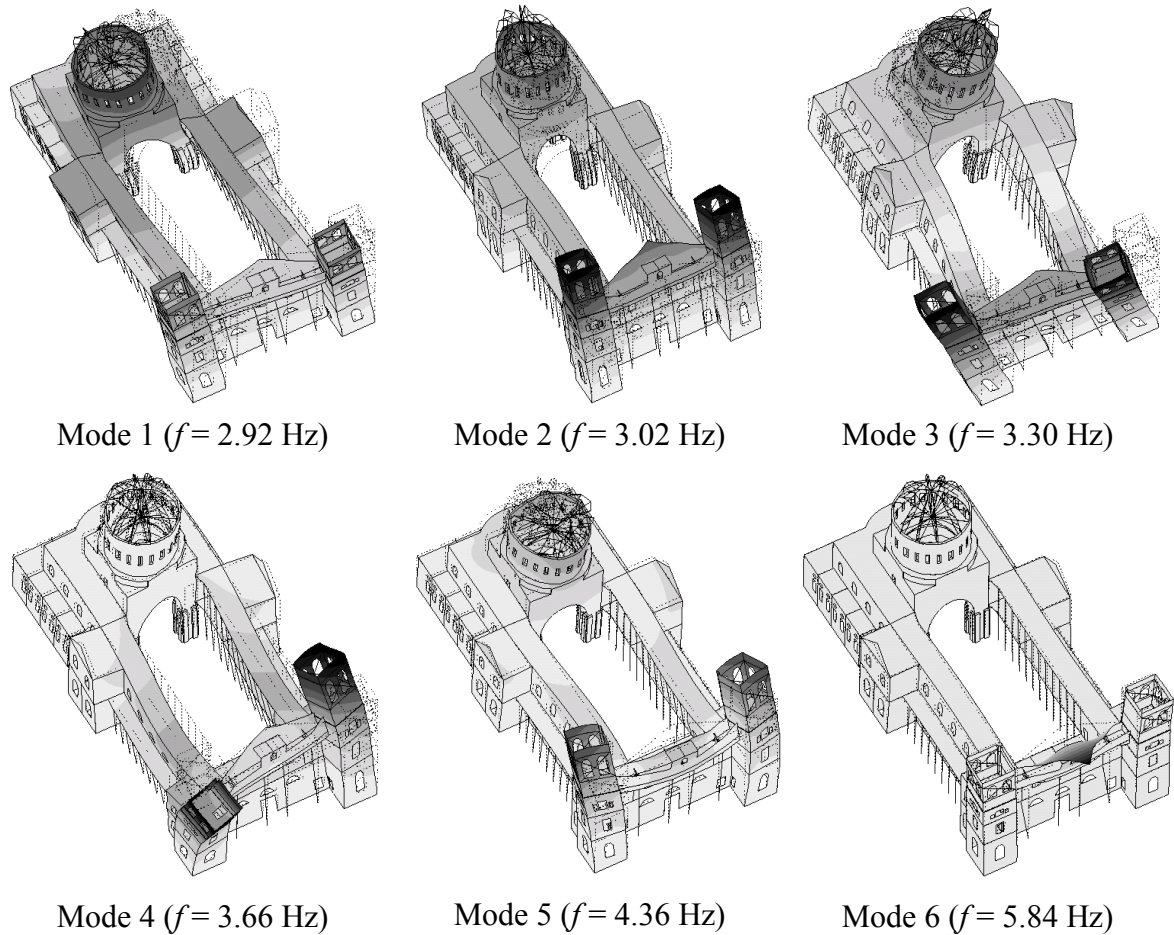


Figure 56 – First six global mode shapes of the non-damaged structure.

#### 4.4 DAMAGED FEM MODEL

After the earthquake of February 22<sup>th</sup>, 2011, dynamic identification tests were carried out to estimate the mode shapes and frequencies of the Basilica [58]. It would be expected that this information could be used to calibrate the numerical model. However, the Basilica was already damaged when the experimental tests were performed and, consequently, the calibration process must be carried out for a numerical model with damage. The damage was inserted in the original FEM model according to two methodologies that create discontinuities and weak boundaries in the structure, aiming at representing the observed

crack patterns: (i) by decreasing the thickness in shell elements and (ii) by decreasing the Young's modulus in solid elements (this operation does not induce cracking but if the stiffness is sufficiently low, it provides a good representation of a pre-existing crack). The stiffness or the strength capacity of beam elements was not changed.

#### 4.4.1 DAMAGE INSERTION

The damage assessment is achieved by gathering information from OPUS<sup>2</sup>, an engineering consultant designated by CERA (Canterbury Earthquake Recovery Authority), with images collected during the dynamic identification tests. In addition to the drawings from OPUS, see Annex A, note that a description of the damage was already made in Section 3.4. The damage considered in the numerical model is the following:

- i. In the North and South façades, all the elements in which crack patterns were registered, for instance in the openings and connections between the nave and the transept walls, had its thickness decreased, see Figure 57a and b;
- ii. In the West façade, the cracking near the windows, walls and corners were inserted by decreasing the element thickness. Due to the partial collapse of the two bell towers, some elements were deleted from the numerical model, see Figure 57c, d, f and g;
- iii. In the East façade, considerable damage was collected mainly in the second floor. Not only in the openings and walls but also in the exterior slabs, see Figure 57e;
- iv. In the solid elements, the damage is mainly related to the North arch, where a high number of elements were deleted due to their collapse (Figure 58a and c), spandrel of South arch, walls of rotunda, and horizontal cracks bellow the walls of the main dome. In the elements where cracks are visible, the Young's modulus was reduced to represent the local weakness (Figure 58a and b).

---

<sup>2</sup> OPUS had the courtesy to share information related to the structural assessment.

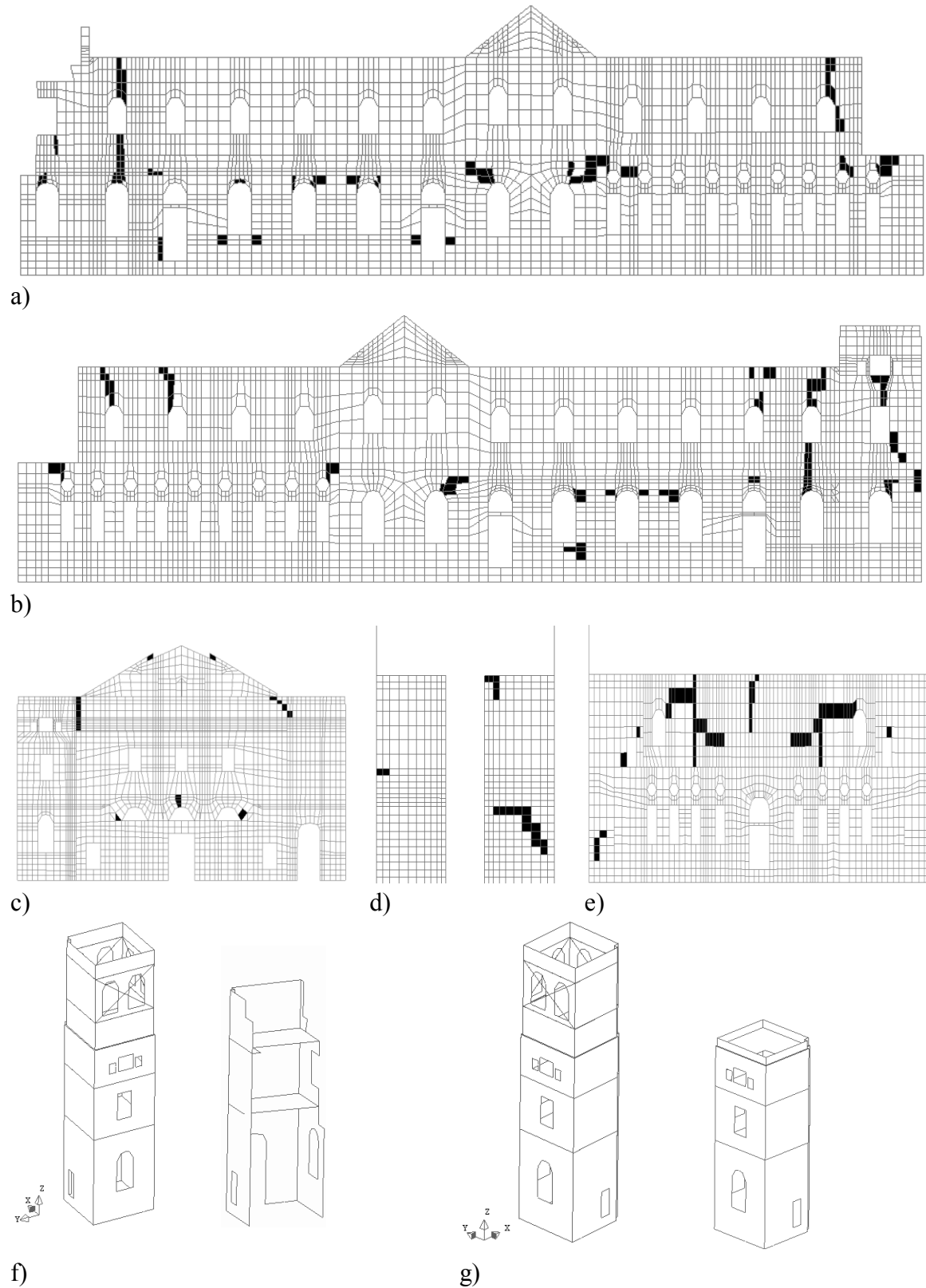


Figure 57 – Damage in shell elements (shadowed elements): a) South elevation; (b) North elevation; (c) West elevation; (d) West façade of the transepts (d) East elevation; (f) Undamaged (left) and damaged (right) South bell tower; (g) Undamaged (left) and damaged (right) North bell tower.

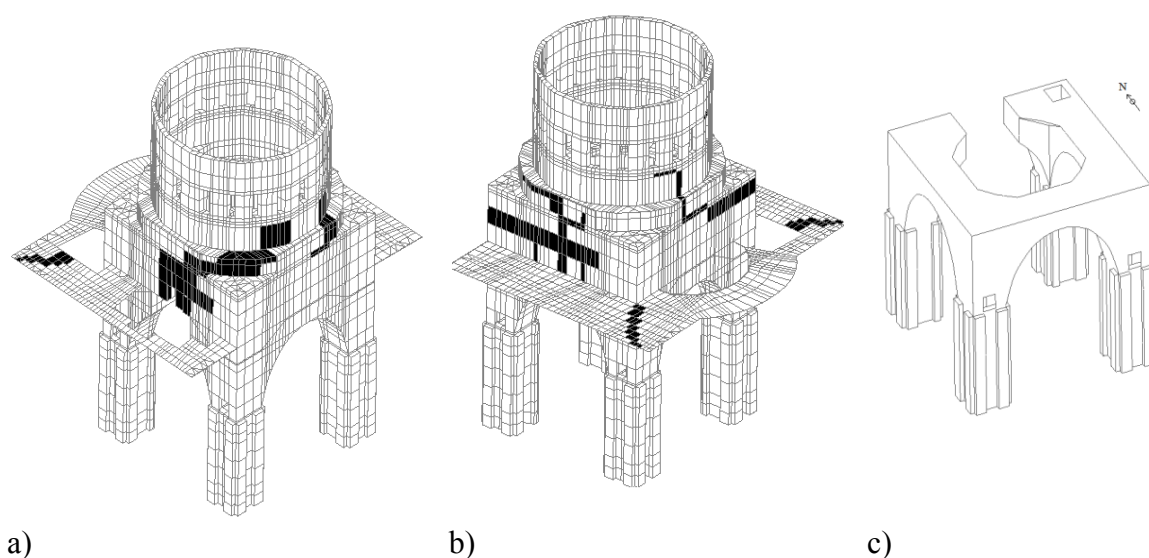


Figure 58 – Damage in solid elements (shadowed elements): a) North-West perspective; b) South-East perspective; c) Deleted elements of the North arch.

#### 4.4.2 CALIBRATION PROCESS

After damage insertion, it is possible to proceed to the next step, i.e. the calibration process. Firstly, a simple methodology was followed in order to evaluate the possibility of calibration and its degree of detail. Due to the damage, some parts of the structure were not considered, which modified the dynamic behavior of the structure. As stated in [58], none of the experimental modes showed a clear global movement. It is possible to conclude that there are local or independent movements of parts of the structure (macro-elements) that directly affect the modal shapes (see Figure 59).

Figure 59 shows the experimental modal shapes and frequencies estimated. The frequencies range from 5.82 Hz to 10.99 Hz. In the first mode, both South and North façade walls (nave and sacristy) have an out-of-plane movement. The second, third and fourth modes are very similar and are mainly local modes with an out-of-plane movement of the North wall of the nave. In the fifth mode, both South and North walls of the nave present an out-of-plane movement. In the sixth mode, an out of-plane-movement of the South-East wall of the sacristy near to the transept also occurs, mainly to the North and South walls of the nave (see the damage in Figure 57e). Finally, the seventh and eighth modes present similar values of frequencies and the North and South façades have identical movement, however, out-of-phase.

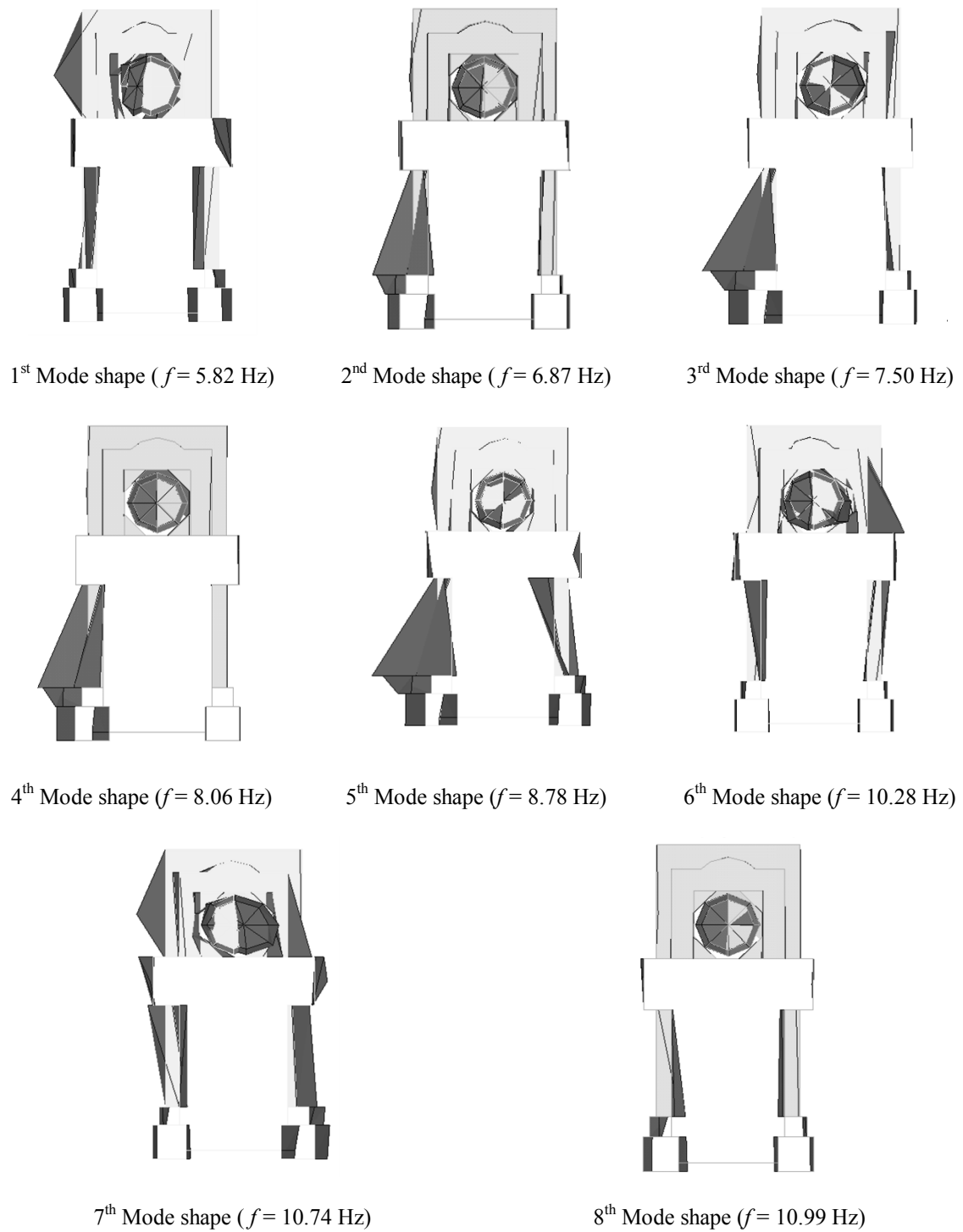


Figure 59 – Experimental mode shapes and frequencies [58].

Six numerical models based on the damaged numerical model presented in Section 4.4.1 were prepared, in which the differences are related to the quantity or severity of damage inserted, i.e. the level of decrease (percentage) in thickness and/or Young's modulus of shells and solid elements, respectively (Table X). The damaged shell elements were

divided in three groups: (i) cracks in openings; (ii) diagonal cracks in walls, and (iii) cracks near façade connections and corners. Furthermore, changes in the Young's modulus of damaged solid elements and in the undamaged masonry elements were also performed, due the uncertainty in their values. The goal of running several numeric models is to analyze the influence of each parameter and to evaluate if the numerical results improve with respect to the experimental modes (mode shapes and frequencies).

Table X – Damaged numerical models used to evaluate the numerical modal response.

<b>Model</b>	<b>Cracks Group 1 (thickness decrease %)</b>	<b>Cracks Group 2 (thickness decrease %)</b>	<b>Cracks Group 3 (thickness decrease %)</b>	<b>E (GPa) Masonry Shell elements</b>	<b>E (GPa) Masonry Damaged solid elements</b>
Model 1	50 %	60 %	85 %	2.00	0.50
Model 2	50 %	60 %	85 %	2.00	1.00
Model 3	50 %	60 %	85 %	1.00	0.50
Model 4	50 %	60 %	85 %	1.50	1.00
Model 5	50 %	70 %	95 %	1.50	0.50
Model 6	30 %	60 %	85 %	2.00	0.50

An eigenvalue analysis was performed for all numerical models of Table X. For each model, the mode shapes and frequencies that resemble the experimental ones were registered. The serious damage of the Basilica has a high influence in the experimental modes, mainly in the local behavior. However, that is not so clear in the numerical models (Figure 56).

In Figure 60, only three modes are presented. They show the difficult of the numerical models to fit the experimental modal parameters. These three mode shapes are general and similar in the eight studied models. The change in the Young's modulus is the option that affects more the modal parameters. Nevertheless, no significant changes in the mode shapes are obtained and it was concluded that the assumed properties and thickness changes do not affect meaningfully the out-of-plane movements of the walls (Table XI).

Still, the error between the numerical and experimental frequencies is quite reasonable for a first step prior to an automatic optimization calibration process. This further step was not carried out as it was noticed that none of the models represent adequately the measured experimental modes. Even for the selected modes (1<sup>st</sup>, 2<sup>nd</sup> and 5<sup>th</sup>), the



difference of local movements is obvious, mainly in the North façade of the nave. Model 5 aims to represent this local movement, by a considerable reduction of thickness in cracks of Group 3 (connection gaps or cracks) and by creating a strong discontinuity between North tower façade and North façade of the nave. Still, the mode shapes were very similar to the other numerical models.

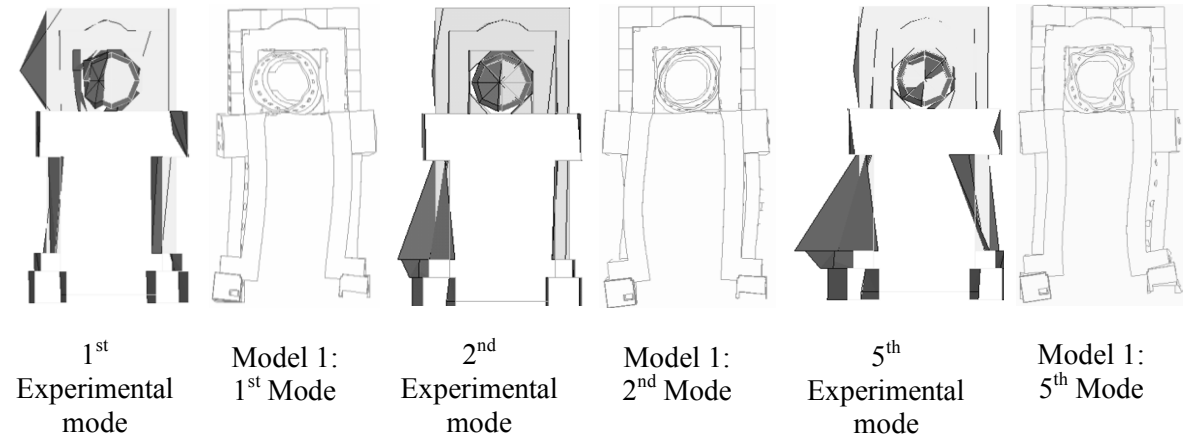


Figure 60 – Comparison between the 1<sup>st</sup>, 2<sup>nd</sup> and 5<sup>th</sup> experimental and numerical mode shapes.

Table XI – Comparison between experimental and numerical modal frequencies.

<b>Model</b>	<b>1<sup>st</sup> Mode frequency (Hz)</b>	<b>2<sup>nd</sup> Mode frequency (Hz)</b>	<b>5<sup>th</sup> Mode frequency (Hz)</b>
Model 1	5.76	6.97	9.80
Model 2	5.76	6.97	9.81
Model 3	5.08	7.25	8.95
Model 4	5.98	6.28	9.00
Model 5	5.96	6.28	8.98
Model 6	5.76	6.61	9.81
Experimental	5.82	6.87	8.78
Maximum error (%)	12.71 %	8.59 %	11.73 %

It is possible to mention, for instance, a study case (*St. James Church*) in which the calibration process had good results and was done taking into account a damaged model too [96]. In this way, it is plausible that other attempts to represent the experimental behavior are possible, e.g. by adding new crack patterns. However, changes in the roof and, possibly, true discontinuities are necessary to obtain the local mechanisms observed

experimentally. This would require major changes in the finite element model and was considered outside the scope of this thesis. The task is difficult, time consuming and risky, without any guarantee of perfect fit, given the complexity of the model. Therefore, a calibration process was not continued and an automatic calibration by optimization was not performed. Still, it is important to refer some final commentaries:

- (i) As reported in [58], dynamic identification does not take into account the two bell towers (severely damaged) neither the West façade. Furthermore, the acquired data from the East façade, dome and rotunda were not used;
- (ii) Figure 59 shows linear mode shapes of the walls. The main reason is the limited number of accelerometers used in the dynamic identification tests. Several setups were needed to perform the acquisition and the accelerometers were placed mainly at the façade connections [58]. Thus, the information about the modal components of several mid-span positions of façades is not available. The lack of information in these positions allows significant doubts on the facades' behavior;
- (iii) At the time of dynamic identification tests, the North bell tower presented a buttress made of containers (a stabilization measure), which was not represented in the numerical model. Although the accelerometers were not placed in this part of the structure, the containers affect the modal parameters of Basilica (frequencies and mode shapes).
- (iv) Safety recommendations led to the use of a controlled iPad flying drone [69] to observe the interior damage of the Basilica. The only damaged inserted in the interior was at the North and South arches (solid elements). As seen in Figure 59, local behavior is dominant and the absence of interior damage near North and South nave façades (for instance, in the interior RC slabs, interior walls or interior beams) could also explain the difficult to reproduce the actual behavior.

# Chapter 5

## Seismic Assessment by Nonlinear Static Analysis

### 5.1 INTRODUCTION

The nonlinear static or pushover analysis is a procedure that allows evaluating the seismic behavior of structures. It is a time-invariant analysis (static) and is, usually, more computational attractive than a nonlinear (dynamic) time history analysis. The seismic forces are simulated by inducing horizontal loads, which are monotonically increased, in the structure under its self-weight (vertical load). In this study case, a uniform pattern was taken into account for the applied horizontal loads, i.e. the applied forces are proportional to the mass of the structure. These lateral loads are applied to the structure considering its nonlinear properties. Moreover, in this type of analysis it is possible to analyze the evolution of the seismic response of the structure, the weaker elements of the structure, the damage distribution and the failure mechanisms.

### 5.2 MATERIAL CONSTITUTIVE MODEL AND NONLINEAR MATERIAL PROPERTIES

In order to predict a nonlinear response it is imperative to use constitutive descriptions for finite elements that are able to reproduce it. Here, for representing the physical nonlinear behavior, the total strain fixed crack model [90] was adopted. This approach allows describing the tensile, compression and shear nonlinear behavior in a continuum model. In this material model, it is assumed that the cracks are orthogonal and fixed, according to the principal strain directions at the onset of cracking, and this direction remains unchanged during the load increase. Furthermore, a shear retention factor, which defines the shear behavior after cracking, has to be defined [97].

Next, the models that represent each material in terms of stress-strain relationship are defined. This selection has also a decisive role, once it controls the response of the structure. Furthermore, a brittle behavior for materials, which considers an immediately decrease of stress when the tensile strength is reached, can provide inaccurate results. It is known that this

particular behavior will lead to a FE model whose convergence is highly dependent on the mesh refinement, specifically the elements size [98], when fracture occurs. In the present case study, the masonry and concrete behavior is given by a parabolic stress-strain relationship for compression and an exponential stress-strain relationship for tension (Figure 61).

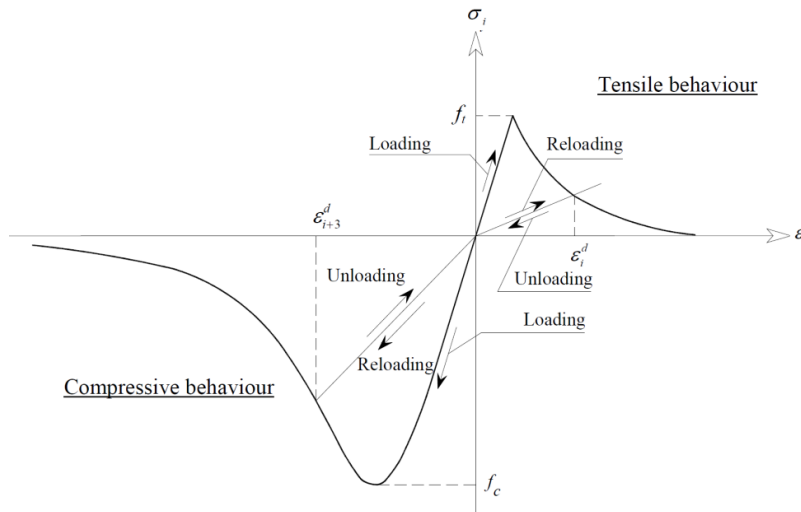


Figure 61 – Adopted hysteretic behavior for masonry and concrete [99].

These relationships are independent from the mesh size, because the crack-bandwidth  $h$  is estimated as function the area  $A$  of the element:

$$h = \sqrt{A} \quad (1)$$

The shear behavior is taken as a linear stress-strain relationship. As already stated, the post-crack shear stiffness ( $G^{cr}$ ) is obtained by reducing the non-cracked shear modulus ( $G$ , which is the elastic shear modulus) through a shear retention factor  $\beta$  ( $0 \leq \beta \leq 1$ ) [90]:

$$G^{cr} = \beta G \quad (2)$$

Finally, the nonlinear material parameters are defined (nonlinear behavior was only assumed for masonry and concrete). The information required includes the compressive and tensile fracture energy  $G_f$ , and the compressive and tensile strength. As mentioned in Section 4.2.3, the information collected from the New Zealand authorities studying the Basilica were adopted, specifically the compressive and tensile strength for masonry and concrete. For the fracture energy, the recommendations presented in the literature were adopted. Thus, the used values for concrete are estimated through Model Code 90 ([100]), meaning that the tensile ( $G_f$  [kN/m]) and compressive ( $G_{fc}$  [kN/m]) fracture energies were obtained by equations (3) and (4), respectively:

$$G_f = 0,025 \times \left(\frac{f_c}{10}\right)^{0,7} \quad (3)$$

$$G_{fc} = 15 + 0.43f_c - 0.0036f_c^2 \quad (4)$$

Here,  $12 \times 10^3 \text{ kPa} \leq f_c \leq 80 \times 10^3 \text{ kPa}$ . For masonry, the compressive fracture energy ( $G_c$ ) can be estimated as  $1.6 \times 10^3 \times f_c$ , for  $f_c$  less than  $12 \times 10^3 \text{ kPa}$  [100]. For the tensile fracture energy, a value equal to  $0.012 \text{ kN/m}$  is recommended [100] for masonry joints, but this might be too low for a masonry assembly. The convergence towards a solution is also highly affected by this parameter in such a complex structure and a value of  $0.12 \text{ kN/m}$  was adopted. Given the rather low value of the masonry tensile strength, it is believed that the results are not significantly affected by the fracture energy. With respect to the shear retention factor, a value of  $0.1$  (10%) was considered. These nonlinear material parameters are summarized in Table XII.

Table XII – Nonlinear material parameters.

Material	Compressive strength ( $f_c$ ) [kPa]	Tensile strength ( $f_t$ ) [kPa]	Compressive fracture energy ( $G_{fc}$ ) [kN/m]	Tensile fracture energy ( $G_f$ ) [kN/m]
Masonry	8000	100	12.8	0.120
Concrete	30000	2000	25.0	0.054

It is also noted that in the nonlinear analysis only the point masses of the belfry towers were taken into account. The others point masses were not considered, due to difficulties in convergence of the solution. It is believed that this will not affect significantly the results despite the location of the point masses, because the mass percentage of these elements in the global model is just  $0.6\%$  of the total mass of the structure (9082 ton).

### 5.3 NUMERICAL INTEGRATION

In the numerical integration of a finite element there are two main concerns, the used (i) integration scheme and the used (ii) integration order. It is possible to choose a full or reduced integration approach and different schemes, for instance the Newton-Cotes or Gauss quadrature. The Newton-Cotes procedure is the more indicated for nonlinear analysis of interface elements (the integration points for stiffness and stress evaluations are located around the elements boundaries) [101]. Here, the usual Gauss quadrature was considered, owing its integration accuracy and attractiveness in terms of time costs. A Simpson

integration scheme was also considered for elements requiring through-thickness integration (see Table XIII) [90].

The main concern related to the integration order is to choose the value that gives accurate results. In general, high order values lead to more effective and accurate solutions, but also to considerable time requirements. In this way, it is expected to find a reasonable integration order that have into account the results quality and processing time until reaching the solution convergence. As seen in Table XIII, the elements integration order is higher for nonlinear analysis, with the exception of the beam elements that are kept under linear elastic regime. The objective is to guarantee more integration points in structurally vulnerable regions, in order to achieve a better and effective spread of plasticity.

Table XIII – In plane Gauss integration points and/or Simpson for linear and nonlinear analysis (in-plane x thickness).

Elements Type	Linear	Nonlinear
L12BE (Beam element)	2	2
Q20SH (Shell element)	2x2x3 <sup>(*)</sup>	2x2x5 <sup>(*)</sup>
T15SH (Shell element)	3x3 <sup>(*)</sup>	3x5 <sup>(*)</sup>
TP18L (Solid element)	1x2	4x3
HX24L (Solid element)	2x2x2	3x3x3

<sup>(\*)</sup> Simpson integration in the thickness direction.

#### 5.4 ITERATIVE PROCEDURE

The calculation procedure and its effectiveness in terms of time costs depend on the number of operations performed. Generally, a total of  $\frac{1}{2}nm_k^2$  operations are required to solve a static equation step by a direct method:

$$\underline{F} = \underline{K} \underline{U} \quad (5)$$

where  $\underline{F}$ ,  $\underline{K}$  and  $\underline{U}$  are the external load, stiffness and displacement matrices, respectively [101], being  $n$  the stiffness matrix order (number of degrees-of-freedom, DOFs) and  $m_k$  the semi-bandwidth of the stiffness matrix (number of columns from the diagonal to the last non-zero value along a row of the stiffness matrix). In this way, and aiming at obtaining a sparse matrix, a proper numbering algorithm that minimizes the  $m_k$  value of each step was chosen (the mesh nodes should be locally numbered in order to avoid a disperse and large value range

between neighboring nodes). This allows decreasing the computational time and the disk storage space.

As briefly referred in Section 5.1, the static nonlinear analysis allows studying the structure response due to lateral loads, incrementally applied, that aim to represent the seismic action. For each load step increment, an equilibrium condition is calculated until reaching numerical convergence and there are several possible approaches to solve these equilibrium equations. Each iterative method has different assumptions, which can lead to an increase of the number of operations and, consequently, to an increase of the calculation time. In addition, convergence might be influenced by the adopted iterative method. Taking in account these aspects, a test on the iterative methods was performed. The test involved three iterative methods, being the goal to identify the method that offers the faster solution convergence. The three iterative procedures considered were the Newton-Raphson method, the Modified Newton-Raphson method and the BFGS method (secant method). For each of them, the same loading increment strategy (number and size of steps) and numerical model were adopted.

In all the procedures, the total displacement increment  $\Delta u$  (equation 6) is calculated for each iteration after estimating the out-of-balance force  $g_i$  and the incremental displacement  $\delta u_i$ . This value is iteratively modified until equilibrium is achieved, i.e. the prescribed criteria tolerance is obtained [90, 101].

$$\Delta u_{i+1} = \Delta u_i + \delta u_{i+1} \quad (6)$$

$$\delta u_i = K_i^{-1} g_i \quad (7)$$

In the Newton-Raphson method, the stiffness matrix ( $K_i$ , iteration  $i$ ) represents the actual tangential stiffness of the structure (equation 8). For the determination of the incremental displacement (equation 7), a tangential stiffness matrix is calculated for each iteration, through the relation between the out-of-balance force and the adopted iteration displacement. In this way, each iteration is dependent on the information related to the last iteration, even if it is not related to an equilibrium condition (Figure 62a).

$$K_i = \frac{dg}{d\Delta u} \quad (8)$$

The regular Newton-Raphson method is the most used iterative procedure in numerical analysis [101]. It has however some disadvantages, for instance, it is possible to verify that a

large order model is considered in this study and a highly demanding computational time is expected for each iteration, because a new stiffness matrix needs to be calculated. Although, it is also known that due to a continuity property of this numerical approach, a faster convergence (quadratic convergence) is obtained if the stiffness matrix is similar between steps (does not suffer considerable changes). The last can be taken into account by applying smaller load steps increments during the structural behavior analysis, provided that the non-linear problem is well-posed.

In the modified Newton-Raphson method the stiffness matrix is estimated using different assumptions [90]. The tangent stiffness matrix is only calculated each time per load step, which means that its update is always achieved on a converged equilibrium state (Figure 62b). Only the incremental displacement and internal force vector are evaluated for each iteration, see equations (6) and (7). It is known that the Modified Newton-Raphson method converges to an equilibrium solution in a slower way, but each iteration has less computational costs than the regular method, meaning that it can be efficient in large models as the present case study.

The BFGS method, also called as a Quasi-Newton method, was the last one tested. In this method, the inverse stiffness matrix (see equation 7) is not explicit calculated and factorized for each iteration. Information from the out-of-balance iteration force  $g_i$  and from the calculated iterative displacement  $\delta u_i$  is used to estimate a better secant approximation (Figure 62c) of the stiffness matrix. In each iteration it is required to calculate a vector to be used in the stiffness matrix approximation. This vector has the order of the total DOF number. In this way, it is expected that, in case of a high number of iterations are needed to achieve convergence, that a considerable amount of disk space is required to record this data [90, 101].

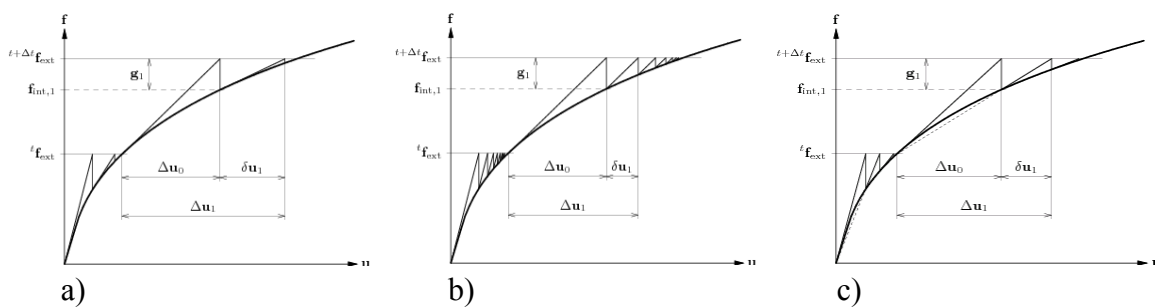


Figure 62 – Iterative methods [90]: a) Regular Newton-Raphson method; b) Modified Newton-Raphson method; c) BFGS method.



For all the iterative procedures just described, the arc-length control method was used. During the iterative process, several numeric problems may arise, mainly, related to a horizontal tangent stiffness matrix (snap-through) and a vertical tangent stiffness (snap-back). To overcome snap-through and snap-back behavior the arc-length changes the displacement based increment. Furthermore, the line search algorithm was also used. If the defined load steps are far away from an equilibrium state, the solution will diverge [102]. The line search algorithm is helpful because it estimates an iterative displacement increment that will possibly provide a faster convergence. Finally, a convergence criterion based on energy and equal to  $1.0 \times 10^{-3}$  was adopted [90].

The preliminary numerical tests were performed using the final finite element model (nonlinear material), but not with the final material properties, as they were not yet available. In these preliminary tests a different value for the compressive strength of masonry was used (1MPa in spite of 8MPa, as is described in Section 5.5). For studying the load-displacement curve two control points were considered: 1, at the top of the West tympanum wall (middle surface); 2, at the top of the main dome wall (Figure 63a and b). The processing time of each iterative method was also registered (Figure 63c). This procedure allows studying the solution accuracy of the methods and to conclude on the one that leads to less computational time (faster convergence). Figure 63b shows that the node 1 has larger displacements, approximately 26mm, for the same  $\alpha$  load coefficient (horizontal load defined as a percentage of the self-weight). In both control nodes, the different solution methods provide similar results.

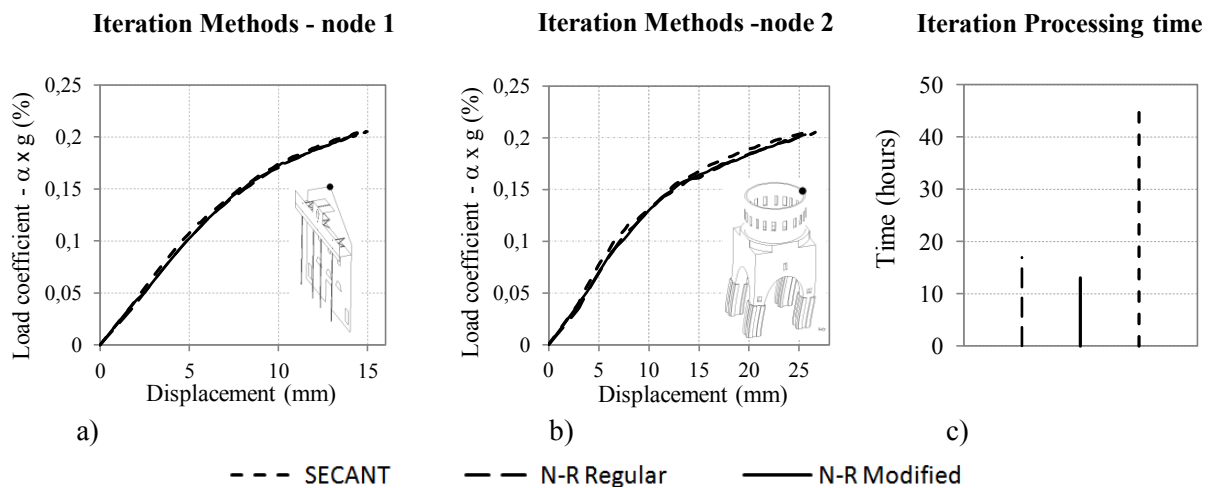


Figure 63 – Iterative methods: (a) Capacity curve in the main dome control node; (b) Capacity curve in the West tympanum wall control node; (c) Processing time.

However, Figure 61c shows evident time differences. A total of 62 load steps was used in all cases and it is possible to conclude that the tangent methods are about 2.5 times faster than the secant method. Furthermore, the Modified Newton-Raphson has a processing time of 13 hours, 4 hours less (i.e. 25% faster) than the Regular Newton-Raphson method (17 hours). Thus, the Modified Newton-Raphson iteration method was adopted for the static nonlinear analysis.

## 5.5 NONLINEAR STATIC ANALYSIS

The nonlinear static, or pushover analysis, was performed by applying a horizontal load proportional to the mass of the structure on the structure under its self-weight. The load direction is in agreement with the global coordinate system of the numerical model and followed the positive and negative axis in the longitudinal direction of the Basilica ( $\pm X$ ). In the transversal direction, only the positive direction was studied ( $+Y$ ) (Figure 64). An analysis in the negative direction along this axis ( $-Y$ ) is redundant because the Basilica has a symmetry axis in this direction. A total of five control nodes were defined for the analysis. The nodes are positioned in elements with higher relative horizontal displacements. These control nodes are identified in Figure 64b. The damage assessment takes in account the maximum principal tensile strains, which is a good indicator of tensile damage (i.e. cracking).

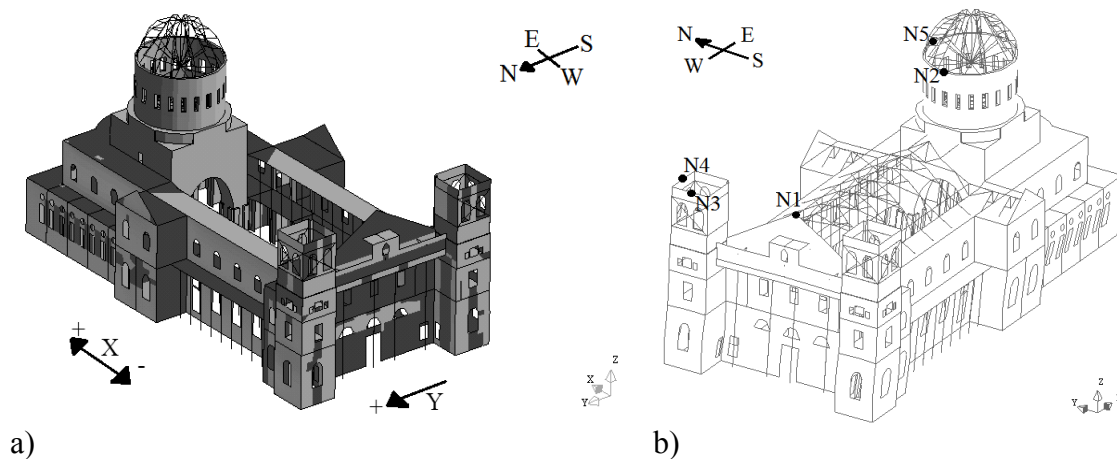


Figure 64 – Pushover analysis: (a) Applied load directions (longitudinal – X; transversal – Y); (b) Control nodes defined.

### 5.5.1 DIRECTION +X

The adopted control nodes for this analysis are located at the West tympanum wall and at the top of the main dome. These points are in agreement with those used in the preliminary numerical analyses. The capacity curves are shown in Figure 65. Both control nodes have a

marked nonlinear behavior, in which the linear limit (initial cracking) occurs for a load factor of about 16%. The top of the tympanum West wall (Node 1) has a slightly larger horizontal displacement than the main dome node (Node 2). A horizontal load of about 30% of the structure self-weight was applied, and a maximum displacement of 30mm for node 1 and 26.3mm for node 2 were obtained. It is also observed in Figure 65a that the capacity curve does not start from the origin position. This was expected, and was already referred in Section 4.3.1, when an out-of-plane movement (negative displacement) was registered due only to vertical loads (self-weight analysis).

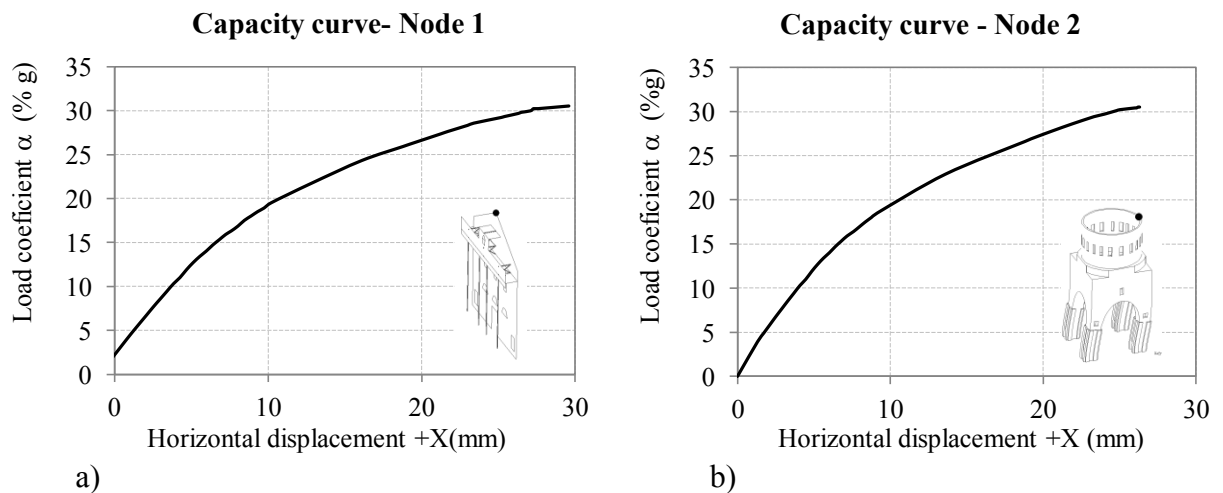


Figure 65 – Capacity curve in +X direction: (a) Node 1; (b) Node 2.

The deformed shape in the positive longitudinal direction is simultaneously represented with the principal tensile strains registered in the South façade walls (Figure 66). It is clear that the larger displacements are located on the top of the elements. However, the horizontal relative displacements do not have a linear increase through the structure height. The first floor walls present the most important in-plane displacement (and damage). This aspect is particularly noted in the deformed shape of the bell tower, where the parabolic shape of the first floor is replaced in height by a linear one. This is due to the added elements in the 2004 strengthening works, i.e. the RC slabs in the bell towers and nave, as well as the steel braces and ring beams of the third bell tower floor improve the seismic behavior of the structure. The principal tensile strains distribution leads to the same conclusion, in which it is observed that the damage concentrates at the first floor walls, i.e. in openings, walls connection (shell elements) and rotunda walls (solid elements).

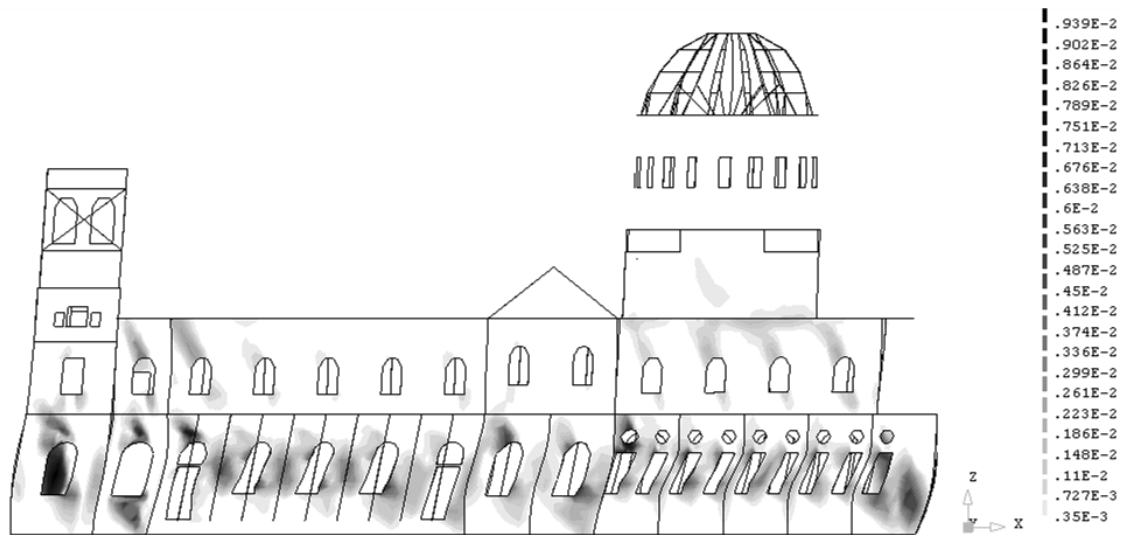


Figure 66 – Principal tensile strains of the south façade walls for a horizontal load of 0.3g in +X direction (the nave roof frame is not represented).

The concentration of damage in walls at the West elevation (Figure 67) is also much relevant. The first floor of the bell towers presents, as aforementioned, a critical behavior. These cracks are developed due to in-plane shear stress and result from the relative displacements between the bell tower storeys. In Figure 68 it is observed that the horizontal in-plane displacement is large in the first story (15mm). The curve of the inter-storey displacements shows this relative difference, which justifies that the shear-cracks are only visible in bell towers' walls of the first and second storeys. On the other hand, the West tympanum wall develops horizontal cracks at the top of the RC slab reinforcement. This damage is in agreement to the expected failure mode, i.e. the out-of-plane movement of a slender element (bending) leads to high stresses, which cause a rotation line, with out-of-plane rocking of the tympanum.

In the solid elements the damage essentially occurs in the rotunda walls and in the four large piers. The piers present two failure modes. The first one is the failure due to the horizontal cracks caused by the uplifting of the foundations. The second one corresponds to the rocking of elements in the piers-arches connection, with a maximum principal stress of  $-7\text{MPa}$  (compression). Once the load direction takes the positive X axis, those stresses are presented on the two piers located at the East side. Nevertheless, for a load factor of 0.30g failure does not occur ( $|7| \text{MPa} < f_{c, \text{masonry}}$ ). In the rotunda the damage is defined by shear cracks in the North and South walls. In fact, the damage is more evident near the second floor opening that allows the passage between the interior arches and exterior balcony.

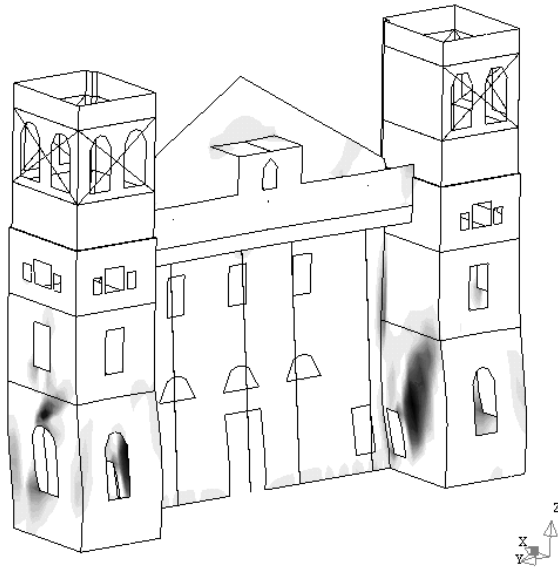


Figure 67– Principal tensile strains for the West façade due to a horizontal load of 0.3g, in +X direction (External surface).

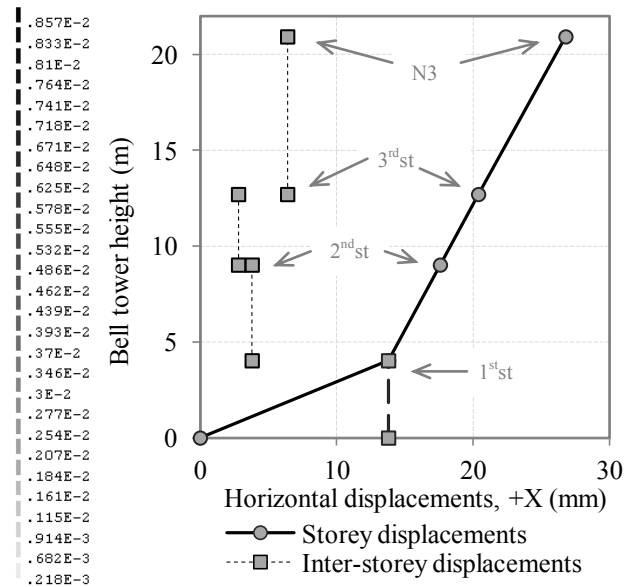


Figure 68 – Bell tower stories' displacements for a horizontal load of 0.3g (+X); (1st: storey; N3: node 3).

### 5.5.2 DIRECTION -X

The maximum horizontal displacement occurs in the top of the bell tower with a value of 30mm. The horizontal displacements decrease to about the half for elements closer of the sacristy. Significant differences in the capacity curve of node 1 are observed, in comparison to the +X direction. The node presents the same maximum displacement but for a load coefficient approximately 5% lower. The same occurs to the initial cracking load, i.e. with a coefficient of 13% rather than 16%. These differences show that the West gable wall has less strength capacity in the -X direction and, consequently, more damage. This can be explained by the confinement action caused by the rotunda walls, which occur in the +X direction (the confinement is only possible due to the modeled roof trusses). This action does not occur for the -X direction, because the out-of-plane movement of the West façade tympanum leads to tensile stresses that cannot be withstand by the rotunda walls, due to the low tensile strength of masonry elements.

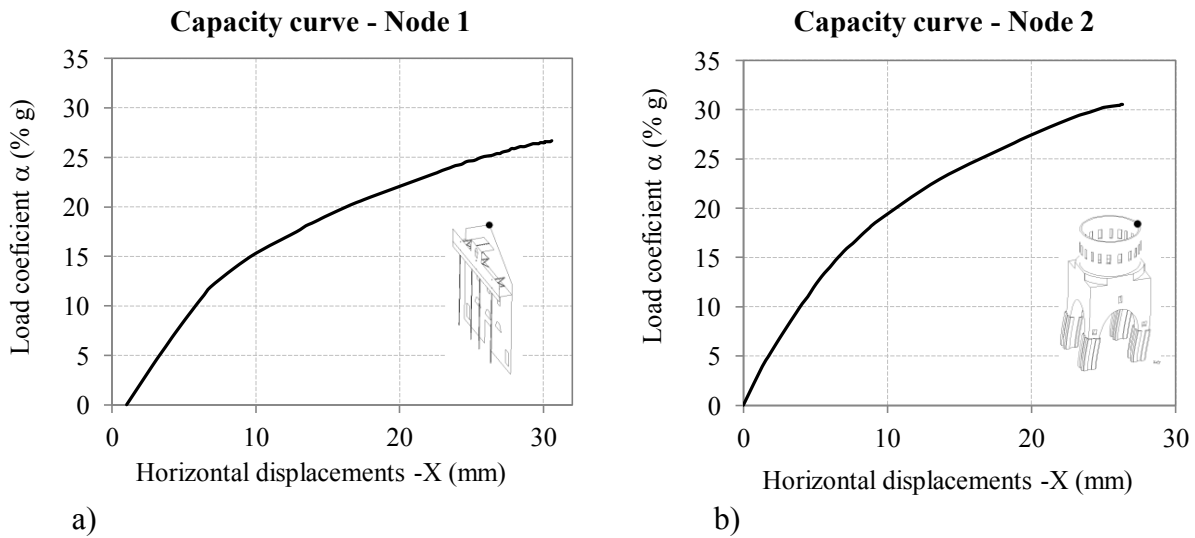


Figure 69 – Capacity curve in -X direction: (a) Node 1; (b) Node 2.

As previously mentioned for the +X direction, it is also possible to observe that the capacity curve does not begin in the origin of the Cartesian coordinate system. In this case the initial point is a positive value (same direction as the load case) and, as already mentioned, this is due to the initial horizontal displacement presented by the node due to vertical loads.

The crack pattern is similar to the one obtained for the +X direction, i.e. a high concentration of cracks in the North, South walls (nave and sacristy) near the openings. It is clear that the damage on the shell elements oriented in the load direction (façade walls) is caused by in-plane shear stresses. Thus, the difference in the -X direction corresponds to the way that cracks propagate (diagonal shear cracks) (Figure 66 and Figure 70).

It is also important to refer another difference in the damage pattern. This is highlighted in Figure 70 and Figure 71 by a dashed circle located in the connection between the South nave and South stairwell wall. This is not related to a shear action but it is instead caused by the push-over action in these elements (tensile stresses). Figure 71 aims to describe the induced damage in the first and second storey RC slabs, where the tensile strength is reached (2 MPa). Thus, if the +X load direction is structurally severe for the bell tower walls, by creating a crack pattern prone to an out-of-plane mechanism, the -X load direction makes it more likely to happen. In fact, for the performed study, a horizontal load of 0.20g (the results of Figure 71 are caused by a 0.27g load, i.e. 27% of the elements self-weight) is the value that initiates cracking to these connections. Similarly to the +X direction, the relative displacements between the storeys of the bell tower are higher between the first and second ones, as seen by

the inter-storey displacements curve of Figure 72. However, even if the horizontal displacement that occurred at the top is 5mm greater (30mm, in comparison to  $\approx 25$ mm), the relative differences are smaller for this direction and consequently the cracks due to in-plane shear stresses occur, but are not as clear as before.

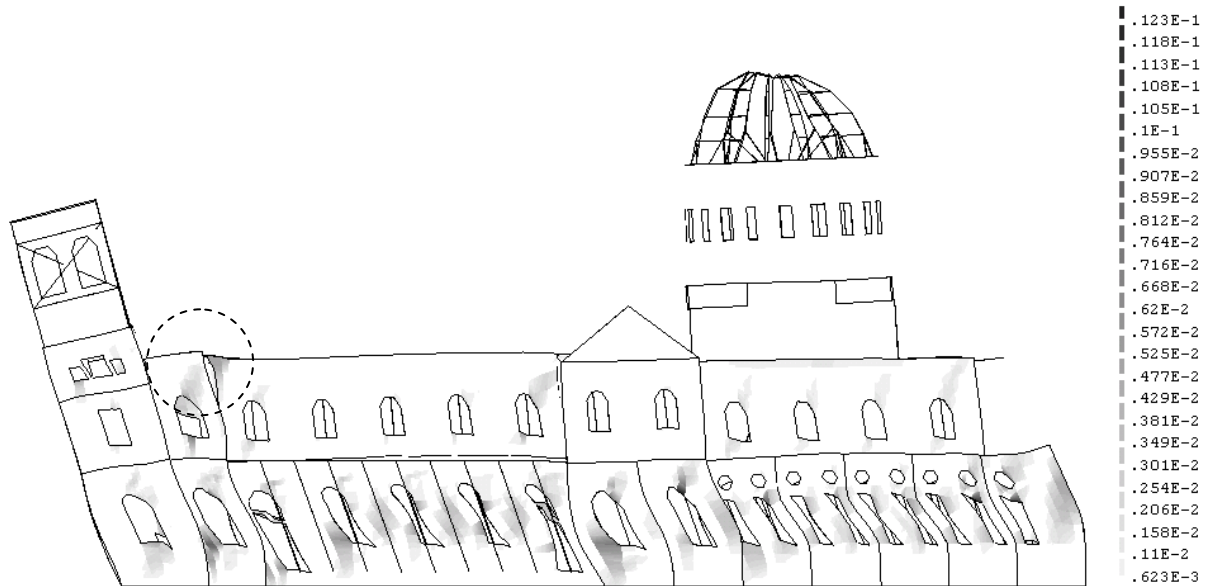


Figure 70 – Principal tensile strains of the South façade walls for a horizontal load of 0.27g in  $-X$  direction (the nave roof frame is not represented).

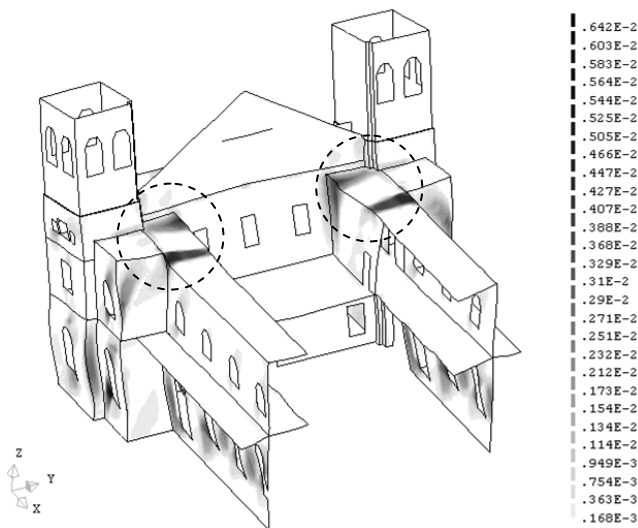


Figure 71 – Side interior view through a North-South cutaway: Principal tensile strains (top Surface) for a horizontal of 0.27g, in direction  $-X$  (top surface).

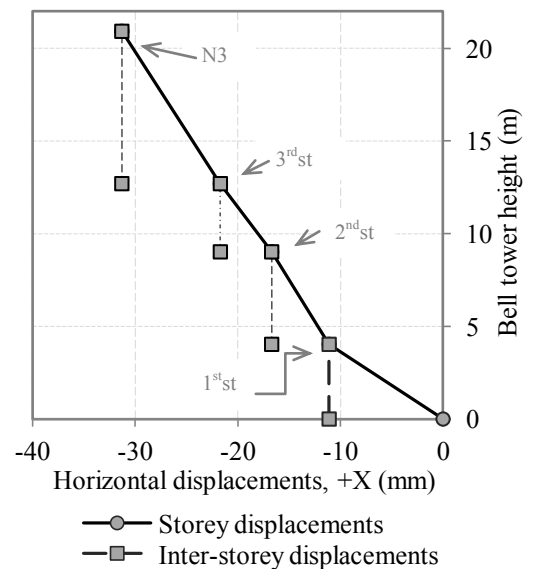


Figure 72 – Bell tower stories' displacements for a horizontal load of 0.27g ( $-X$ ); (st.: storey; N3: node 3).

### 5.5.3 DIRECTION +Y

Concerning the analysis in the direction +Y, it is possible to verify from Figure 73 that control nodes different from the previous analysis were used. Node 1 was not assumed because the gable West wall is transversally positioned with respect to the Y direction. This wall has a high stiffness and a maximum displacement of 12mm is obtained for this action, which is much smaller than the displacements obtained in the X direction. Thus, node 4 and node 5 were taken as control nodes, as they are located in elements that exhibit the maximum horizontal displacement in the Y direction. In Figure 73 it is possible to identify that for the considered capacity curves the initial cracking load ranges from 10% to 13% of the self-weight. For both nodes a maximum load coefficient of 22% was obtained and it is possible to conclude that the main dome node has, for the same load, a less significant nonlinear behavior.

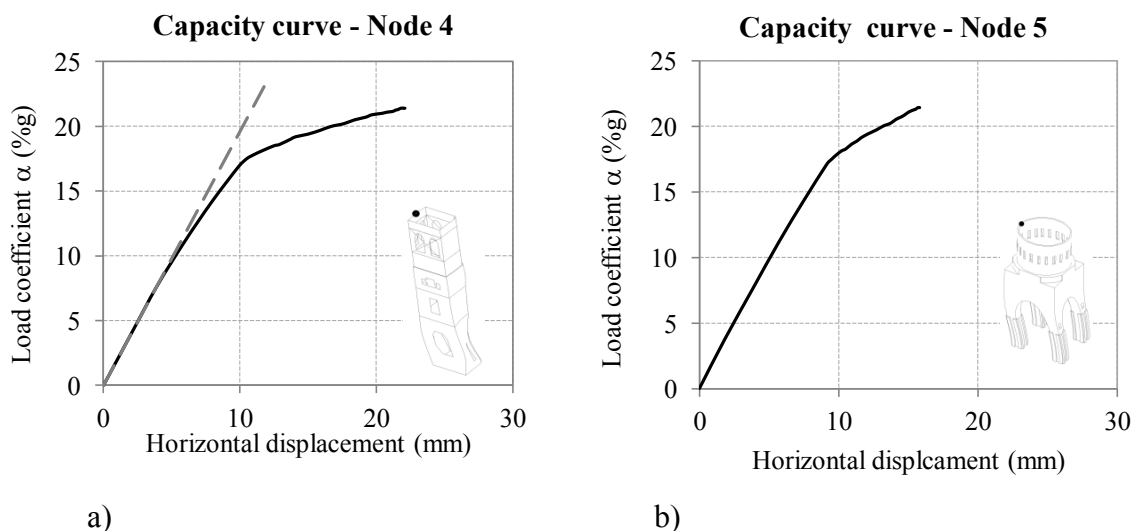
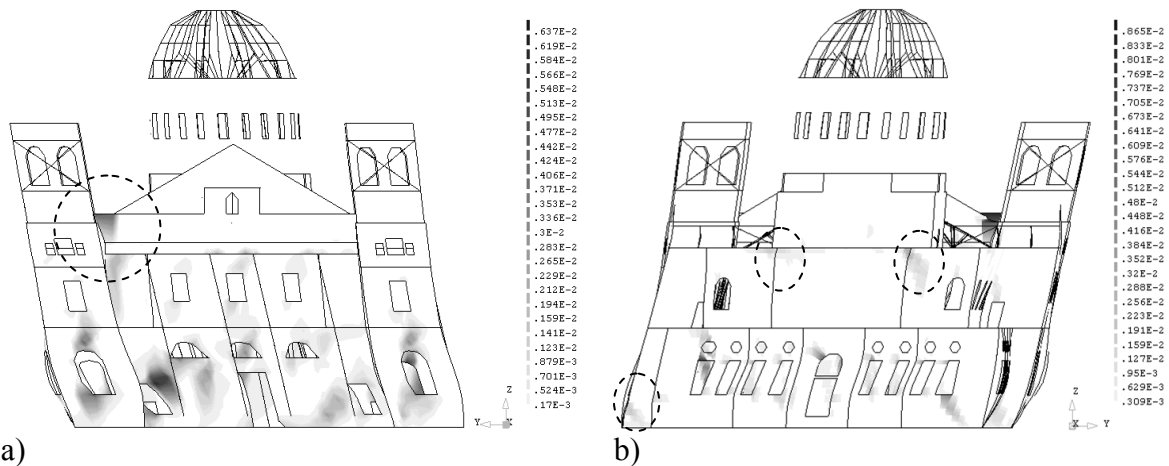


Figure 73 – Capacity curve in +Y direction: (a) Node 4; (b) Node 5.

The main numerical damage obtained from the +Y direction analysis is presented next. Figure 74a indicates with a dashed line the initial cracking occurrence, caused by the concentration of tensile stresses due to the difference of behavior between macro-elements, i.e. the North bell tower has larger displacements than the main West façade wall (if the load had the -Y direction, it would be symmetric). This is valid to the North end of the West entablature and also for the finite elements at the connection between the West façade and North bell tower, where a vertical crack is prone to be active. Nevertheless, for a load coefficient of 22% of the self-weight the demand for tensile action is small, leading to cracking that has by itself no further repercussions on a macro-elements failure collapse. A set of diagonal cracks is also



presented in Figure 74b, due to in-plane shear stresses near the openings of the West and East elevations and near the walls connections, specifically in the transversal walls of the transepts and in the second floor of the East wall (dashed circles).



a) Figure 74 – Principal tensile strains due to a horizontal load in +Y direction: (a) West façade; (b) East façade.

On the other hand, interior damage is also observed. The arrows of Figure 75 show interior damage in the first floor at the transversal bell tower wall, near the arch passage and near the aisle passage of the second floor. Furthermore, diagonal shear cracks are very clear at the transversal walls of the South and North façades. There is no occurrence of toe crushing and, similarly to what occurs in direction X, the difference between displacements of the first and second storeys is considerable, being the main cause of the concentration of shear cracks in both bell tower walls at the first floor level (Figure 76).

In addition to the damage already reported in the transversal direction ( $\pm Y$ ), it is important to address more features. Being the Y axis the less stiff direction of the structure, the control nodes present an analogous horizontal displacement to those seen in the  $\pm X$ , but for a lower load coefficient. As expected, there is lower capacity to dissipate energy, as it is easily observed in Figure 77a by the damage of the transversal interior walls. The same cracking pattern appears at the exterior walls of the North transept (Figure 77b). This makes possible an out-of-plane movement of the North sacristy wall and transept façade, which can be mainly prevented by the four large piers and the structure longitudinal walls.

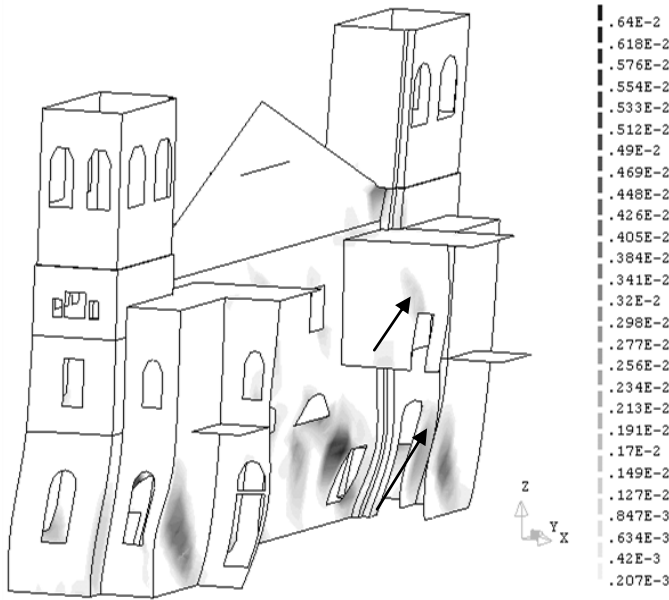


Figure 75 – Side interior view through a north-south cutaway: Principal tensile strains (external surfaces to façades, top surfaces of slabs and North surfaces to interior walls), direction +Y (interior damage, pointed out by the arrows).

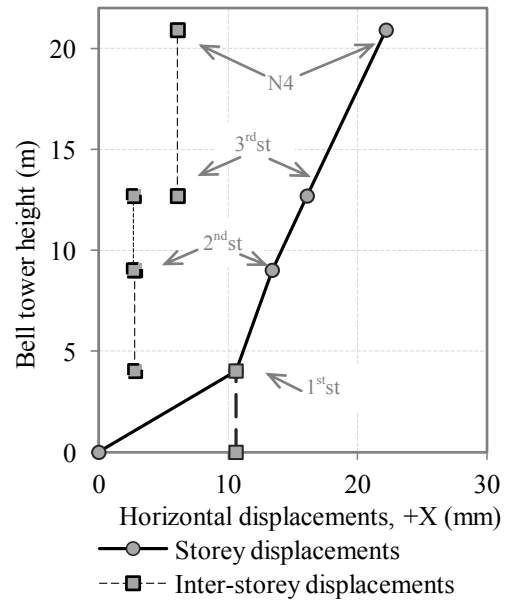


Figure 76 – Bell tower storeys' displacements (+Y); (1st.: storey; N4: node 4).

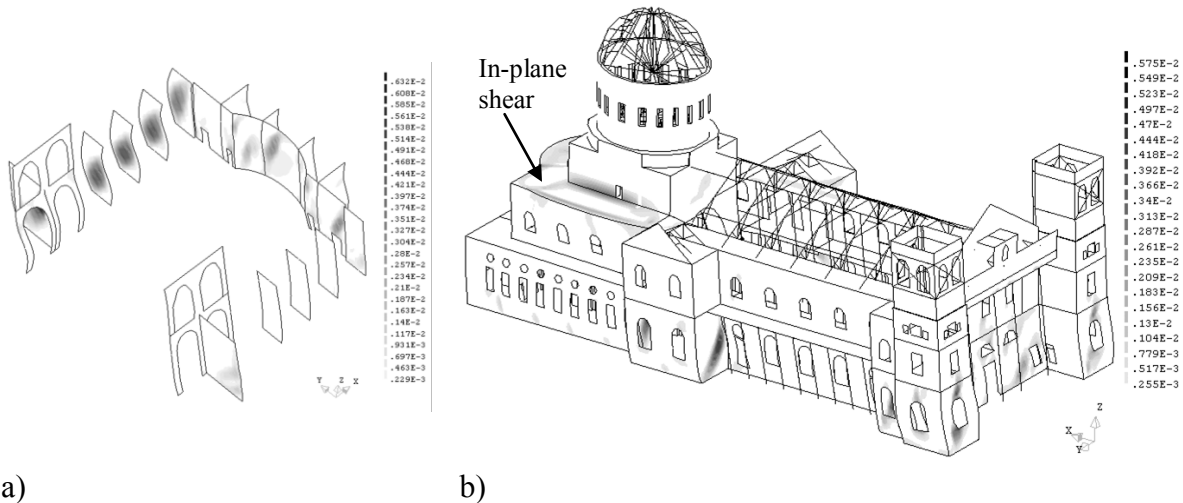


Figure 77 – (a) Damage at the interior transverse walls; (b) Global overview of the damage in the north elevation.

It is also noted that a good connection between elements must be guaranteed to improve the distribution of horizontal loads. The so-called box behavior, which is presented in the Basilica (at least in the numerical model) has also a decisive role. This structural effect due to a diaphragm action is quite atypical in historical constructions [103], but has an important effect

in the maintenance of the façades stability. The in-plane stiffness avoids flexible movements of the façades (even if it increases the stresses between the façades-slab connections) and allows lower vertical displacements in the RC slabs. For instance, and as represented in Figure 77b, the tensile stresses of 3MPa (top surface) leads to the cracking located at the second floor slab near the North rotunda wall. It is also possible to observe a diagonal in-plane shear crack (see arrow). This damage is mainly explained by the relative difference of stiffness and consequently of vertical displacements between the shell façades and solid elements, seen in the analysis of the structure due to its self-weight (Section 4.3.1).

Finally, the South, East and West rotunda wells also present cracking, even if not so meaningful. The same occurs in the four large piers, which present horizontal cracking due to tensile stresses caused by the outward movement (bending).

## **5.6 FINAL REMARKS**

After the nonlinear static analysis, it is possible to put forth several final remarks about the structural behavior of the Christchurch Catholic Basilica due to horizontal loads. The weaker direction of the structure is the Y one (transversal direction), as the maximum applied load coefficient is equal to 20% and 30% for the transversal and longitudinal directions, respectively. This analysis enables to obtain the cracks patterns and failure mechanisms. According to the latter, several in-plane and out-of-plane mechanisms were observed, caused by in-plane shear stresses and orthogonal loads, respectively.

The areas with concentration of damage are the two bell towers, the interior and transept walls transversally positioned, the top of the West gable wall, the North and South walls of the rotunda, and the second floor RC slab near to the rotunda walls. Furthermore, cracks were observed near the openings throughout all the external façades of the structure and at the interior walls and RC slabs, which were not considered in the calibration process at Section 4.4.2 (interior damage was not inserted in the damaged numerical model, because it is unknown).

It is also important to highlight that the obtained damage in the four piers are caused by tensile stresses due to the bending action. The piers do not present large inelastic areas or high displacements at the top. The main reason can be related with the high stiffness of the piers that leads to lower horizontal displacements at its top. The normal ratio (height / transversal

dimension) for Cathedral piers ranges 7 or 8 [92] but, in this case, the ratio is about 3 (only the non-confined zone was taken into account, i.e. the first floor).

Finally, the elements of the main dome wall do not present any relevant damage which leads to the conclusion that the installed RC ring beams have an effective action. In general, it is possible to conclude that the damage obtained from the numerical model is in reasonable agreement with the observed crack pattern after the series of earthquakes. The model also indicates that the structure is unsafe for an earthquake such as the one experienced, so significant damage would be expected.

# Chapter 6

## Conclusions and Future Works

### 6.1 CONCLUSIONS

Cultural heritage buildings have an intangible contribution and importance in terms of cultural and social enrichment, besides the obvious tangible contributions. The reflection made in Chapter 2 allows highlighting the inherent consequences of a sudden collapse of these structures. The collected examples and moreover the adopted decisions do not allow to create, by themselves, a methodology to the question of how to act in cases of cultural heritage sudden collapse. In fact, the different variables that contribute to the definition of value and significance make harder the final decision. Still, it is possible to affirm that social, technical and economical matters have a substantial weight in this decision.

In the present study, the seismic performance of the Christchurch Catholic Basilica (New Zealand) was studied and the main issues are related to technical and economic criteria. The earthquake sequence of 2011 led to severe damage in the Basilica's structure. The decision between partial, total reconstruction (strengthening strategies) or demolition is highly dependable of the structural assessment. In this way, a FEM model of the Christchurch Catholic Basilica was prepared. The calibration of the numerical model, based on the experimental results obtained from the dynamic identification tests, was the initial purpose. Therefore, several numerical models were prepared, taking into account the damage that the structure presented. However, none of the models seems reasonable to guarantee a proper model calibration and one possible cause is the unknown interior damage, which was not represented. Seismic assessment was performed in a non-calibrated Basilica's FEM model and through a pushover analysis, by considering only the non-linear material behavior. Three analyses were carried out ( $\pm X$  and  $Y$ ), and the assumed material properties followed the literature and NZ authorities recommendations. As the numerical model is very large, some studies were carried out on the proper choice for the mesh refinement and the iterative method to be used in nonlinear analysis. The Modified Newton-Raphson was selected, taking into account the required analysis time.

The seismic assessment was useful to obtain the crack patterns and to identify the most vulnerable elements. The structural strengthening performed in 2004 have a decisive role to avoid more damage, mainly to the West façade walls but also to prevent the local failure mechanisms, i.e. a structure without box behavior. It is possible to define the bell towers (slender elements) as the more vulnerable ones, as they present high damage for all the studied directions. Furthermore, the damage of the rotunda walls, the four piers, the second floor RC slab and the elements around openings throughout the North, South and East (even with less relative importance) elevations is also highlighted. The main causes of damage are in-plane shear stresses (diagonal cracks), pure tensile action (tensile strength is reached), in-plane cracking due to bending stresses and base uplifting of the piers (due to rocking).

It is concluded that the weaker direction of the structure is the transversal one (Y). The maximum applied coefficient load (self-weight percentage) is equal to 20% and 30% in the transversal and longitudinal directions, respectively. Finally, it is important to stress the good agreement between the numerical and real damage. The numerical results support the initial idea that the interior damage, specifically the interior walls and RC slabs, have a significant effect in the calibration process. The damage is mainly located in the South and North walls, which were the elements that presented an out-of-plane movement that was hardly adjustable in the calibration.

## **6.2 FUTURE WORKS**

Two main tasks are proposed to be developed in future works:

- (1) The first one is to change the mesh refinement and the adopted types for the finite elements discretization, i.e. use elements with 20 and 15 nodes for solid elements, 8 and 6 nodes for shells and 3 nodes for beam elements. These aims to improve the convergence of the nonlinear static analysis, allowing obtaining the post-peak response of the structure.
- (2) Taking into account the modified undamaged model, another task is to study different strengthening interventions. The crack patterns and the capacity curves will be compared in order to achieve safer solutions, also taking into consideration the cost of the works proposed.







# REFERENCES

- [1] M. F. Bernanard, *Conservation of Historic Buildings*, 3rd ed., pp. (1-9). Elsevier Ltd: Architectural Press, 2003.
- [2] "Environmental Policy and Planning Unit Christchurch City Council," [10/03/2013; <http://resources.ccc.govt.nz/files/HeritageConservationPolicydocs.pdf>.
- [3] D. Watt, *Surveying Historic Buildings*, 2nd ed.: DonHead, 2011.
- [4] P. Roca, "The study and Restoration of Historical Structures: From Principles to Practice." pp. 9-25.
- [5] E. Verstrynge, L. Schueremans, D. Van Gemert *et al.*, "Modelling and analysis of time-dependent behaviour of historical masonry under high stress levels," *Engineering Structures*, vol. 33, no. 1, pp. 210-217, 2012.
- [6] "Heritage Listings - Christchurch City Council," [10/03/2003; <http://resources.ccc.govt.nz/files/HeritageListings-docs.pdf>.
- [7] A. Russell, Ingham, J., and Griffith, M., "Comparing New Zealand's Unreinforced Masonry Details with those Encountered in Other Seismically Active Countries," *7th International Masonry Conference*, 30 October - 1 November, 2006.
- [8] G. Milania, P. B. Lourenço, and A. Trallia, "3D homogenized limit analysis of masonry buildings under horizontal loads," *Engineering Structures*, vol. 29 (11), pp. 3134-3148, 2007.
- [9] G. Croci, "The Conservation and structural restoration of Architectural Heritage," *Advances in Architecture*, vol. 1, pp. 251, 1998.
- [10] A. F. Alba, "Teoria e historia de la restauracion," *Master de restauracion y rehabilitacion del patrimonio. Editorial Munilla.*, no. 1, pp. 269, 1997.
- [11] P. Roca, "The Study and Restoration of Historical Structures: From Principles to Practice," in *Structural Analysis of Historical Construction New Delphi 2006*, pp. 9-25.
- [12] J. Jokilehto, "Definition of Cultural Heritage References to documents in history," *ICCROM Working Group 'Heritage and Society*, 2005.
- [13] M. B. Armaly, Carlo; Hannah, Lawrence "Stari Most: rebuilding more than a historic bridge in Mostar," *Museum International* vol. 56, pp. 103, December, 2004.
- [14] L. T. Krstevska, Lj.; Kustura, M, "Ambient vibration testing of old bridge in Mostar. Protection of Historical Buildings," *Conference on Protection of Historical Buildings* vol. 1, pp. 10, 21-24 JUNE, 2009.
- [15] "Detailed Analysis of the Design Issues. Rehabilitation Design of the Old Bridge of Mostar," [http://www.gen-eng.florence.it/starimost/04\\_archany/04e\\_others/others.htm](http://www.gen-eng.florence.it/starimost/04_archany/04e_others/others.htm).
- [16] A. Curry, "Cronwning glory " *smithsonianmag.com* vol. 36, no. 12, pp. 92-94, March, 2006.
- [17] W. Jäger, "A short summary of the history of the Frauenkirche in Dresden," *Construction and Building Materials*, vol. 17, no. 8, pp. 641-649, 2003.
- [18] F. Pohle, and W. Jäger, "Material properties of historical masonry of the Frauenkirche and the masonry guideline for reconstruction," *Construction and Building Materials*, vol. 17, no. 8, pp. 651-667, 2003.
- [19] A. Clayton, "War and Faith in Dresden," *History Today*, vol. 47, no. 4, April, 1997.
- [20] "Warsaw Uprising 1944," [10/03/2013; <http://www.warsawuprising.com/>.
- [21] "Old Town Warsaw," <http://www.scrapbookpages.com/Poland/Warsaw/Warsaw02.html>
- [22] A. Wójcik, M. Bilewicz, and M. Lewicka, "Living on the ashes: Collective representations of Polish-Jewish history among people living in the former Warsaw Ghetto area," *Cities*, vol. 27, no. 4, pp. 195-203, 2010.
- [23] *Heritage at Risk*, International Council on Monuments and Sites, 2010.
- [24] S. Weinberger. "Researchers Say They Can Restore 1 of Destroyed Bamiyan Buddhas," 02/02/2013; <http://www.aolnews.com/2011/03/01/researchers-say-they-can-restore-1-of-destroyed-bamiyan-buddhas/>.
- [25] A. O. Sidi, "Maintaining Timbuktu's unique tangible and intangible heritage," *International Journal of Heritage Studies*, vol. 18, no. 3, pp. 324-331, 2012.

- [26] E. Greenspan, "A global site of heritage? Constructing spaces of memory at the World Trade Center site," *International Journal of Heritage Studies*, vol. 11, no. 5, pp. 371-384, 2005.
- [27] "One World Trade Center," [10/03/2013; <http://www.wtc.com/about/freedom-tower>.
- [28] "'Freedom Tower (New York)," *Glass Steel and Stone*," [10/03/2013; <http://www.glassteelandstone.com/BuildingDetail/439.php>.
- [29] R. M. "Remembering to forget: sublimation as sacrifice in war memorials," *The Art of Memory*, K. S. Forty A, ed., p. 131, Oxford: Berg, 1999.
- [30] P. J. Gough, "'Invicta pax' Monuments, Memorials and peace: An Analysis of the Canadian Peacekeeping Monument, Ottawa.," *International Journal of Heritage Studies*, vol. 8, no. 3, pp. 201-223, 2002.
- [31] L. L. Ramos, P. B. , "Análise das Técnicas de Construção Pombalina e Apreciação do Estado de Conservação Estrutural do Quarteirão do Martinho da Arcada.," *Engenharia Civil* vol. 7, pp. 35-46, 2000.
- [32] H. Murteira, "A Place for Lisbon in Eighteenth Century Europe: Lisbon, London and Edinburgh a town-planning comparative study", Architecture, University of Edinburgh, 2004.
- [33] T. Maria, "Reabilitação de edifícios pombalinos. Análise experimental de paredes de frontal," Universidade do Minho, 2010.
- [34] A. S. Pereira, "The Opportunity of a Disaster: The Economic Impact of the 1755 Lisbon Earthquake," *The Journal of Economic History*, vol. 69, no. 02, pp. 466-499, 2009.
- [35] L. F. Ramos, and P. B. Lourenco, "Modeling and vulnerability of historical city centers in seismic areas: a case study in Lisbon," *ENG STRUC*, vol. 26, no. 9, pp. 16-16, 2004.
- [36] M. Lopes, "Construção Pombalina: Património histórico e estrutura sísmo-resistente," in 8º Congresso de Sismologia e Engenharia Sísmica Universidade de Aveiro, 2010, pp. 15.
- [37] F. V. F. L. Mayer, "Estrutura Geral de Custos em Obras de Reabilitação de Edifícios," Instituto Superior Técnico - Universidade Técnica de Lisboa, 2008.
- [38] M. J. Goulão, "Déstruction, reconstruction, préservation: le cas du Chiado, à Lisbonne," *Les Ateliers des interprètes: revue européenne pour étudiants en histoire de l'art*, no. 3, pp. 28-39, 1991.
- [39] C. J. L. Balsas, "City Centre Revitalization in Portugal: A Study of Lisbon and Porto," *Journal of Urban Design*, vol. 12, no. 2, pp. 231-259, 2007/06/01, 2007.
- [40] Á. Siza, *A Reconstrução do Chiado Lisboa*, 2nd ed., 2000.
- [41] D. F. B. Martins, "Renovação e Reabilitação de interiores de Quarteirão na Baixa do Chiado," Instituto Superior Técnico, 2008.
- [42] J. P. Henriques, "Masonry under compression : failure analysis and long-term effects," Escola de Engenharia, Universidade do Minho, 2005.
- [43] B. Anzani A., L., Mirabella Roberti G., "The Effect of Heavy Persistent Actions into the Behaviour of Ancient Masonry," *Materials and Structures*, pp. 251-261, 2000.
- [44] D. Ferretti, and Z. P. Bažant, "Stability of ancient masonry towers: Moisture diffusion, carbonation and size effect," *Cement and Concrete Research*, vol. 36, no. 7, pp. 1379-1388, 2006.
- [45] P. M. Smith, "A concise history of New Zealand," Cambridge Concise Histories Series, 2012.
- [46] "Cook, James (1728-1779) F.R.S.," [10/03/2013]; <http://www.anbg.gov.au/biography/cook-james.html>.
- [47] "The Endeavour," [10/03/2013; <http://www.anmm.gov.au/site/page.cfm?u=1372>.
- [48] J. Wilson, "Government and nation – The origins of Nationhood," *Te Ara – The Encyclopedia of New Zealand*, 2009.
- [49] P. a. H. Boxall, Peter, "Strategy and Trade Union Effectiveness in a Neo-liberal Environment " *British Journal of Industrial Relations*, vol. 35, no. 4, pp. 567–591, 1997.
- [50] B. Easton, "Economic history - Interwar years and the great depression," *Te Ara - the Encyclopedia of New Zealand*, 2010.
- [51] "The Fund for Peace, The Failed States Index," [10/03/2003; <http://ffp.statesindex.org/rankings-2012-sortable>.
- [52] "Corruption by Country/Territory," [10/03/2013; <http://www.transparency.org/country>.

- [53] "OECD Better Life Index," [10/03/2013; <http://www.oecdbetterlifeindex.org/countries/new-zealand/>].
- [54] D. B. Wynn-Williams, "The Basilicas of F.W. Petre," University of Canterbury, 1982.
- [55] "Darfield (Canterbury), September 4 2010," [10/03/2013; <http://www.geonet.org.nz/earthquake/historic-earthquakes/top-nz/quake-13.html>].
- [56] P. Hamilton, "Francis Petre, 1847–1918: An Investigation into New Zealand Architectural Biography," University of Auckland, 1986.
- [57] L. Locations. "Christchurch City Libraries "; <http://christchurchcitylibraries.com/heritage/photos/>
- [58] J. M. Leite, Nuno; Lourenço, Paulo B., *Ambient Modal Analysis of the Cathedral of the Blessed Sacrament, Christchurch, New Zealand*, Report 11-DEC/E-35, 2011.
- [59] D. I. Dizhur, Jason; Moon, Lisa; Griffith, Mike; Schultz, Arturo; Senaldi, Ilaria; Magenes, Guido; Dickie, Jocelyn; Lissel, Shelley; Centeno, Jose; Ventura, Carlos; Leite, João C.; Lourenço, Paulo B., "Performance of Masonry Buildings and Churches in the 22 February 2011 Christchurch Earthquake' " *Bulletin of the New Zealand Society for Earthquake Engineering*, vol. 44, no. 4, December, 2011.
- [60] D. Dizhur, Ismail, N., Knox, C., Lumantarna, R. & Ingham, J. , "Performance of unreinforced and retrofitted masonry buildings during the 2010 Darfield earthquake," *Bulletin of the New Zealand Society for Earthquake Engineering*, vol. 43, no. 4, pp. 321-339, 2010.
- [61] M. B. Anagnostopoulou, Michel; Gavin, Henry P. , "Performance of Churches during the Darfield Earthquake of September 4, 2010," *Bulletin of the New Zealand Society for Earthquake Engineering*, vol. 43, no. 4, pp. 374-381, 2010.
- [62] K. Gledhill, Ristau, J., Reyners, M., Fry, B., Holden, C. , "The Darfield (Canterbury, NewZealand) Mw 7.1 Earthquake of September 2010: A Preliminary Seismological Report," *Seismological Research Letters*, vol. 82, no. 3, pp. 378-386, May/June, 2011.
- [63] D. Alexander, "A tale of three cities and three earthquake disasters," *Tarfter Journal*, no. 50, August, 2012.
- [64] B. A. B. a. M. Cubrinovski, "Near-source Strong Ground Motions Observed in the 22 February 2011 Christchurch Earthquake," *Seismological Research Letters*, vol. 82, no. 6, pp. 853-865, November/December 2011.
- [65] J. Berrill, "Some Aspects of the M6.3 February 22nd Earthquake," Civil Engineering, University of Canterbury, 2011.
- [66] G. A. M. R. P. Dhakal, "Lessons from the February 2011 M6.3 Christchurch Earthquake." p. 8.
- [67] "Christchurch Earthquake Fact Sheets 2011. IPENZ Engineers New Zealand," [10/03/2013; <http://www.ipenz.org.nz/ipenz/forms/pdfs/ChChFactSheets-Overview.pdf>].
- [68] J. B. Lester, A.; Ingham, J., "Christchurch Cathedral of the Blessed Sacrament: Lessons learnt on the Stabilization of a Significant Heritage Building," in 2012 Annual Technical Conference Christchurch, New Zealand 2012.
- [69] J. R. Lester, A. G. Brown, and J. M. Ingham, "Stabilisation of the Cathedral of the Blessed Sacrament following the Canterbury earthquakes," *Engineering Failure Analysis*, 2013.
- [70] "Resource Management Act 1991," [10/03/2013; <http://www.legislation.govt.nz/act/public/1991/0069/latest/DLM230265.html>].
- [71] "Building Act 2004," [10/03/2013; <http://www.legislation.govt.nz/act/public/2004/0072/latest/DLM306036.html>].
- [72] "Civil Defence Emergency Management Act 2002," [10/03/2013; <http://www.legislation.govt.nz/act/public/2002/0033/latest/DLM149789.html>].
- [73] K. B. Warwick D. Smith, "Earthquake Hazard in New Zealand: Inferences from Seismology and Geology," *Seismological Observatory bulletin S*, 306., pp. 223-242, 1986.
- [74] G. M. Mark Stirling, Matthew Gerstenberger, Nicola Litchfield, Russ Van Dissen, Kelvin Berryman, Philip Barnes, Laura Wallace, Pilar Villamor, Robert Langridge, Geoffroy Lamarche, Scott Nodder, Martin Reyners, Brendon Bradley, David Rhoades, Warwick Smith, Andy Nicol, Jarg Pettinga, Kate Clark, and Katrina Jacobs "National Seismic Hazard Model for New Zealand: 2010 Update," *Bulletin of the Seismological Society of America*, vol. 102, no. 4, pp. 1514-1542, August 12, 2012.

- [75] "GNS Science Consultancy Report 2011," [10/03/2013; [http://canterbury.royalcommission.govt.nz/vwluResources/SEI.GNS.0002D.pdf/\\$file/SEI.GNS.0002D.pdf](http://canterbury.royalcommission.govt.nz/vwluResources/SEI.GNS.0002D.pdf/$file/SEI.GNS.0002D.pdf)].
- [76] "A Safer New Zealand. IPENZ Engineers New Zealand.," [10/03/2013; <http://www.ipenz.org.nz/news-policy/Documents/NaturalHazards2012.pdf>].
- [77] P. C. f. t. Environment., "Historic and Cultural Heritage Management in New Zealand," 1996, p. 93.
- [78] *The Concise Oxford Dictionary*, H. W. F. a. F. G. Fowler, ed., 1976.
- [79] "Manual de Desconstrucció (Institut de Tecnologia de la Construcció de Catalunya)," [10/03/2013; <http://www20.gencat.cat/docs/arc/Home/LA Agencia/Publicacions/Residus%20de%20la%20construccio/desconstr.pdf>].
- [80] B. G. M. E. Rinker, "A guide to deconstruction. ," 2003, p. 93.
- [81] C. Gates. "Cardboard cathedral 'will go ahead'," November 2, 2012; <http://www.stuff.co.nz/national/christchurch-earthquake/6118504/Cardboard-cathedral-will-go-ahead>.
- [82] D. B. Johnston, Julia; Paton, Douglas "Multi-agency community engagement during disaster recovery: Lessons from two New Zealand earthquake events," *Disaster Prevention and Management* vol. 21, no. 2, pp. 252 - 268, 1992.
- [83] L. E. S. E. S T, Yeung; S W, Chan "Strike a Balance – Repair or Replace ?," *Advanced Materials Research* vol. Volume 133-134, pp. 997-1002, 2010.
- [84] A. Orduña , and P. B. Lourenço, "Limit analysis as a tool for the simplified assessment of ancient masonry structures," pp. 511-520, *Historical Constructions*, 2001.
- [85] A. Brencich, and L. S., "A macroelement dynamic model for masonry shear walls," *Proceedings of the Fourth Int. Symposium on Computer Methods in Structural Masonry (STRUMAS), Firenze*, 1997.
- [86] G. Box, and N. R. Draper, *Empirical Model-Building and Response Surfaces*: John Wiley & Sons, 1987.
- [87] E. Oñate, *Structural Analysis with the Finite Element Method – Linear statics: Basis and solids*, Lecture Notes on Numerical Methods in Engineering and Sciences, Springer-Verlag. Berlin, Germany, 2009.
- [88] F. Teixeira-Dias, J. Pinho-da-Cruz, R. A. Fontes Valente *et al.*, *Método dos Elementos Finitos - Técnicas de Simulação Numérica em Engenharia*, 2009.
- [89] P. B. Lourenco, "Computational Strategies for masonry structures," Delft University of Technology, PhD Thesis, 1996.
- [90] TNO, "DIANA, Displacement method ANALyser," *User's Manual, Release 9.4. The Netherlands.*, 2009.
- [91] P. B. Lourenço, Gregorczyk, P. , "A2F - A filter from AutoCad to Femgv, ," *Diana World*, 2000(2), p. 11-13 (2000). 2000.
- [92] P. Roca, M. Cervera, L. Pelà *et al.*, "Continuum FE models for the analysis of Mallorca Cathedral," *Engineering Structures*, vol. Volume 46, pp. 653-670, January 2013.
- [93] S. Russo, "Testing and modelling of dynamic out-of-plane behaviour of the historic masonry façade of Palazzo Ducale in Venice, Italy," *Engineering Structures*, vol. Volume 46, pp. 130-139, January 2013.
- [94] A. Arêdê, C. Almeida, A. Costa *et al.*, "Dynamic identification and seismic analysis of the 'Serra Do Pillar' Monastery Church," *Proceedings of SPIE*, vol. Vol. 4753(2), pp. 1237-1243, 2001.
- [95] S. E. Benzley, E. Perry, K. Merkley *et al.*, "A comparison of all hexagonal and all tetrahedral finite element meshes for elastic and elasto-plastic analysis," *Proceedings, 4th International Meshing Roundtable, Sandia National Laboratories*, pp. 179-191, October 1995.
- [96] Ana S. Araújo, Paulo B. Lourenço, D. V. Oliveira *et al.*, "Seismic Assessment of St James Church by Means of Pushover Analysis – Before and After the New Zealand Earthquake " *The Open Civil Engineering Journal*, vol. 6, pp. 160-172, 2012.
- [97] M. Boonpichetvong, and J. G. Rots, "Fracture Analyses of Walls Under Non-Proportional Loadings," in *5th International conference on fracture mechanics of concrete and concrete structures*, 2004, pp. 941-948.

- 
- [98] Z. Bazant, and J. Planas, "Fracture and size effect in concrete and other quasi-brittle materials," *CRC Press, Boca Raton, Florida.*, 1998.
- [99] N. Mendes, "Seismic Assessment of Ancient Masonry Buildings: Shaking Table Tests and Numerical Analysis," *Engenharia Civil, Escola de Engenharia, Universidade do Minho*, 2012.
- [100] P. B. Lourenço, "Recent advances in masonry structures: Micromodelling and homogenisation.," *Multiscale Modeling in Solid Mechanics: Computational Approaches*, U. Galvanetto and M. H. F. Aliabadi, eds., pp. 251-294, Imperial College Press, 2009.
- [101] K. J. Bathe, *Finite Element Procedures*, Upper Saddle River, New Jersey: Prentice-Hall, 1996.
- [102] M. Bashir-Ahmed, and S. Xiao-zu, "Arc-length technique for nonlinear finite element analysis," *Journal of Zhejiang University SCIENCE*, vol. 5(5), pp. 618-628, 2004.
- [103] P. B. Lourenço, N. Mendes, L. Ramos *et al.*, "Analysis of masonry structures without box behaviour," *International Journal of Architectural Heritage*, vol. 5, no. 4-5, pp. 369-382, 2011.

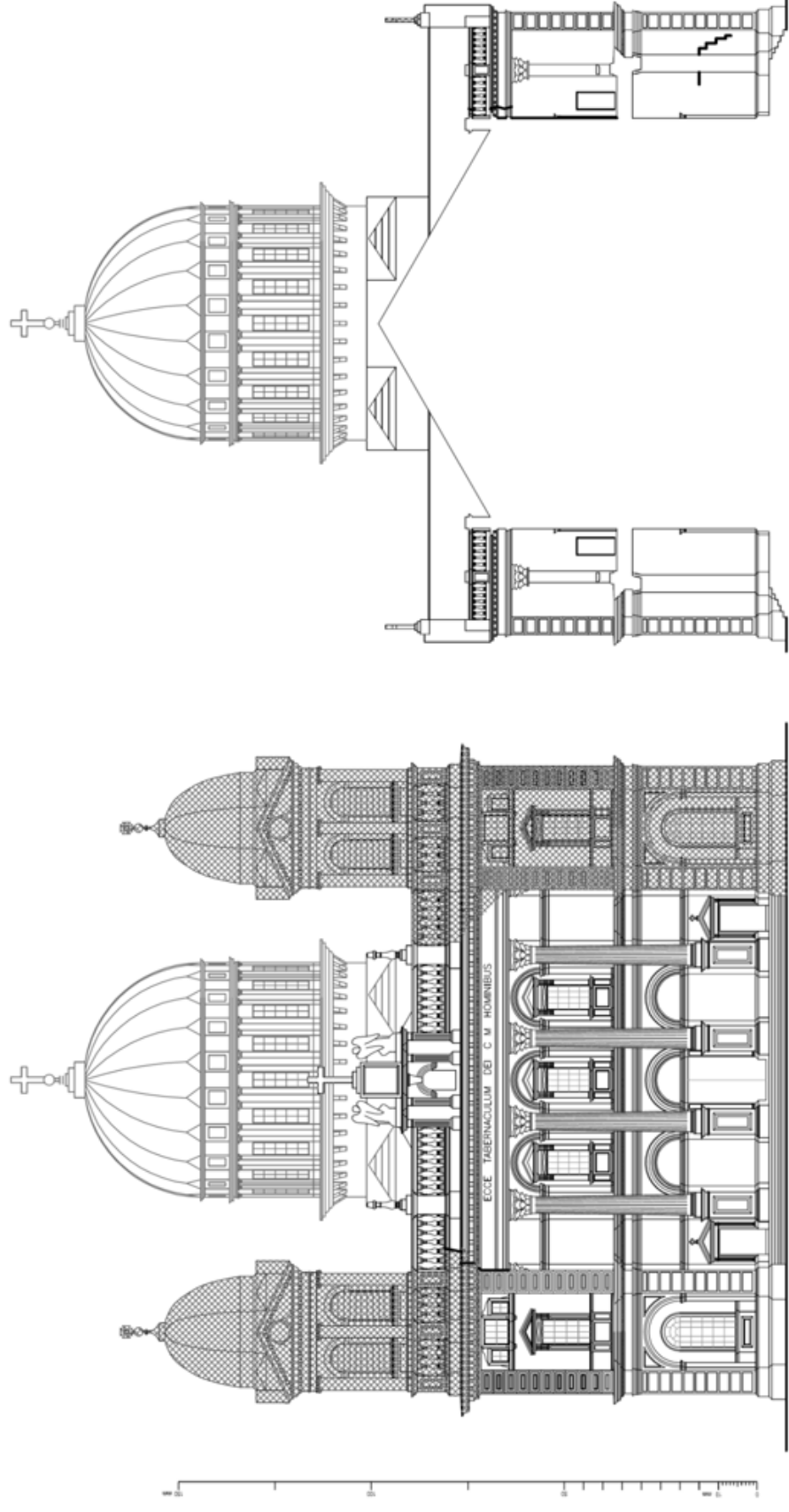


# **ANNEX A**

## **Damage Assessment**





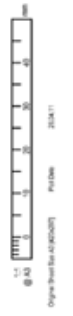


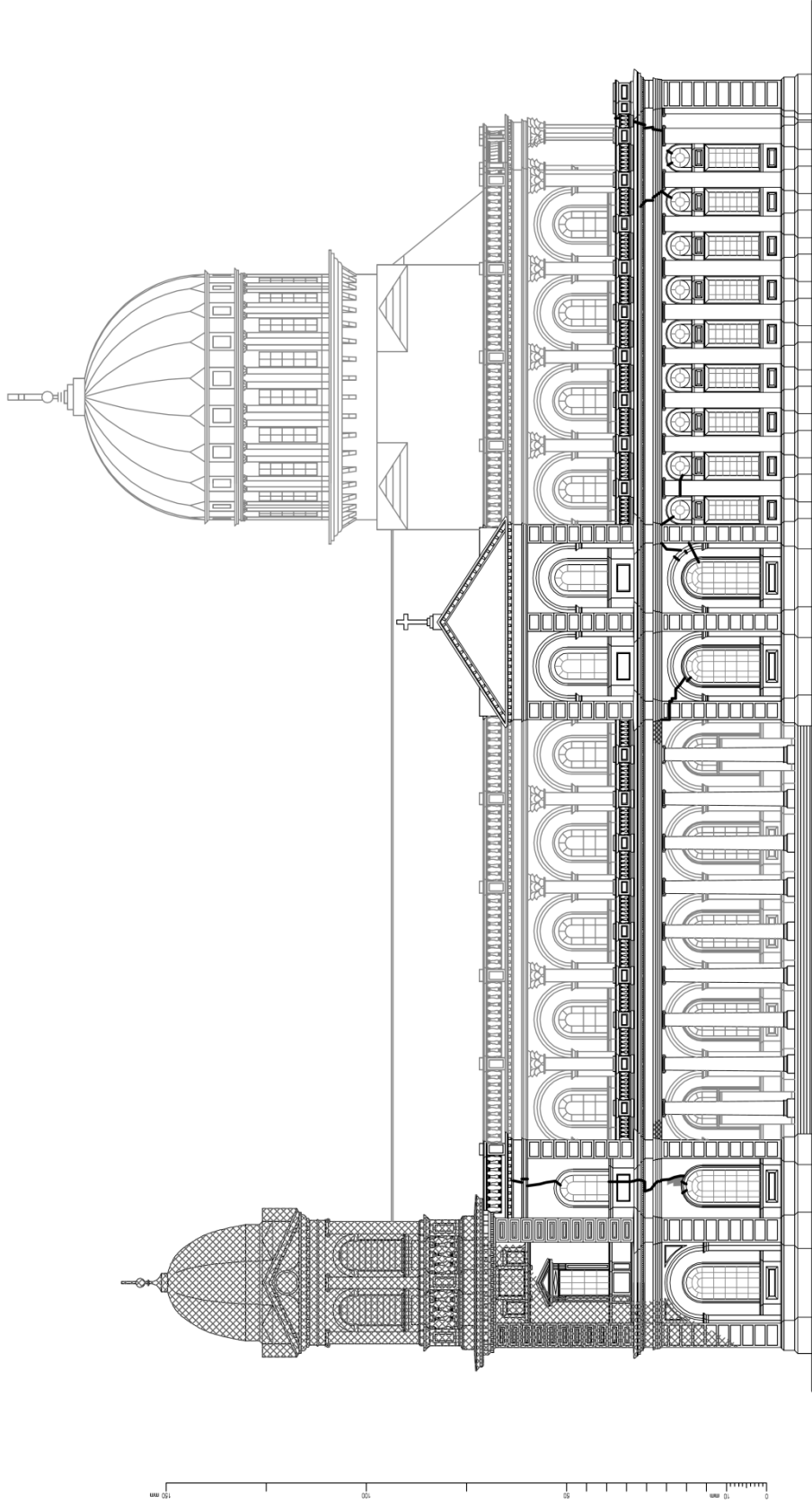
Report

**OPUS**  
Civil Office  
Christchurch Buildings  
Post Earthquake Structural Assessment  
1001 Hicoria Street, Dunedin, New Zealand  
PO Box 480, Dunedin, New Zealand  
Tel: +64 (0)3 477 1722

West Elevation & West Walls of Transepts

1:200





Project: Christchurch Basilica  
Post Earthquake Structural Assessment

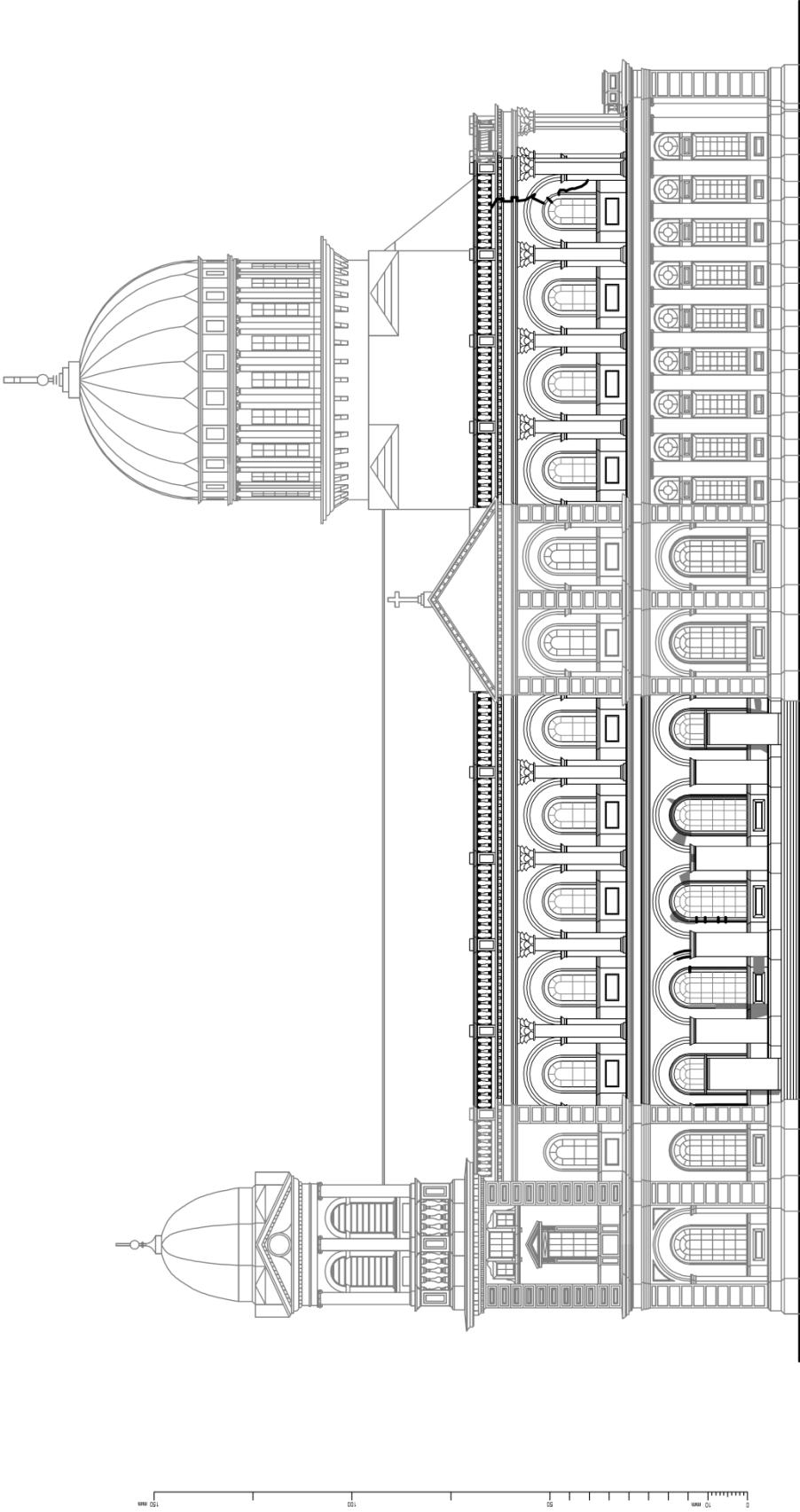
Client: Christchurch City Council  
101-107 Ferris Court, Ferris Lane,  
Blenheim, Central Otago 7773  
+44 (0)20 2077 7773


OPUS  
Structural Engineering  
100-1000  
AW

Drawn: [Name]  
Checked: [Name]  
Approved: [Name]

Scale: 1:200

Sheet No.: 2

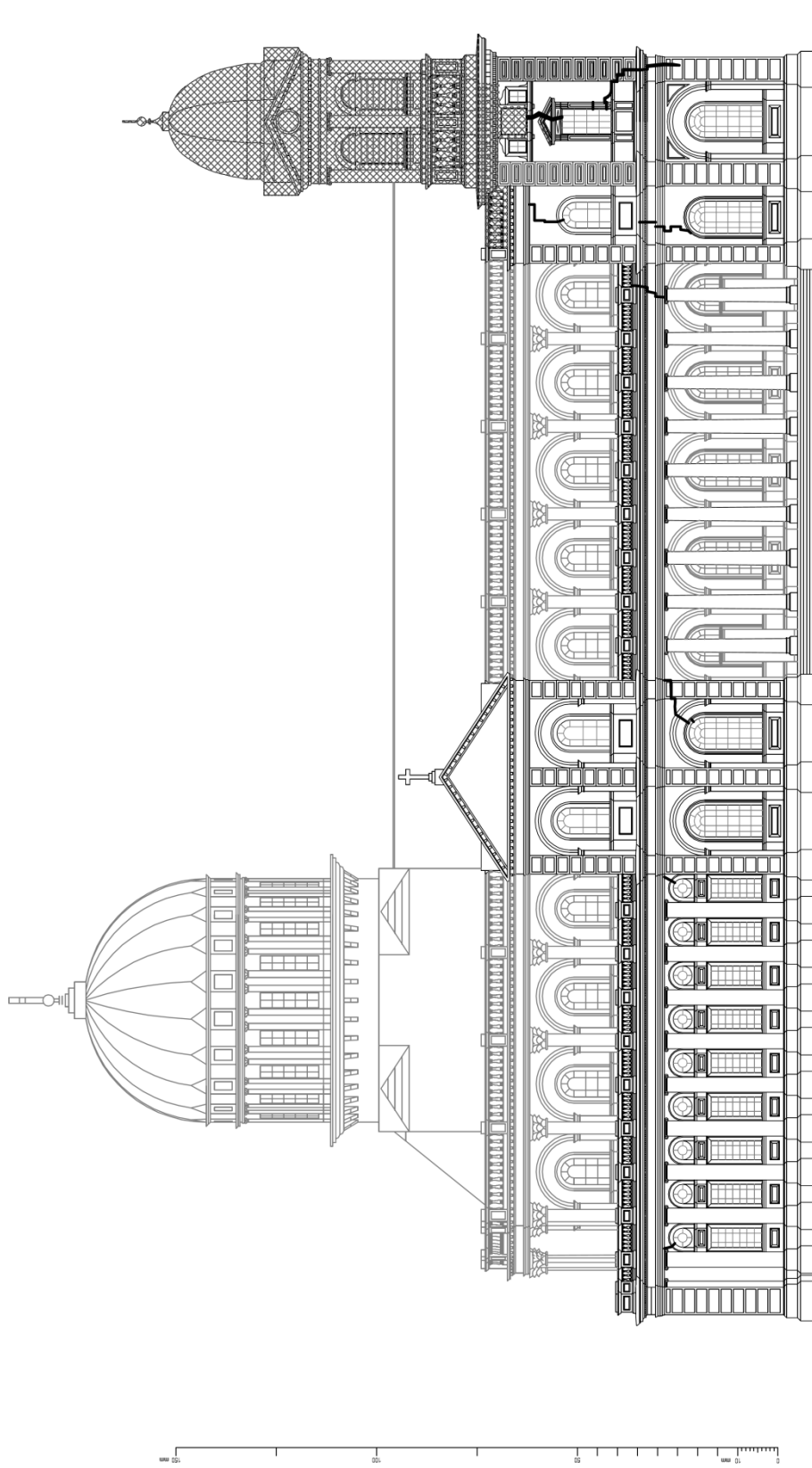



**Christchurch Basilica**  
 Post-Earthquake Structural Assessment  
 South Elevation (Inner)

Client: Christchurch Basilica  
 101-117 Lambton Quay, Christchurch, New Zealand  
 Phone: +64 (0)3 377 1721

Project No: 1200  
 Date: 2014/11

1:1  
 @ A3  
 Original Sheet Size: A3 (420x594) Plot Date: 2014/11

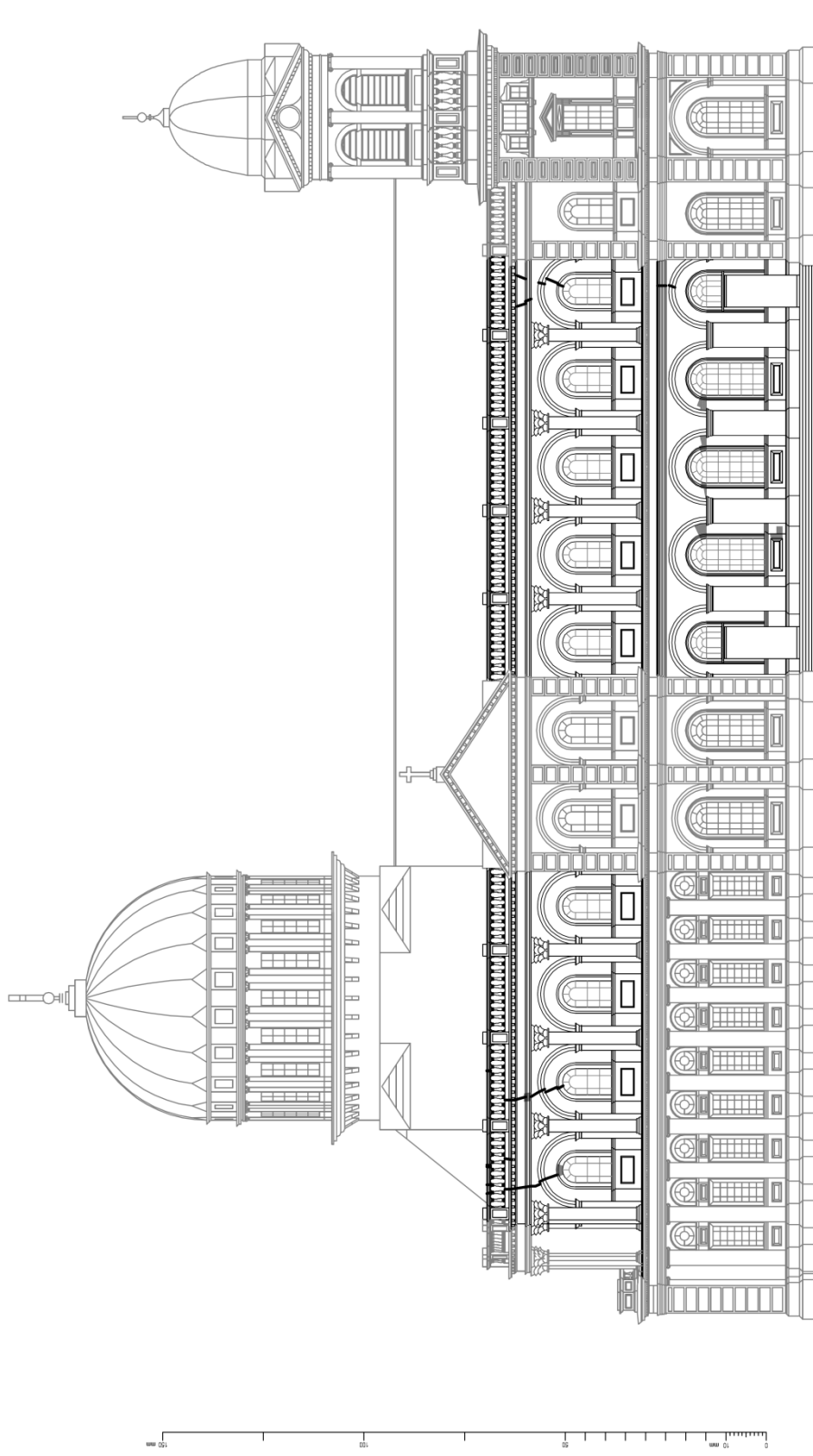


OPUS  
Christchurch Basilica  
Post Earthquake Structural Assessment

North Elevation (Outer)

1:200

4



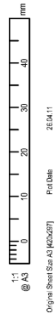
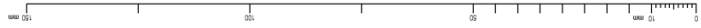
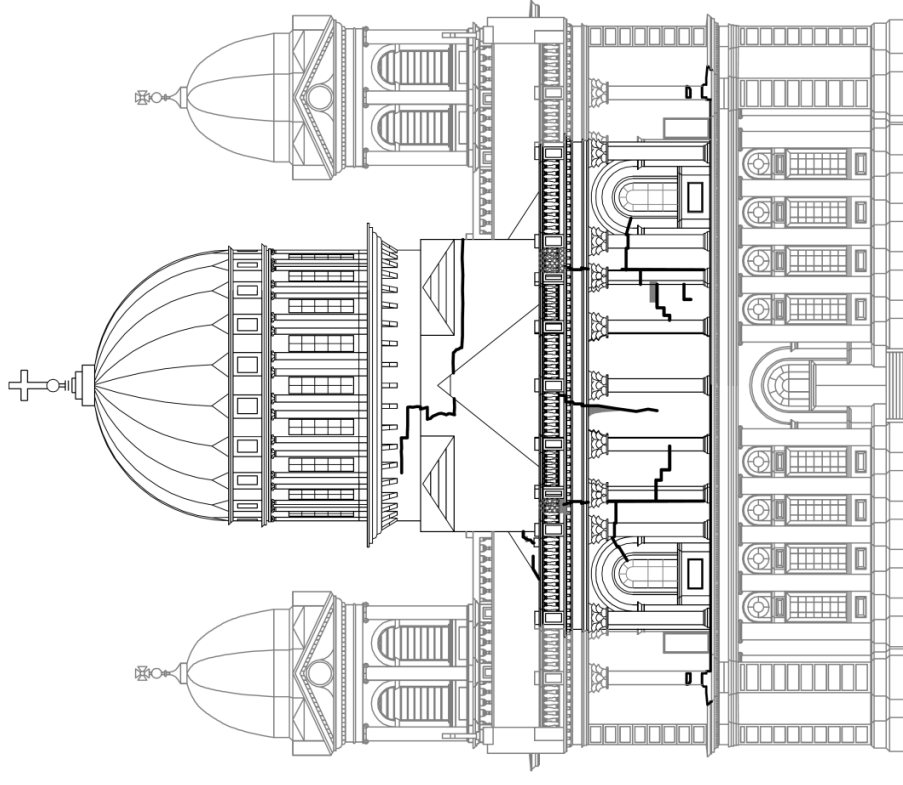
Christchurch Basilica  
Post Earthquake Structural Assessment

OPUS  
Civil Engineering  
100 The Terrace, Christchurch, New Zealand  
Phone: +64 (0)3 371 1974  
Fax: +64 (0)3 371 1973

North Elevation (Inner)

1:1  
@ A3  
0 10 20 30 40 50  
mm

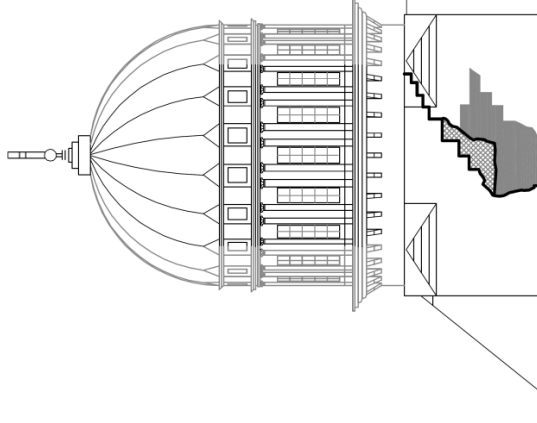
Project: Christchurch Basilica  
Drawing No: 2618.11  
Date: 26/04/11



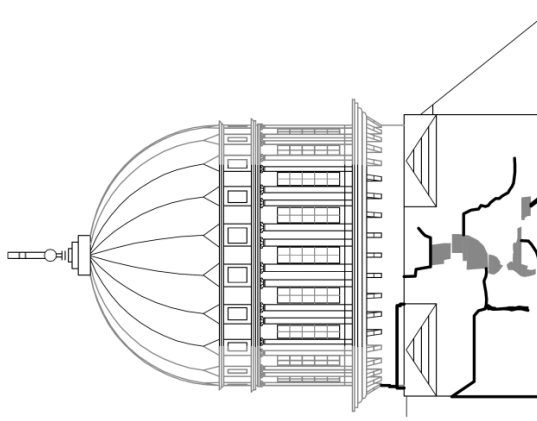
Christchurch Basilica  
Post Earthquake Structural Assessment

**OPUS**  
Civil Office  
100 The Terrace, Christchurch  
P.O. Box 480, Christchurch 8140  
+61 (0)3 2277 272

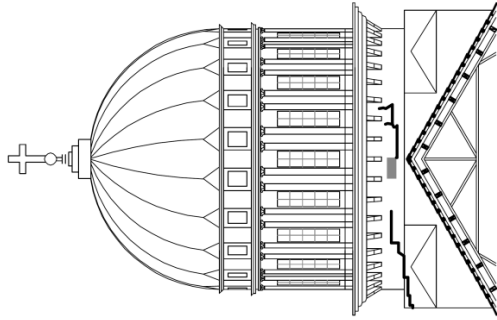
AW  
1:200  
6



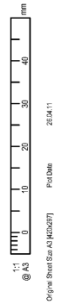
Rotunda - North Elevation




Rotunda - South Elevation



Rotunda - West Elevation




**OPUS**  
 CONSULTANTS  
 1000 West Broadway, Suite 1000  
 Vancouver, BC V6H 4G1  
 Tel: 604.277.7373

Christchurch Bealifa  
 Post Earthquake Structural Assessment  
 1000 West Broadway, Suite 1000  
 Vancouver, BC V6H 4G1  
 Tel: 604.277.7373

Rotunda & Dome  
 1:200  
 7